NUREG/CP-0191
Vol. 2, Part 2

Proceedings of the Conference on Vessel Penetration Inspection, Crack Growth and Repair

Held at
Gaithersburg Marriott at Washington Center
Gaithersburg, MD
September 29 – October 2, 2003

Presentation Graphics
Session IV: Crack Growth Rate Studies for the Disposition of Flaws
Session V: Mitigation of Nickel-base Alloy Degradation and Foreign Experience

U.S. Nuclear Regulatory Commission
Office of Nuclear Regulatory Research
Washington, DC 20555-0001

AVAILABILITY OF REFERENCE MATERIALS IN NRC PUBLICATIONS

NRC Reference Material

As of November 1999, you may electronically access NUREG-series publications and other NRC records at NRC's Public Electronic Reading Room at http://www.nrc.gov/reading-rm.html. Publicly released records include, to name a few, NUREG-series publications; *Federal Register* notices; applicant, licensee, and vendor documents and correspondence; NRC correspondence and internal memoranda; bulletins and information notices; inspection and investigative reports; licensee event reports; and Commission papers and their attachments.

NRC publications in the NUREG series, NRC regulations, and *Title 10, Energy*, in the Code of *Federal Regulations* may also be purchased from one of these two sources.

1. The Superintendent of Documents
   U.S. Government Printing Office
   Mail Stop SSOP
   Washington, DC 20402–0001
   Internet: bookstore.gpo.gov
   Telephone: 202-512-1800
   Fax: 202-512-2250
2. The National Technical Information Service
   Springfield, VA 22161–0002
   www.ntis.gov
   1–800–553–6847 or, locally, 703–605–6000

A single copy of each NRC draft report for comment is available free, to the extent of supply, upon written request as follows:

Address: Office of the Chief Information Officer,
Reproduction and Distribution
Services Section
U.S. Nuclear Regulatory Commission
Washington, DC 20555-0001
E-mail: DISTRIBUTION@nrc.gov
Facsimile: 301–415–2289

Some publications in the NUREG series that are posted at NRC's Web site address http://www.nrc.gov/reading-rm/doc-collections/nuregs are updated periodically and may differ from the last printed version. Although references to material found on a Web site bear the date the material was accessed, the material available on the date cited may subsequently be removed from the site.

Non-NRC Reference Material

Documents available from public and special technical libraries include all open literature items, such as books, journal articles, and transactions, *Federal Register* notices, Federal and State legislation, and congressional reports. Such documents as theses, dissertations, foreign reports and translations, and non-NRC conference proceedings may be purchased from their sponsoring organization.

Copies of industry codes and standards used in a substantive manner in the NRC regulatory process are maintained at—

The NRC Technical Library
Two White Flint North
11545 Rockville Pike
Rockville, MD 20852–2738

These standards are available in the library for reference use by the public. Codes and standards are usually copyrighted and may be purchased from the originating organization or, if they are American National Standards, from—

American National Standards Institute
11 West 42nd Street
New York, NY 10036–8002
www.ansi.org
212–642–4900

Legally binding regulatory requirements are stated only in laws; NRC regulations; licenses, including technical specifications; or orders, not in NUREG-series publications. The views expressed in contractor-prepared publications in this series are not necessarily those of the NRC.

The NUREG series comprises (1) technical and administrative reports and books prepared by the staff (NUREG–XXXX) or agency contractors (NUREG/CR–XXXX), (2) proceedings of conferences (NUREG/CP–XXXX), (3) reports resulting from international agreements (NUREG/IA–XXXX), (4) brochures (NUREG/BR–XXXX), and (5) compilations of legal decisions and orders of the Commission and Atomic and Safety Licensing Boards and of Directors' decisions under Section 2.206 of NRC's regulations (NUREG–0750).

DISCLAIMER: Where the papers in these proceedings have been authored by contractors of the U. S. Government, neither the U.S. Government nor any agency thereof, nor any U.S. employee makes any warranty, expressed or implied, or assumes any legal liability or responsibility for any third party's use or the results of such use, of any information, apparatus, product, or process disclosed in these proceedings, or represents that its use by such third party would not infringe privately owned rights. The views expressed in these proceedings are not necessarily those of the U. S. Regulatory Commission.

NUREG/CP-0191
Vol. 2, Part 2

Proceedings of the Conference on Vessel Penetration Inspection, Crack Growth and Repair

Held at
Gaithersburg Marriott at Washington Center
Gaithersburg, MD
September 29 - October 2, 2003

Volume 2 - Presentation Graphics, Part 2
Session IV: Crack Growth Rate Studies for the Disposition of Flaws
Session V: Mitigation of Nickel-base Alloy Degradation and Foreign Experience

Manuscript Completed: July 2005
Date Published: September 2005

Compiled and edited by:
T. S. Mintz and W. H. Cullen, Jr.

Prepared by
Division of Engineering Technology
Office of Nuclear Regulatory Research
Washington, DC 20555-0001
NRC Job Code Y6722

ABSTRACT

These two volumes of proceedings contain the visual projections (in Volume I), and the contributed manuscripts (in Volume II) from the Conference on Vessel Head Penetration, Crack Growth and Repair, held at the Gaithersburg Marriott at Washingtonian Center on September 29 – October 2, 2003. The conference was co-sponsored by the U. S. Nuclear Regulatory Commission and Argonne National Laboratory. Over two hundred attendees were provided with 45 presentations, divided into five sessions: (I) Inspection Techniques, Results, and Future Developments, (II) Continued Plant Operation, (III) Structural Analysis and Fracture Mechanics Issues, (IV) Crack Growth Rate Studies for the Disposition of Flaws, and (V) Mitigation of Nickel-Base Alloy Degradation and Foreign Experience. The conference opened with a plenary session including presentations giving the overview from the NRC Office of Nuclear Regulatory Research, and an overview of nickel-base alloy cracking issues worldwide. The conference closed with a panel session consisting of industry representatives and NRC management discussing the prognosis for future issues in this area of concern.

FOREWORD

Stress-corrosion cracking of nickel-base alloys used in both wrought and welded vessel penetration components has been an increasing and worldwide challenge for the nuclear industry and regulatory authorities since the mid-1980s. Cracks and resultant leaks were initially discovered in components fabricated from Alloys 600 and 182 exposed to higher temperatures, particularly in pressurizer heater sleeves and nozzles. Over time, cracks and leaks have also been discovered in components operating at lower temperatures, including vessel head and bottom-mounted instrumentation penetrations.

Given the safety-significance of this issue, the U.S. Nuclear Regulatory Commission (NRC) hosted a 4-day conference on September 29 – October 2, 2003, to provide a forum for presentations and discussions concerning inspection, stress analysis, flaw evaluation, and mitigation of stress-corrosion cracks in vessel penetrations. This conference also provided a valuable opportunity for participants from several venues — regulatory, research, and plant operations — to meet face-to-face to formally and informally exchange data and concepts with the individuals who are at the forefront of the cracking issue.

As such, the conference brought together much of the worldwide expertise in the area of nickel-base alloy cracking. More than 200 individuals attended the 4-day conference, which included 45 presentations that provided a wide-ranging perspective on the issue. Many of the presentations were prepared by researchers involved in crack growth rate studies and nondestructive inspection; those presentations described successes and difficulties in developing testing and inspection procedures. Several discussed the stochastic nature and statistical analysis of cracking incidents, predictive algorithms for this type of degradation, and the prognosis for the future, including head replacement strategies, mitigation of the cracking process, and the likelihood of increased resistance to cracking of the replacement materials (Alloys 690 and 152). Other presentations were prepared by reactor component vendors, utility representatives, and regulatory participants, who described plant responses to component degradation, structural integrity evaluation, or the repair and mitigation of cracking. Many of those presentations were marked by completeness and candor in the discussion of observed problems and the related solutions. In addition, several presentations described the experiences of non-domestic institutions, providing contrasts and alternative approaches to the same problem.

The complete proceedings package consists of all conference presentations and available manuscripts, in both printed and electronic formats. The broad, public distribution of the proceedings ensures that the presentations will be subject to the greatest possible scrutiny and accreditation. As a result, the conference organizers believe that these proceedings will give readers an overview of the current status of inspection technology and crack growth rate studies, as well as an understanding of reactor safety and the economic impact of the degradation of nickel-base alloys on plant operation.

Carl J. Paperiello

Carl J. Paperiello, Director
Office of Nuclear Regulatory Research

CONTENTS

ABSTRACT iii
FOREWORD v
EXECUTIVE SUMMARY xiii
ACKNOWLEDGEMENTS xvii

1. Opening Session 1

1.1 A Review of Alloy 600 cracking in Operating Nuclear Plants: Historical Experience and Future Trends 3
W. H. Bamford and J. F. Hall

2. Session I: Inspection Techniques, Results, and Future Developments 19
Chairpersons: S. Doctor, Pacific Northwest National Laboratory
D. Jackson, US Nuclear Regulatory Commission

2.1 NDE of Austenitic Materials: A Review of Progress and Challenges 21
F. Ammirato

2.2 Inspection Reliability of Reactor Vessel Head Penetrations 49
S. R. Doctor

2.3 The Evolution of Inspection and Repair Approaches for Reactor Vessel Head Penetrations 81
D. Schlader

2.4 Summary of U.S. PWR Reactor Vessel Head Nozzle Inspection Results 97
G. White, N. Nordmann, L. Mathews, and C. King

2.5 Inspection Technology for BMI Penetrations 125
M. S. Lashley, R. F. Cole, and S. W. Glass

2.6 EPRI MRP Alloy 600 RPV Head Penetration Inspection Demonstration Program 149
T. Alley, E. K. Kietzman, and F. Ammirato

2.7 Production of Realistic Flaw in Alloy 600 for Qualification Purposes 181
M. Kemppainen, I. Virkkunen, J. Pitkänen, K. Hukkanen, and H. Hänninen

2.8 Generic Guidance for an Effective Boric Acid Inspection Program for Pressurized Water Reactors 197
G. Rao, S. Sharma, and D. Weakland

2.9 Risk-Informed Evaluation of PWR Reactor Vessel Head Penetration Inspection Intervals 221
G. White, S. Hunt, and N. Nordmann

2.10 Reactor Vessel Head Penetration Inspection Technology, Past, Present and Future 241
J. P. Lareau and D. C. Adamonis

3. Session II: Continued Plant Operation 261
Chairpersons: W. H. Bamford, Westinghouse Electric Company, LLC
A. L. Hiser, Jr.,US Nuclear Regulatory Commission

3.1 Background and Technical Basis: Evaluation of Upper Head Penetration Flaws in the ASME Code 263
W. Bamford and G. DeBoo

3.2 Maintenance Strategy of the Inconel Components in PWR Primary System in France . 283
F. Champigny, F. Chapelier, C. Amzallag, and F. Vaillant

3.3 Strategic Planning for RPV Head Operation 307
S. Hunt and G. White

3.4 Reactor Vessel Bottom-Mounted Instrumentation (BMI) Nozzle Repair Development and Implementation at South Texas Project 327
D. Waskey

3.5 Bottom Mounted Instrument Penetration Condition Resolution 347
S. Thomas

3.6 The Embedded Flaw Process for Repair of Reactor Vessel Head Penetrations 379
W. Bamford and P. Kreitman

3.7 Weld Overlay to Reduce Tensile Stresses in Alloy 82/182 Butt Welds 401
S. Hunt, J. Broussard, S. Ahnert, P. O'Regan, and D. Covill

4. Session III: Structural Analysis and Fracture Mechanics Issues 423
Chairperson: G. Wilkowski, Engineering Mechanics of Columbus, Corp.

4.1 Probabilistic Fracture Mechanics Analyses of RPV Top Head Nozzles 425
P. Riccardella, N. Cofie, and A. Miessi

4.2 Parametric Studies of CRDM Head Failures 457
W. J. Shack

4.3 Analysis of Weld Residual Stresses and Circumferential Through-Wall Crack K-Solutions for CRDM Nozzles 477
D. Rudland, G. Wilkowski, Y.-Y. Wang, and W. Norris

4.4 International Cooperative Project: PWSCC and NDE in Ni-Base Alloys and Dissimilar Metal Welds 511
C. E. Moyer

4.5 Welding Residual and Operating Stress Analysis of RPV Top and Bottom Head Nozzles 517
J. Broussard and D. Gross

4.6 Predicting the First Failure 543
R. W. Staehle

4.7 Elevated Temperature Grain Boundary Embrittlement and Ductility-Dip Cracking in Ni-base Weld Metals 573
J. C. Lippold

4.8 Impact of PWSCC and Current Leak Detection on Leak-Before-Break 607
D. Rudland, R. Wolterman, G. Wilkowski, and R. Tregoning

5. Session IV: Crack Growth Rate Studies for the Disposition of Flaws 635
Chairpersons: K. Gott, Swedish Nuclear Power Inspectorate (SKi)
T. Shoji, Institute of Fracture Mechanics, Tohoku University, Japan

5.1 US Regulatory Experience and Prognosis with RPV Head Degradation and VHP Nozzle Cracking 637
A. L. Hiser

5.2 Stress Corrosion Crack Growth Rates (SCCGRs) for Alloy 182 and 82 Welds 661
S. A. Attanasio, J. V. Mullen, J. W. Wuthrich, W. W. Wilkening, and D. S. Morton

5.3 Influence of Temperature on Primary Water Stress Corrosion Cracking of Alloy 600 Weld Metals 693
Y. Nishikawa, N. Totsuka, and K. Arioka

5.4 Experimental and Numerical Approaches for Characterizing the Crack Growth Behavior of Alloy 600 in PWR Primary Water, and Lifetime Predictions for Welded Structures 713
T. Shoji, Z. Lu, and Q. Peng

5.5 Hydrogen Assisted Fracture Model Predictions for Alloy 600 PWSCC: Sensitivities of Crack Growth Rate to Applied Stress Intensity Factor, Temperature, Carbon Concentration, Yield Stress, Crack Growth Orientation and coolant-borne hydrogen 745
M. M. Hall, W. C. Moshier, and D. J. Paraventi

5.6 SCC Growth Rate of Nickel Based Alloy 132 Weld Metal 767
T. Yonezawa, K. Tsutsumi, H. Kanasaki, K. Yoshimoto, Y. Nomura, and S. Asada

5.7 The Stress Corrosion Crack Growth Rate of Alloy 600 Heat Affected Zones Exposed to High Purity Water 799
G. A. Young, N. Lewis, and D. S. Morton

5.8 In-situ Raman Spectroscopic Study on Alloy 600 CRDM Nozzle Material and Its Implications 819
J. H. Kim, I. S. Hwang, and T. R. Kim

5.9 Analysis Alloy 600 Stress Corrosion Cracking with an Artificial Neural Network 849
M. J. Pattison, S. Belsito, S. Banerjee, and W. H. Cullen

5.10 Results of Accelerated SCC Testing of Alloy 82, Alloy 182, and Alloy 52M Weld Metals 867
R. J. Jacko, R. E. Gold, G. V. Rao, A. Kroes, and K. Koyama

5.11 Metallurgical Investigation and Root Cause Assessment of the Reactor Vessel Head Penetration Alloy 182/82 J-groove Weld Cracking in Two Rotterdam Vessels 889
G. Rao, G. Embring, J. Bennetch, and W. Gahwiller

5.12 French Regulatory Experience and Views on Nickel-Base Alloys PWSCC Prevention & Treatment 913
G. Turluer, G. Cattiaux, B. Monnot, D. Emond, J. Reuchet, and P. Chartier

6. Session V: Mitigation of Nickel-base Alloy Degradation and Foreign Experience 933
Chairpersons: P. Scott, Framatome ANP, France
S. Fyfitch, Framatome ANP, USA

6.1 Belgian Activities on Alloys 600 and 182 Issues 935
R. Gerard and Ph. Daoust

6.2 German Experience with RPV Head Penetrations 963
K. Degmayr

6.3 Activities on Alloy 600 Cracking of PWRs in Japan 995
M. Toyoda, S. Asada, and N. Hori

6.4 Tsuruga Unit-2 Pressurizer; Leakage from the Dissimilar Weld (Alloy 600) of the Relief Nozzle (informal presentation by T. Yonazawa) 1013

6.5 RPV Heads: Inspection vs. Replacement Strategies for Ringhals-PWR 1021
P. Efsing and C. Jansson

6.6 Alloy 600 PWSCC Mitigation: Past, Present, and Future 1043
S. Fyfitch

6.7 A Reactor Vessel Upper Head Temperature Reduction Program to Prevent and Mitigate Alloy 600 Cracking 1067
D. R. Forsyth, P. L. Strauch, and P. J. Kreitman

6.8 Status Report on the Effect of Zinc Additions on Mitigation of PWSCC in Alloy 600 1081
J. Hickling

6.9 An Assessment of MSIP for PWSCC Mitigation of PWR Thick Wall Piping Welds by Instrumented Monitoring of Full-Scale Mock-up Test 1099
G. Rao, M. Badlani, E. Ray, and T. Damico

7. Session Summaries 1115

7.1 Session I: Inspection Techniques, Results, and Future Developments 1117
S. Doctor and D. Jackson

7.2 Session II: Continued Plant Operation 1129
A. Hiser and W. Bamford

7.3 Session III: Structural Analysis and Fracture Mechanics Issues 1137
G. Wilkowski

7.4 Session IV: Crack Growth Rate Studies for the Disposition of Flaws 1139
T. Shoji

7.5 Session V: Mitigation of Nickel-base Alloy Degradation and Foreign Experience 1159
S. Fyfitch and P. Scott

8. Panel Discussion 1169

8.1 NRC Perspective on the Management of Materials Degradation 1171
R. Barrett

8.2 Integrated Inspection Model for Managing Materials Issues 1177
J. Strosnider

EXECUTIVE SUMMARY

The purpose for this conference was to examine the current state of technology for vessel head penetrations with respect to inspection, cracking, and repair. This subject is being examined because of penetration cracking which has been occurring for over a decade. The first reactor head penetrations to show signs of leakage occurred in France in the early 90's at Bugey 3. After this incident the French inspected a large number of their penetrations and reported that roughly 3% of their inspected nozzles had some type of indication. Because of the cracking in France, many power plants in the US and elsewhere started to examine penetrations and found ultimately that a large number were similarly cracked. The next leakage from a vessel head penetration occurred in the United States at Oconee 3 in 2000. Following Oconee there have been many other plants with cracked or leaking penetrations. This type of degradation led to one of the most serious nuclear incidents in the U.S. at Davis Besse. A crack in a vessel head penetration, possibly combined with the presence of substantial boric acid deposits, led to corrosion of the low-alloy steel, and the formation of a large cavity in the reactor head. Another significant event included the first leaking bottom mounted instrument penetrations discovered at the South Texas Project Plant in the United States. These instances of failure are a concern to the public, industry, and regulators. Knowledge gained from this conference will help reduce future incidents from occurring. The five sessions listed below were held at the conference and covered several topical areas.

Session I: Inspection Techniques, Results, and Future Developments
Session II: Continued Plant Operation
Session III: Structural Analysis and Fracture Mechanics Issues
Session IV: Crack Growth Rate Studies for the Disposition of Flaws
Session V: Mitigation of Nickel-base Alloy Degradation and Foreign Experience

The first session examined the area of inspection techniques for the vessel head penetrations. This is important research, since inspection capability is one of the first lines-of-defense against vessel head penetration leakage. A range of topics were discussed including how nondestructive examination (NDE) has evolved over time. Advancements in NDE were examined which included Phased Array Ultrasonic Testing and Eddy Current Testing Arrays. With regards to the area of NDE testing tools, cracked penetration mockups and performance demonstrations were discussed. This included examining new techniques for developing realistic flaws. The issue of reliability of NDE data was another topic of concern. This led into presentations about in-service inspections (ISI). One main area of discussion for ISI is the frequency of inspections. One question that was raised asked what should be the bases for determining the inspection frequency. Should the ISI be based on avoiding any leakage at a plant or should it be based on avoiding core damage? The discussion of inspection techniques carried over to the next session of Continued Plant Operation.

The second session examined Continued Plant Operation, and one of the first presentations examined the analytical and repair approaches for continued plant operation. Included in this session was a description of the cracking which occurred at South Texas Project in the bottom mounted instrument (BMI) nozzles. The repair techniques for these bottom mounted nozzles were discussed in detail. With regards to upper head penetrations, there is an understanding that evaluation methods are being developed and will be included in section XI of the ASME code sometime in 2004. The French discussed the initial leak at Bugey and investigations which followed. In France it was determined that the best choice of action was to replace the vessel heads with Alloy 690 nozzles and Alloy 152 weld material. The subject of how power plants in the United States have reacted to the nickel-based material cracking issues was similarly covered. In examining how to operate after repair or mitigation, taking into consideration cost and downtime, the optimum solution to this problem was to reduce the reactor vessel head temperatures. There were two repair techniques presented, which included embedded flaw repair and weld overlay

repair. In determining the acceptable usage for these two repair techniques, structural analysis must be taken into consideration, a discussion which provided a segue into the next session.

Structural Analysis and Fracture Mechanics Issues was the title of session three. The initial presentations focused on using probabilistic analysis to determine the probability that the head penetrations will either leak or be ejected. It seems that through this type of analysis, in conjunction with reasonable inspection plans, the top heads meet the safety limit for nozzle ejection. However, there are conservatisms still inherent in these calculations. The next topic focused on residual stresses present in the nozzle and how they may affect cracking. There are different variables that need to be considered to determine accurately the hoop and axial residual stresses. Some of these variables are nozzle thermal properties, welding procedure, joint configuration, and mechanical properties. The research presented suggests that residual hoop stresses are larger then the residual axial stresses. In the peripheral nozzles the stresses will depend upon the location in the nozzle, with respect to the downhill or uphill side. Specifically, as the weld height increased the axial stresses decreased while the hoop stresses increased. A logical consequence is that some type of medium weld height might be used in order to achieve a balance between both hoop and axial residual stresses. The session included discussion on the subject of ductile-dip-cracking, which seems to be a much larger problem for alloys 152/52 then it is for alloy 182/82. There was also some examination of the leak before break (LBB) concept. Initial LBB calculations utilized cracks which were more characteristic of fatigue cracks than PWSCC cracks. A reanalysis of LBB using PWSCC crack geometries leads to some new results. The presentation noted that it is difficult to satisfy LBB criteria using the PWSCC crack geometries. Another feature is that PWSCC could result in long circumferential surface cracks which may be more prone to failure than than the currently-utilized, simple, through-wall circumferential crack. The LBB screening criteria is not satisfied by this type of circumferential cracking. Finally, the last subject in this session examined the subject of predicting first failure by creating an all inclusive equation. This equation would predict failure by using past experience as a guide. Auxiliary equations would take into consideration variables such as temperature or stress, which affect failure. These small individual equations would be combined to create an overall cracking equation. However, this work is still in the beginning phase of development.

The fourth session of the conference was titled Crack Growth Rate Studies for the disposition of flaws. This is a very important subject because crack growth rates can be used to predict when an identified crack will lead to leakage of reactor coolant solution. A discussion of the history of Alloy 600 cracking at plants in the United States and France was followed by a description of new testing techniques for stress corrosion cracking growth rates (SCCGR). This description included the design details of compliant, self-loaded compact tension (CT) specimens and the conduct of accelerated crack growth tests with a clearly-defined acceleration factor. With regards to SCCGR evaluation procedures, there was discussion about using a maximum or average SCCGR. There was also discussion about the pros and cons of periodic unloading for more continuous crack tip activation. The next subject covered examined the SCCGRs for the materials such as Alloy 600, 182, 152, 132, 82, and 52. The conclusion is that SCCGR for alloy 182 is larger then alloy 82. Alloy 132 has a SCCGR on the order of Alloy 182 SCCGR. The crack growth rates in the heat affected zone (HAZ) in Alloy 600 may be 30 times larger then the non-HAZ material. Alloy 52M has been tested but no cracking was found in this material. In service, an alloy 182 weld with 5-10 effective full power years (EFPY) cracked. Alloy 600 showed cracking in a material with 6-13 EFPY. The participants discussed the effect of dissolved hydrogen on SCCGRs in this session. There was agreement that the SCCGRs are maximized when exposed to electrochemical conditions around the Ni/NiO equilibrium line on a Pourbaix diagram. Another subject covered was models for SCCGRs. The physical and mechanical-chemical models discussed are useful tools that can be utilized to examine the SCCGR inter-workings. The combination of models with the SCCGR data should provide a more accurate assessment of SCCGR curves.

The final session for the conference examined Mitigation of Nickel-Base Alloy Degradation and Foreign Experience. During previous sessions the experiences from both the United States and France had been presented. This session allowed other countries affected by the same degradation to present the issues occurring in their country. This foreign experience included presentations from Belgium, Germany, Sweden, and Japan. In Belgium, a proactive approach has been taken to repair, replace, or mitigate any alloy 600 cracking before leakage occurs. In Germany, the Obrigheim power plant is the only plant in that country which contains Alloy 600 in the reactor vessel head penetrations. As a result, Obrigheim uses leakage detection systems. In Japan, reactor heads were replaced in older plants, while newer plants have lowered the reactor vessel head temperature. Minor indications in the bottom mounted instrument nozzles have also been discovered in Japan. Sweden plants replaced the reactor vessel heads. The next subject of this session was mitigation techniques for nickel-based alloy degradation. One of the main directions industry is headed is to replace Alloy 600 parts with Alloy 690. Other then replacing the material, there are three ways to alleviate degradation. These mitigation strategies are mechanical surface enhancement, environmental barriers or coatings, or changes to the environment. The geometry of the component influences the choice of a particular strategy. One type of mitigation technique that has been employed is to reduce the head temperature of the vessel. This has the effect of reducing the rate of increase of effective degradation years. Another mitigation technique which is being tested is low-level zinc additions to the primary coolant. There has been some evidence that zinc reduces the initiation time for PWSCC. However, there is less evidence that zinc additions reduce the PWSCC crack growth rate. The last mitigation technique discussed was the mechanical stress improvement procedure (MSIP). MSIP has been demonstrated on thick walled PWR piping. The results from this demonstration show that compressive stresses are formed in the inner weld region and that the profile of the pipe after MSIP is still acceptable for in-service inspections.

ACKNOWLEDGEMENTS

The bulk of the arrangements for this conference were handled by the Conference Office at Argonne National Laboratories. Ms. J. Brunsvold of that office negotiated with the lodging and conference staffs at the Marriott/Gaithersburg – Washingtonian Center, and arranged for a trouble-free four days of conferencing. The assistance of the staff at the Conference Center was managed by K. Natesan, Argonne National Laboratory, who is the program manager for several NRC-funded programs. Speaking for all the attendees, we appreciate the hard work of both Ms. Brunsvold, and Mr. Natesan.

Actually, Ms. Brunsvold and Mr. Natesan planned the logistics for this conference twice. The conference was originally scheduled for September 24, 2001, which turned out to be less than two weeks following the attacks of Sept. 11. The conference was successfully postponed, thanks to the efforts of the Argonne staff and the gracious understanding of the Marriott-Gaithersburg conference office staff. All participants were successfully contacted; not one person showed up at the venue expecting a conference to actually take place.

The organization of the sessions and contributing authors was handled by Ms. Karen Gott, Swedish Nuclear Power Inspectorate (SKi), who was participating in a rotational assignment at the NRC in the months preceding the original conference. We appreciate her hard work and diligence in this effort was extremely helpful in getting this conference off the ground successfully. At the rescheduled conference, Dr. T. Mintz was indispensable in his seemingly effortless handling of the audiovisual logistics during the course of the conference, and with his able assistance in the preparation of the proceedings. The registration and logistics table at the conference site was staffed by Ms. Brunsvold, together with Ms. C. Briggs and Ms. E. Miller, both of the NRC's Office of Nuclear Regulatory Research. Their contribution is much appreciated. T. Mintz also assisted in the compilation, tabulation and electronic linking of the written and electronic versions of the proceedings.

W. Cullen, NRC Program Manager

Section 5:
Session 4: Crack Growth Rate Studies for the Disposition of Flaws

US REGULATORY EXPERIENCE AND PROGNOSIS WITH RPV HEAD DEGRADATION AND VHP NOZZLE CRACKING

Presented by

Allen L. Hiser, Jr.
Materials and Chemical Engineering Branch
Office of Nuclear Reactor Regulation

Conference on Vessel Penetration Inspection, Cracking & Repairs

October 1, 2003

OUTLINE

- Background
- Order EA-03-009 (issued February 11, 2003)
  - Inspection requirements
  - Relaxation requests
  - Possible Modifications to Order EA-03-009
- Outlook
- Bulletin 2003-02

BACKGROUND

- Fall 2000
  - Oconee Unit 1 identifies deposits - axial leak
- Spring 2001
  - Oconee Unit 2 and 3 identify circumferential cracks
  - ANO Unit 1 identifies a leaking nozzle
- **NRC issues Bulletin 2001-01 - August 2001**
  - Focus is safety issue (circumferential cracks) for high susceptibility plants
  - Visual examinations considered acceptable
- Fall 2001
  - Circumferential cracks identified - Crystal River 3 and Oconee 3
  - Leaks and repairs at Surry 1, North Anna 2 and TMI

BACKGROUND (cont.)

- Spring 2002
  - Davis-Besse identifies RPV head wastage & circumferential cracking
- **NRC issues Bulletin 2002-01 - March 2002**
  - Focus is safety issue is RPV wastage for all plants
- Spring 2002
  - Millstone identifies part through-wall cracks (moderate plant)
- **NRC issues Bulletin 2002-02 - August 2002**
  - Focus is adequacy of inspection programs - methods (non-visual NDE for high susceptibility) and frequency
  - Licensee responses generally vague on future program, many cite MRP-75 program

BACKGROUND (cont.)

- Fall 2002
  - North Anna 2 identifies
    - ✓ Prevalent weld cracking, & leak from a repaired nozzle
    - ✓ Circumferential cracking at weld root without boron deposits
  - ANO Unit 1 identifies leak from a repaired nozzle
  - Oconee Unit 2 identifies possible through-wall cracking without boron deposits on the RPV head
  - Head corrosion at Sequoyah Unit 2 - above head boron source

- **NRC issues Order EA-03-009 - February 2003**
  - Mandates inspections for all PWRs

- Spring 2003
  - South Texas Project Unit 1 - boron deposits on the lower head

- **NRC issues Bulletin 2003-02 - August 2003**
  - Focus is inspections of bottom head Alloy 600 nozzles of PWRs

- Fall 2003
  - Oconee Unit 1 - Leak from a plugged thermocouple nozzle
  - (Alloy 690 plug and 152 weld)

OVERVIEW OF ORDERS

- Issued February 11, 2003
- Issued to all PWRs
- Adequate protection basis
  - ASME Code inspections are inadequate
  - Revisions to inspection requirements are not imminent
  - RPV head degradation and nozzle cracking pose safety risks if not promptly identified and corrected
- Provides a clear regulatory framework pending the incorporation of revised inspection requirements into 10 CFR 50.55a

ORDER REQUIREMENTS

- Evaluate susceptibility - effective degradation years (EDY), based on operating temperature and time
- High plants - bare metal visual AND non-visual NDE at EVERY RFO
- Moderate plants - BMV and non-visual NDE at alternating RFOs
- Low plants - BMV by next 2 RFOs (repeat every 3rd RFO or 5 years), non-visual by 2008 (repeat every 4th RFO or 7 years)
- Non-visual NDE is EITHER:
  - Ultrasonic with evaluation of interference fit leakage, OR
  - Wetted-surface examination

Order EA-03-009
Required Inspection Surfaces

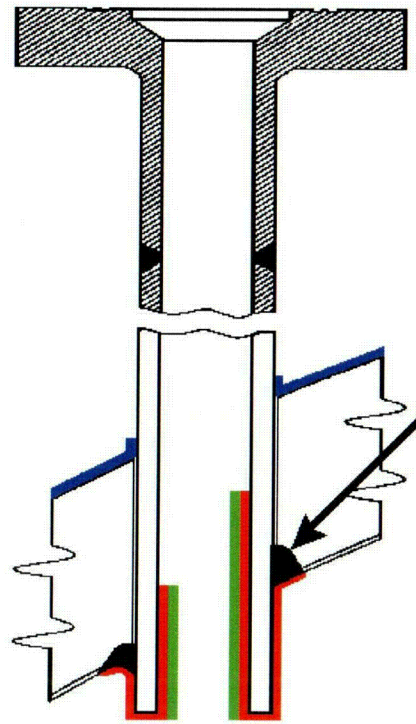

C01

ORDER REQUIREMENTS

- Explicit requirements and criteria to inspect repaired nozzles/welds
- Each RFO, must perform visual inspections to identify boric acid leaks from components above the RPV head - follow-up actions include inspections of potentially-affected RPV head areas and nozzles
- Flaw evaluation per NRC guidance (Strosnider letter fall 2001, revised guidance in Barrett letter April 2003)
- Orders also apply to new RPV heads, either Alloy 600 (Davis-Besse) or Alloy 690 (North Anna 2 and many others)
- Post-outage report 60 days after restart

LICENSEE OPTIONS

- Request Director of NRR to relax or rescind requirements of the order based on "good cause"

- Requests for relaxation for specific VHP nozzles will be evaluated using procedures for proposed alternatives to the ASME Code in accordance with 10 CFR 50.55a(a)(3)
  - The proposed alternative will provide an acceptable level of quality and safety
  - Compliance would result in hardship or unusual difficulty without a compensating increase in the level of quality and safety

646

NEED FOR ORDERS

- Past process of issuing Bulletins unwieldy, inconsistent, not stable, and has no regulatory weight (licensee commitments only)
- Rulemaking would take at least 1 or 2 years
- Orders can be revised or rescinded as necessary
- Although inspection plans for the next RFOs were generally acceptable, NRC wanted to provide licensees with planning time to meet order requirements
- Concerns that above RPV head leakage could result in undetected RPV head degradation

RELAXATION REQUESTS

- Limitations above the J-groove weld
  - Centering tabs & step on nozzle ID
  - Stress in non-inspected area below 28 ksi
  - Hardship - would have required guide sleeve removal and re-welding of a guide funnel onto nozzle

- Limitations below the J-groove weld
  - Guide funnel threads (ID & OD) and tapers on end of nozzles
  - Transducer coupling for time-of-flight-diffraction

- Bare metal visual examinations
  - Localized insulation and support shroud interferences
  - Insulation prevents total access to RPV head surface
    - ✓ Low frequency eddy current to demonstrate head integrity
    - ✓ Enhanced UT to detect "triple-point" cracking

Calvert Cliffs
Order Inspection Limitations

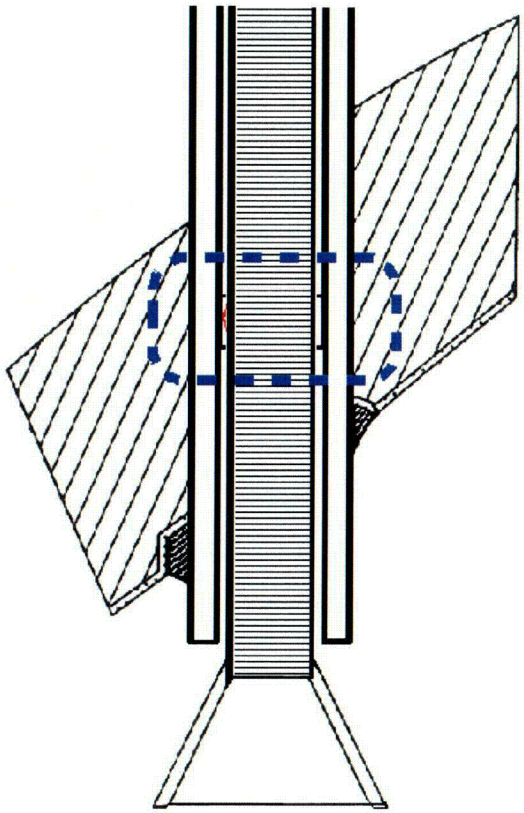

Thermal/Guide Sleeve

Sleeve Expansion Points

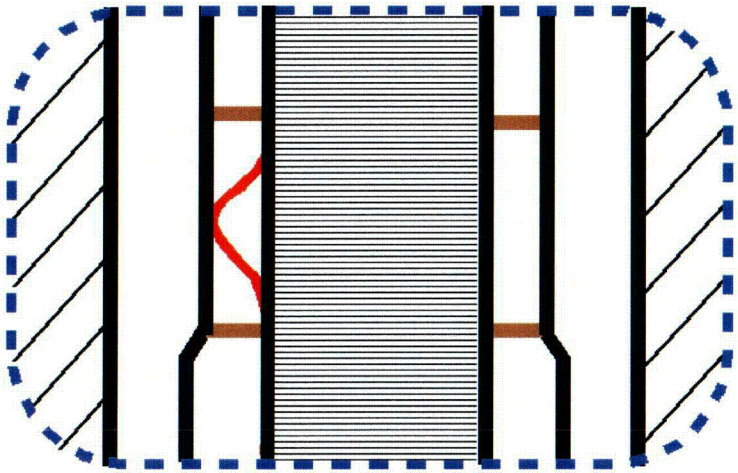

C02

Farley Funnel Thread Inspection Limitation

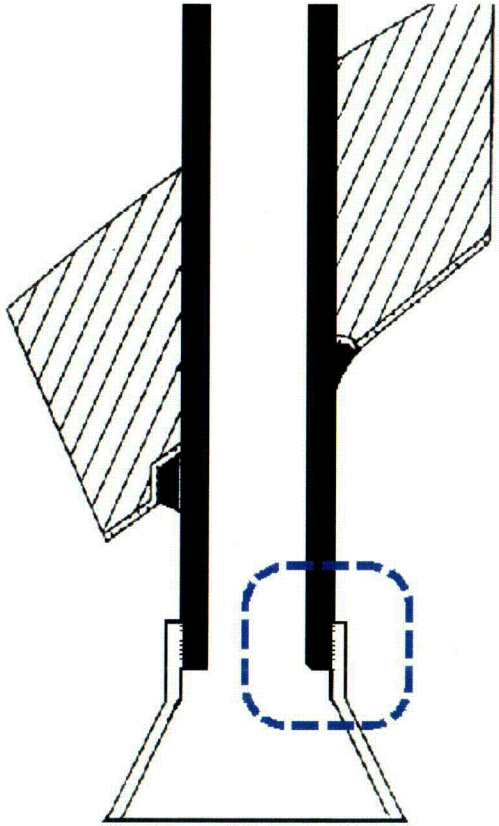

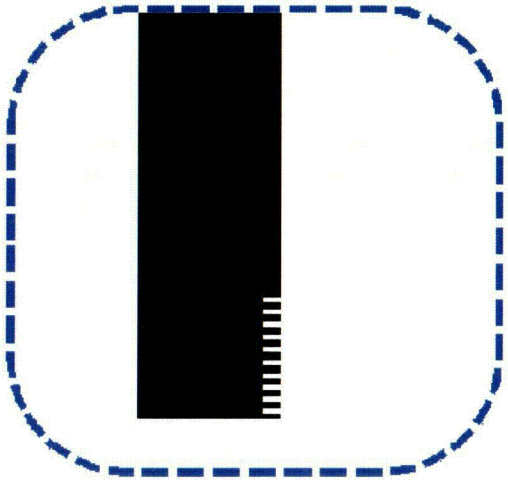

Threaded Surface

C03

St. Lucie Unit 2
Typical RPV Nozzle With Threaded Guide Funnel

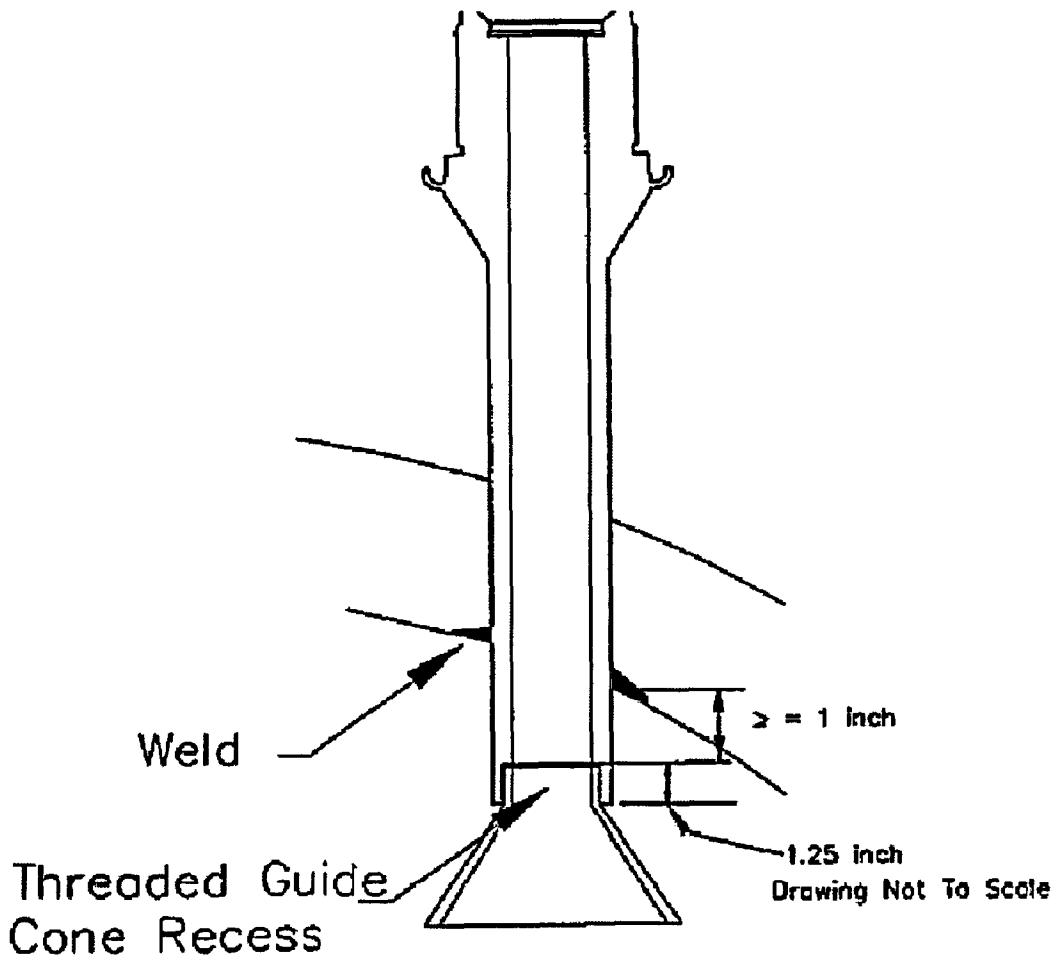

TOFD Transducer Coupling Limitations

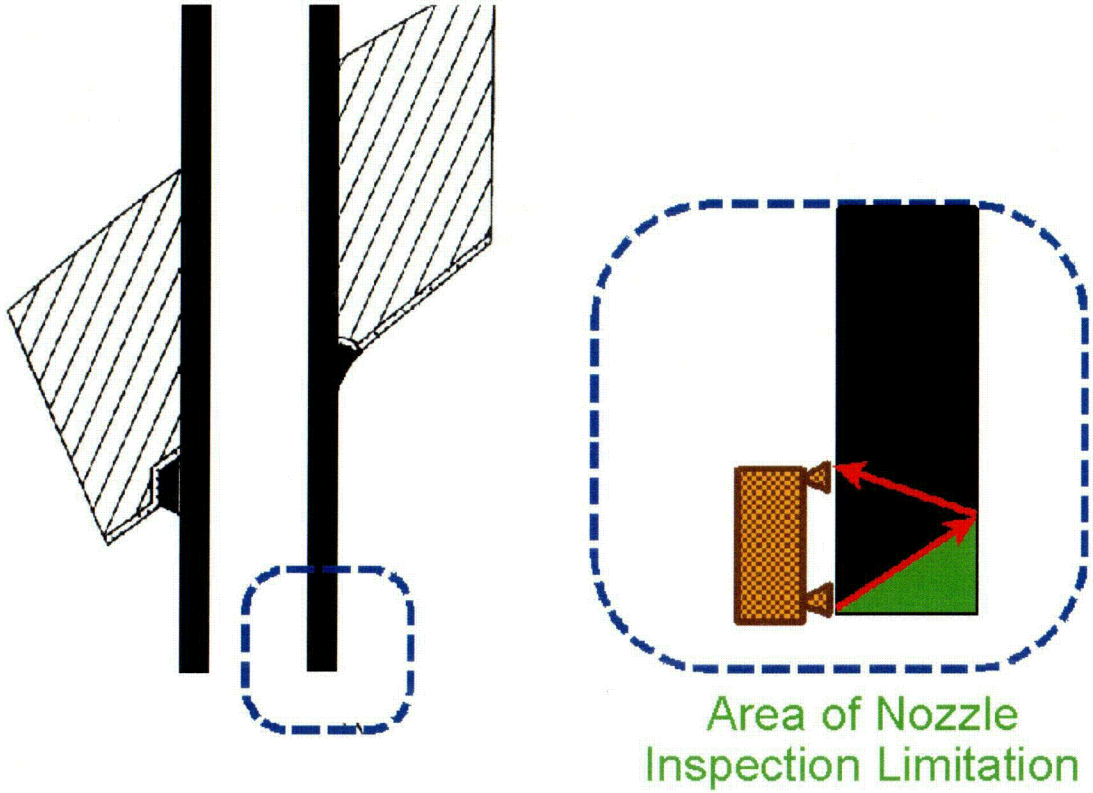

C04

Millstone Power Station
Bare Metal Visual Inspection Restraints

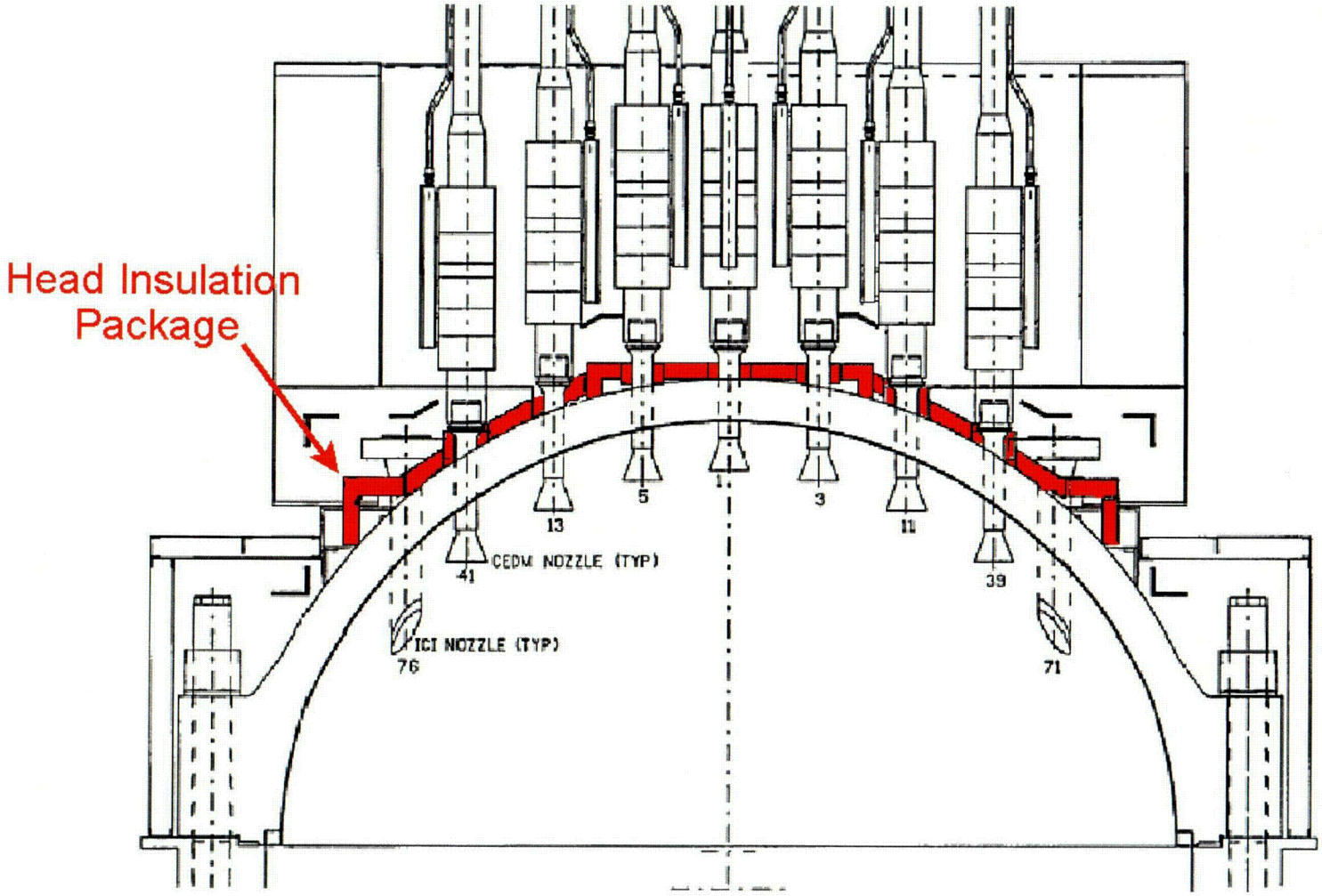

C05

OUTLOOK

- Goal is "permanent" requirements for inspections to ensure structural integrity of the RPV head and VHP nozzles

- ASME Code is working to develop inspection requirements
  - Has been based upon industry report (MRP-75)
  - NRC staff has provided comments - report is not acceptable as submitted, acceptability is not certain
  - NRC has suspended review pending revisions by the industry based on fall 2002 findings
  - ASME Code adoption of requirements may not be complete until 2004 or later

- Inspection requirements will be implemented in 10 CFR 50.55a
  - Endorse the new ASME Code requirements (if acceptable) under expedited implementation, OR
  - Codify alternative inspection requirements
  - Will take 1-2 years once acceptable requirements are identified

POSSIBLE MODIFICATIONS TO ORDER EA-03-009

- Initially mentioned with industry on June 12
- Staff highlighted a high volume of similar relaxation requests for non-safety significant portions of the VHP nozzles and a potential for the industry to provide a generic analysis that could provide a technical basis for modifications to the Order - **report received September 26**
- The modification would result in a significant reduction in the burden on both the industry and the staff by reducing the number of repetitive evaluations, without impacting the level of safety provided by the Order

POSSIBLE MODIFICATIONS TO ORDER EA-03-009

- Allow combinations of non-visual NDE (UT and surface examinations) to be used on a RPV head to obtain full coverage for the head
  - Order currently specifies UT <u>or</u> surface examinations of **each** VHP nozzle or weld
- Modify scope of bare metal visual examination for support structure interferences (outside of VHP nozzle area) - examine above and below support structure
- Refine scope of coverage for each VHP nozzle to some elevation above the bottom of the nozzle, or some established stress level
  - Limitations due to internal or external threads (for guide cones or funnels) and bottom end chamfers restrict access and usefulness of examination data - this was not anticipated prior to Order issuance
  - Possible modification would eliminate need to examine areas with low stress and limited crack growth potential

RECENT INDUSTRY PROPOSAL

- Reduce frequency of UT or eddy current examinations for high susceptibility plants with a prior CLEAN examination (no leaks or cracks)
  - Proposed during teleconference July 8 - licensee submittal August 17
  - Small number of affected plants (4-5?), beginning this fall
  - Basis would be deterministic and/or probabilistic
  - May be a generic approach or plant-specific
- Considerations
  - A high threshold for the acceptability of prior inspections - must be consistent with the inspection criteria of the Order with current state-of-the-art techniques
  - Are two clean Order inspections necessary?

OTHER CONSIDERATIONS

- Use of Bulletins and early inspections for emergent issues intended to establish prevalence of issue - avoid significant events
  - Role of continuing "permanent" ISI activities is to re-establish defense-in-depth considerations
  - Tech. Spec requirements for no pressure boundary leakage
  - GDC 14 - "extremely low probability of abnormal leakage"

- Cause for leakage from plugged thermocouple nozzle (Alloy 690 plug and 152 weld) at Oconee Unit 1

BULLETIN 2003-02: INFORMATION REQUEST

- RPV lower head penetration inspections performed to date and findings
- Description of inspection program during next and **SUBSEQUENT** refueling outages
- If unable to perform BMV inspection of each penetration during next refueling outage, describe inspections able to perform and actions to be taken to permit inspection of each penetration during subsequent refueling outages
- If do not intend to perform either BMV or volumetric exam, provide basis for concluding requirements are and will continue to be met

BULLETIN 2003-02 (continued)

- Within 30 days after plant restart following next lower head inspection, summary of the inspections performed, conditions found, and any actions taken
- Provide response within 30 days if entering refueling outage before end of 2003
- All other addressees, provide response within 90 days

660

LOCKHEED MARTIN

Stress Corrosion Crack Growth Rates (SCCGRs) for Alloy 182 and 82 Welds

Steven A. Attanasio, John V. Mullen, John W. Wuthrich,
Weldon W. Wilkening, and David S. Morton

Lockheed Martin Corporation
Schenectady, NY

Alloy 600 SCC Workshop
Gaithersburg, MD
September 2003

Outline

- Background
- Data Overview
- Description of Compliant Self-Loaded Compact Tension Specimens
- Context - EPRI Materials Reliability Program (MRP)
- Use of Average Crack Growth Rate and Maximum-to-Average Ratio
- Alloy 182 and Alloy 82 SCCGR Data
  - Comparison to data from other investigators
  - Comparison of the two alloys
  - Modeling approaches
- Aqueous Hydrogen Effects on SCC of Ni-base alloys, including Alloy 82

Background

- Both Alloys 182 and 82 are susceptible to primary water SCC
  - VC Summer hot leg (*http://www.nrc.gov/NRC/REACTOR/SUMMER/index.htm*)

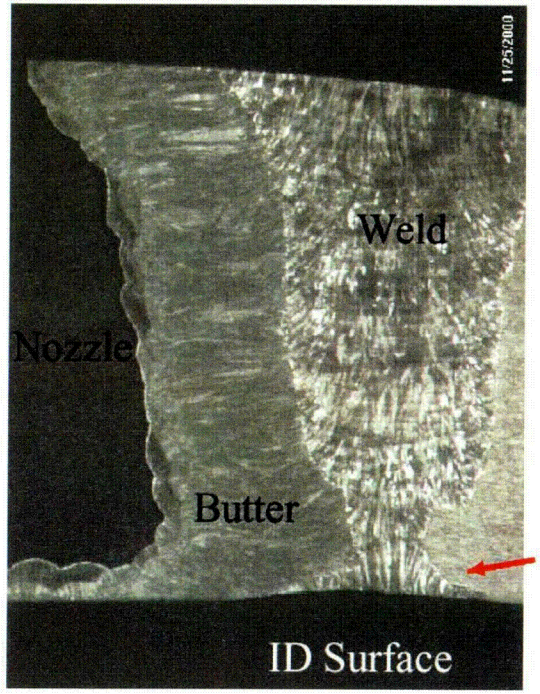

Weld repair

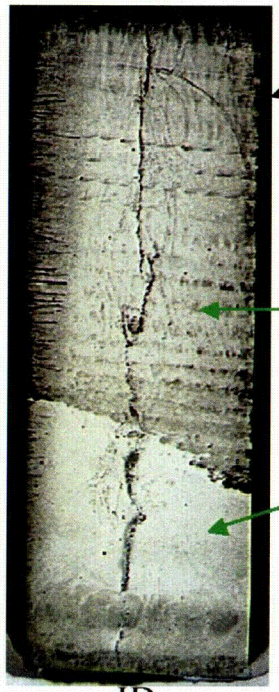

Cross-Section of Weld

Main Crack

Alloy 82

Alloy 182 butter

LOCKHEED MARTIN

C06

Data Overview

- SCCGR data - compact tension (CT) specimens (most side-grooved)
  - Active load, bolt load, compliant self-loaded (CSLCTs) - precracked
- Alloy 182 and 82 welds
  - Yield strengths of 454 to 530 (182) and 439 to 465 (82)
  - Carbon levels ~ 0.02 and 0.03 wt% (182) and ~ 0.045 wt% (82)
- High temperature hydrogenated water ($pH_T \sim 6.6$)
  - Single hydrogen concentration in each test (20, 30, 35, or 40 scc/kg)
- Single temperature tests - 316 to 360°C
- Average K_I of 33 to 46 MPa√m (182) and 23 to 55 MPa√m (82)
- All T-S Orientation (growth from root to crown; parallel to dendrites)
- 11 Alloy 182 data points - 2 heats
- 20 Alloy 82 data points - 3 heats
  - Subjected to screening criteria similar to that used by EPRI-MRP group

LOCKHEED MARTIN

Compliant Self-Loaded Compact Tension Specimens

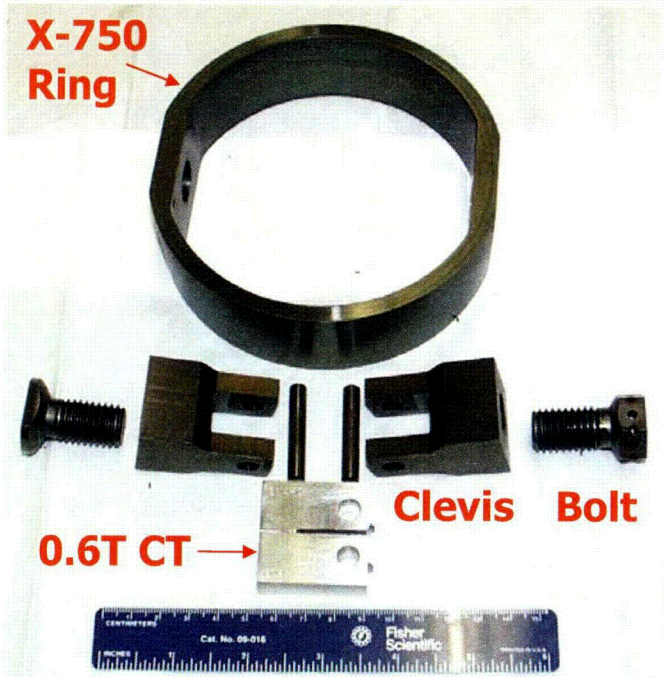

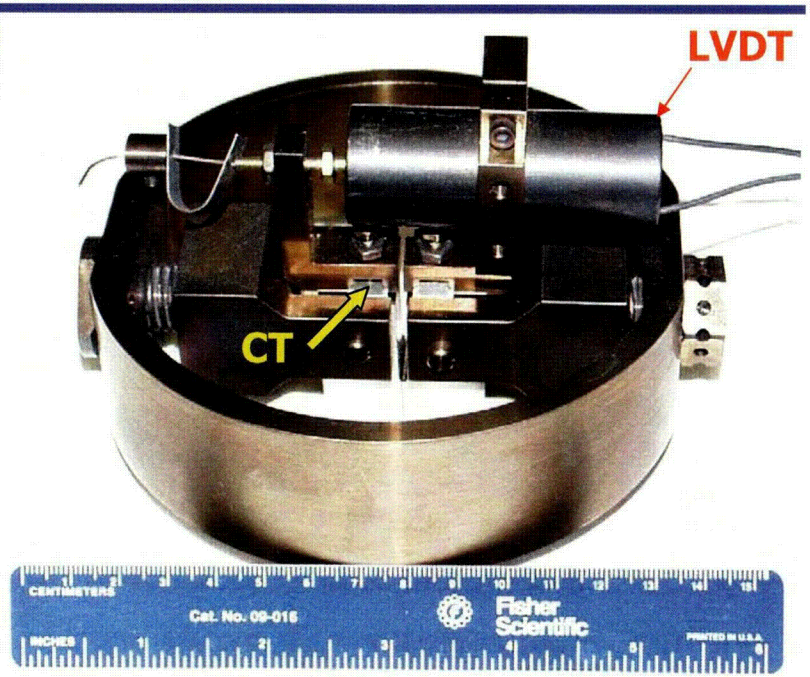

Loading Method:

- Compress ring using Instron machine, rotate bolt to apply 'setup' load to CT specimen
- Release Instron load slowly - CT specimen is loaded as ring expands
- Exact load is determined *via* measurement of ring spring constant and ring displacement
- Account for modulus changes due to heatup by increasing room temperature load

LOCKHEED MARTIN

C07

CSLCT Specimen Qualification

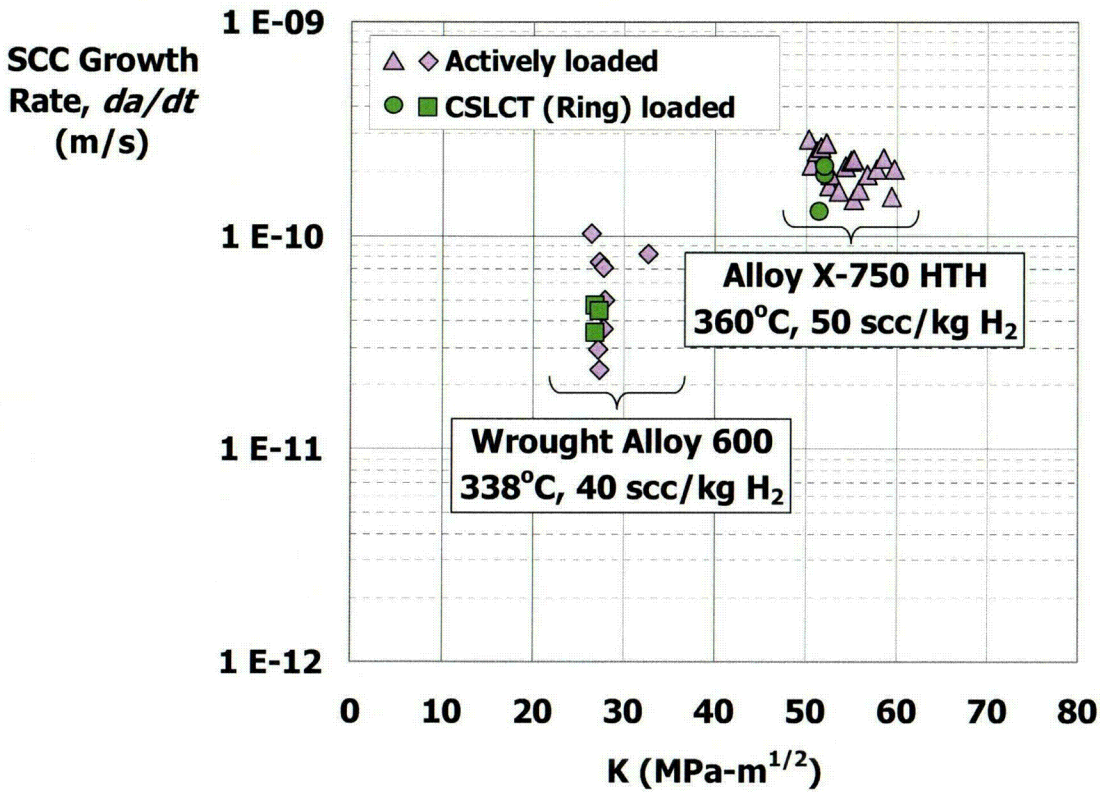

- Due to the compliance of the ring, load relaxation is minimal - even as SCC crack grows
- Can test up to 10 CSLCTs in a single 60 liter flowing autoclave (with LVDTs) - efficient

LOCKHEED MARTIN

C08

Specimen Fabrication

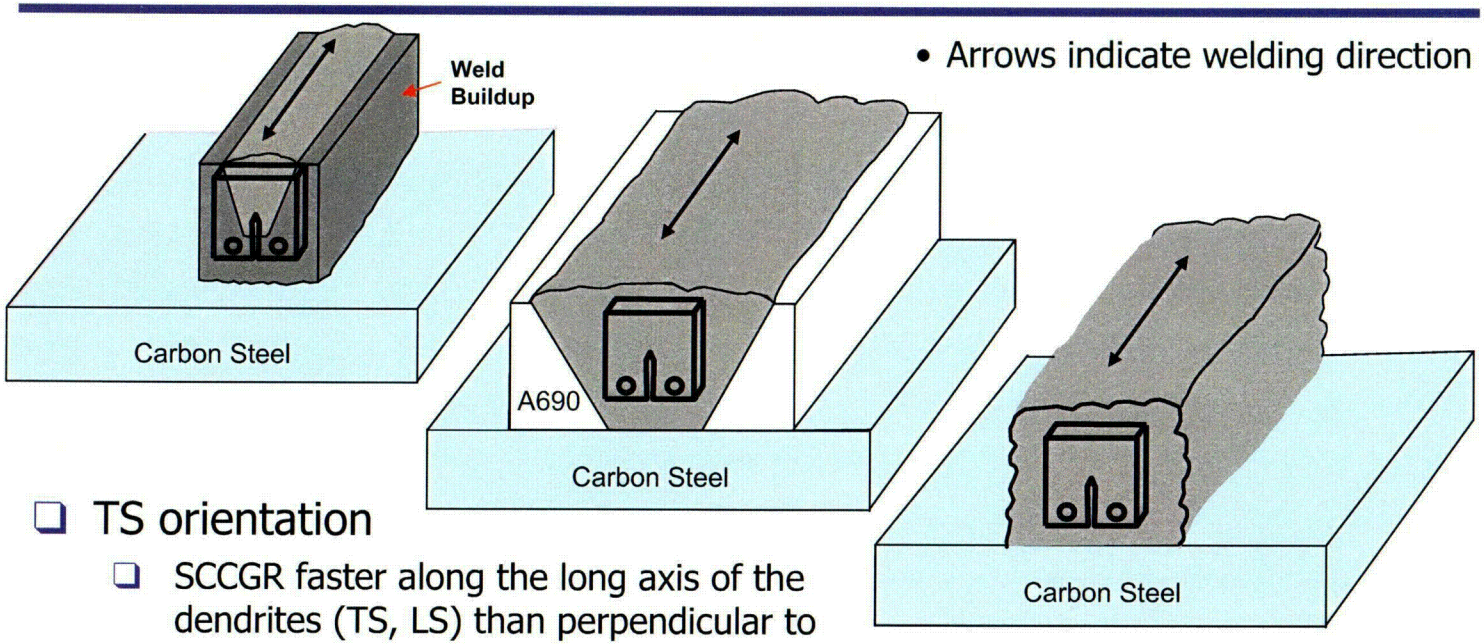

- Arrows indicate welding direction

- TS orientation
  - SCCGR faster along the long axis of the dendrites (TS, LS) than perpendicular to dendrites (e.g., TL)
    - Proven by Bamford *et al.* and others
- Weld process:
  - 182: Manual shielded metal arc welding
  - 82: Automatic gas tungsten arc welding

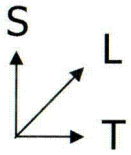

LOCKHEED MARTIN

C09

EPRI Materials Reliability Program (MRP) Work

- MRP: Develop a SCCGR Model for Alloy 182 and 82 Weld Metals
  - Similar to the work performed for Wrought Alloy 600
- EPRI MRP-55 - Wrought Alloy 600 SCCGR Model (2002)
  - View/analyze present weld data *in part* using methods from MRP-55
  - Scott model - uses threshold K_I of 9 MPa√m
  - Thermal activation energy (Q_{SCCGR}) = 130 kJ/mole (31 kcal/mole)

$$\frac{da}{dt} = \alpha \cdot (K_I - 9)^{1.16} \cdot exp\left[-\frac{130{,}000}{8.314}\left(\frac{1}{T} - \frac{1}{598.15}\right)\right]$$

(*da/dt* in m/s, K_I in MPa√m, *T* in Kelvin)

  - Each heat described by its value of α
  - Data from different temperatures normalized to 325°C
    - Le Hong *et al.* - Alloy 182 Q_{SCCGR} is ~ 130 kJ/mole (EDF, ETH, CEA data)
    - Mills and Brown - Alloy 82 Q_{SCCGR} = 130 to 150 kJ/mole (31-35 kcal/mole)
      - In the present work, Alloy 82 and 182 data normalized using 130 kJ/mole

Data Screening Criteria

- Single condition test
- ASTM E647 Size Criteria (flow strength at temperature)
- Minimum average crack extension = 0.2 mm
- Data based on post-test destructive examination (DE)
- Periodic unload-reload only if hold time > 60 minutes
- Careful autoclave chemistry control (including H_2)
- Minimum 'engagement' of fatigue precrack = 50%
  - Quantifies the percentage of precrack length with SCC
- All Lockheed Martin (LM) SCCGR data herein pass these screening criteria

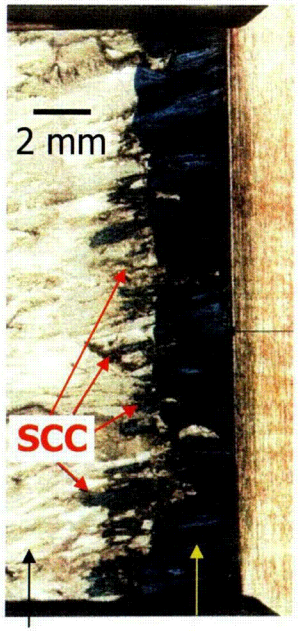

- LM Data reported as $SCCGR_{ave}$, rather than as $SCCGR_{max}$
  - Also report maximum-to-average SCC extension ratio (RATIO)
  - RATIO used by Lockheed Martin (LM) and by Mills (Bechtel)

LOCKHEED MARTIN

C10

Max./Ave. Ratio Decreases as the Crack Grows

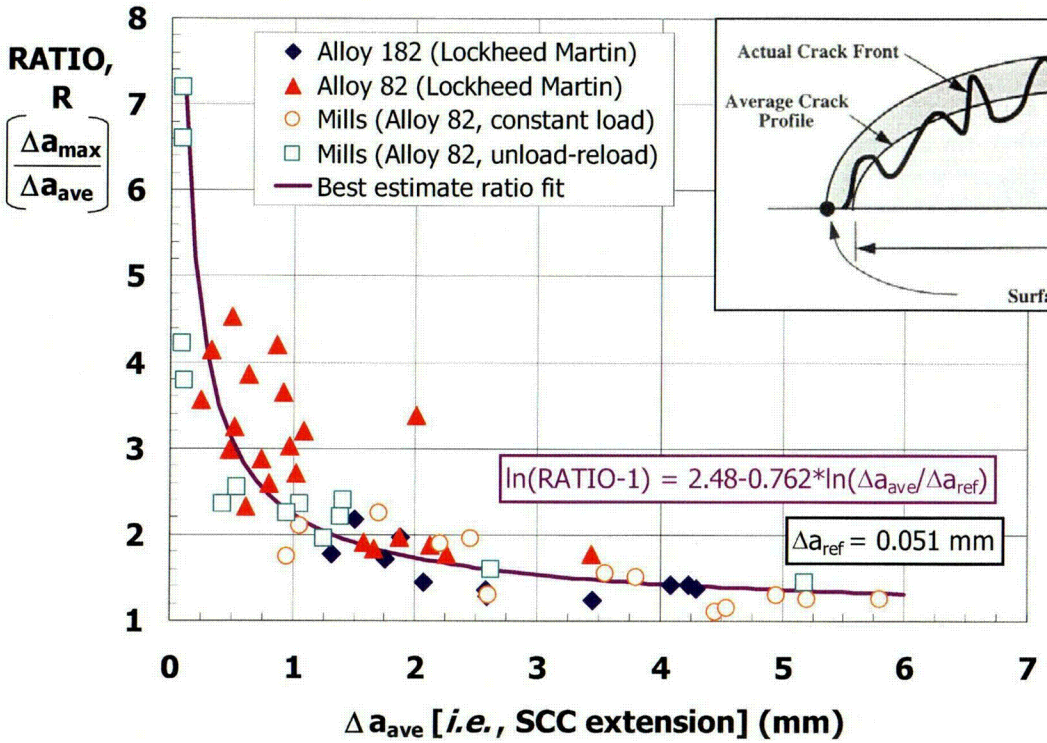

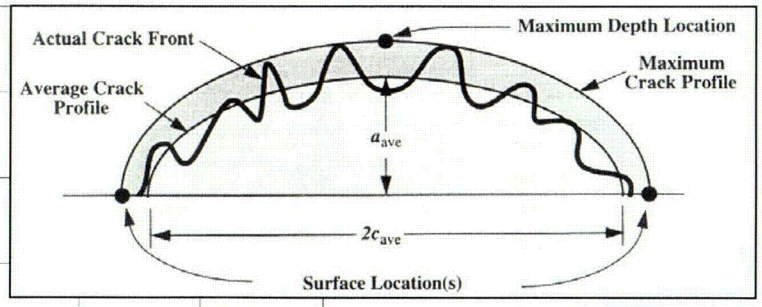

- Crack fronts often uneven
- Cracking initially occurs as discrete 'fingers', then becomes more uniform

- To broaden the ratio data set, some data were used that do not pass the screening criteria
- LM: Δa_{max} is maximum SCC depth at any location along the crack front
- Mills: Δa_{max} is maximum SCC depth at the DE measurement locations (ASTM E813)

LOCKHEED MARTIN

C11

Maximum SCCGR Depends on Test Duration

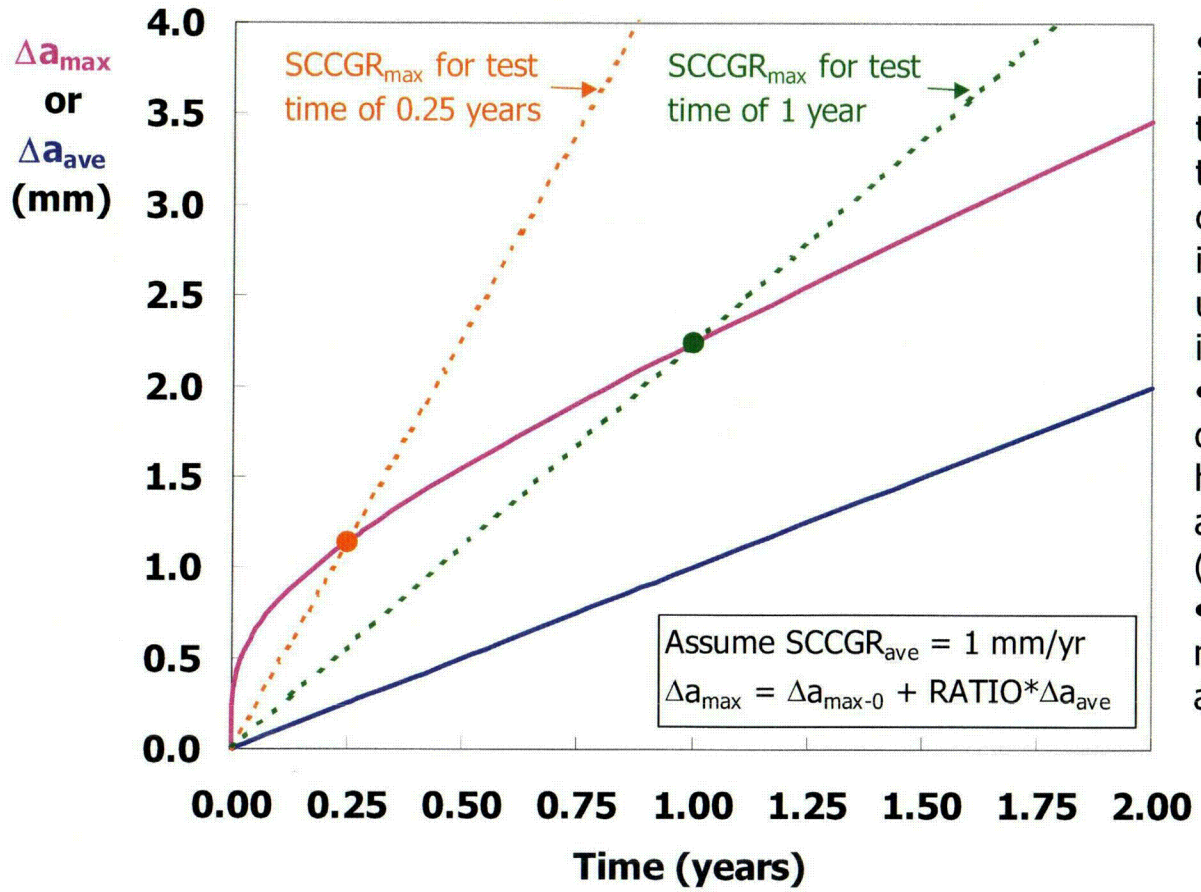

- Assumes no incubation time, or that the data are corrected for incubation time using *in-situ* instrumentation
- All SCCGR data reported herein are average rates ($SCCGR_{ave}$)
- Also report the maximum-to-average ratio

LOCKHEED MARTIN

C12

Use RATIO to Infer % Engagement

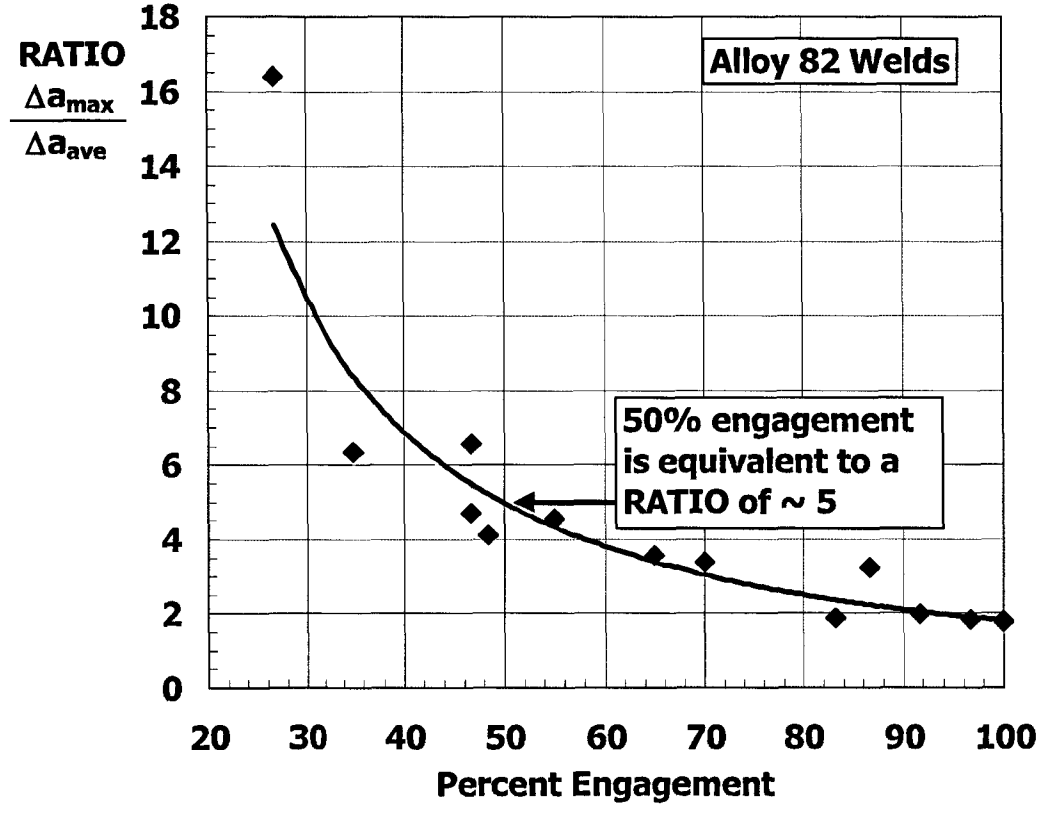

- Some of the data shown in this plot did not meet the screening criteria

LOCKHEED MARTIN

Use SCC Extent to Infer % Engagement

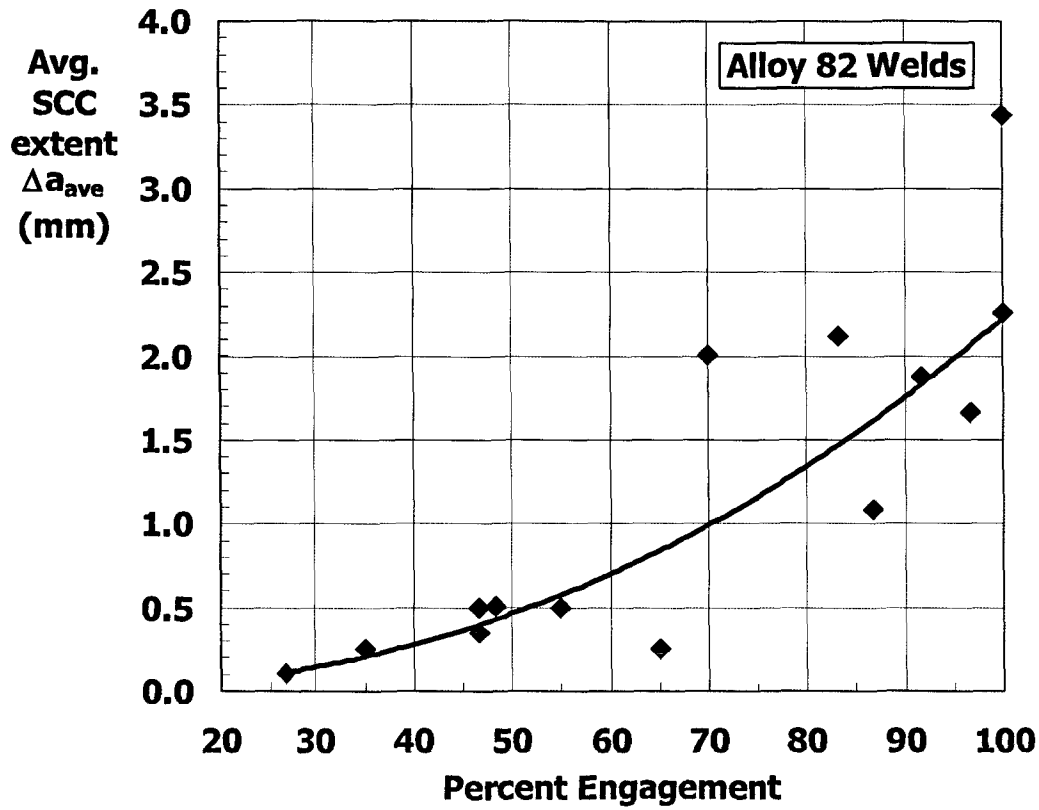

- Some of the data shown in this plot did not meet the screening criteria

LOCKHEED MARTIN

Alloy 182 SCCGRs and Comparison to Other Data

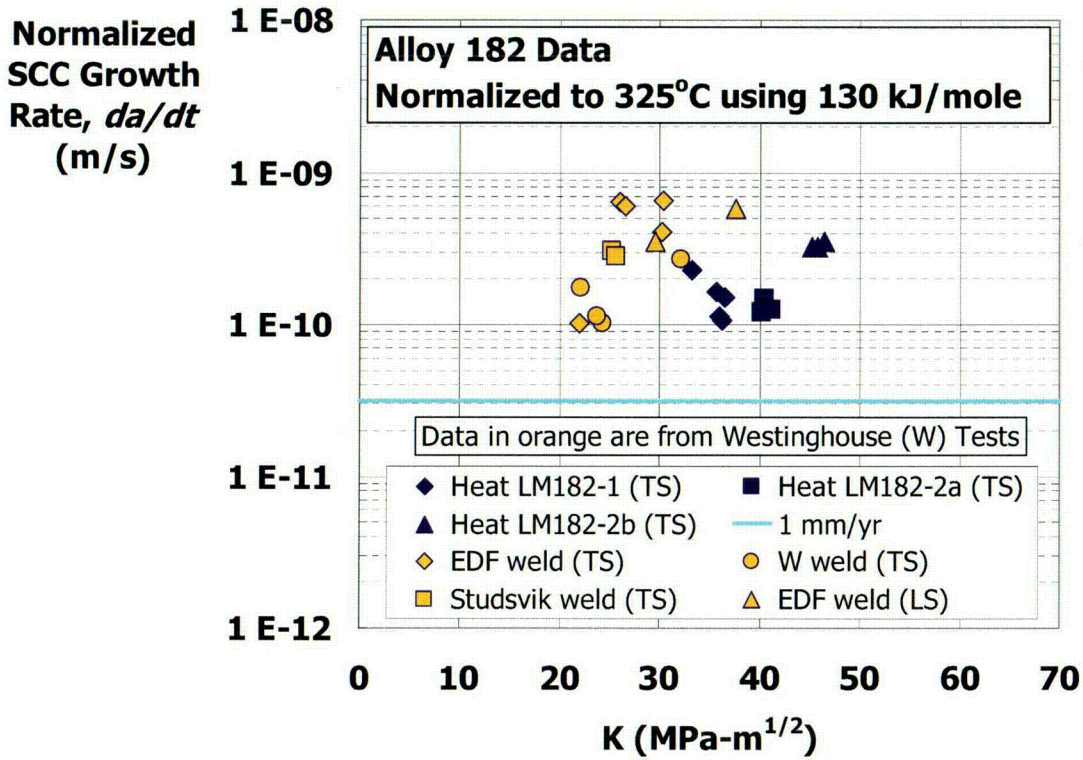

- 3 Westinghouse data points screened due to $\Delta a_{ave} < 0.2$ mm
- LM refers to Lockheed Martin

- Compare to published data where *average* SCCGR was reported (fairest comparison)
- Westinghouse data - 3 welds (W, EDF, Studsvik); carbon 0.025 to 0.053 wt%
- All root-to-crown growth; LM - 35 or 40 scc/kg H_2, Westinghouse (W) - 25 scc/kg H_2

LOCKHEED MARTIN

C13

Alloy 82 SCCGRs and Comparison to Other Data

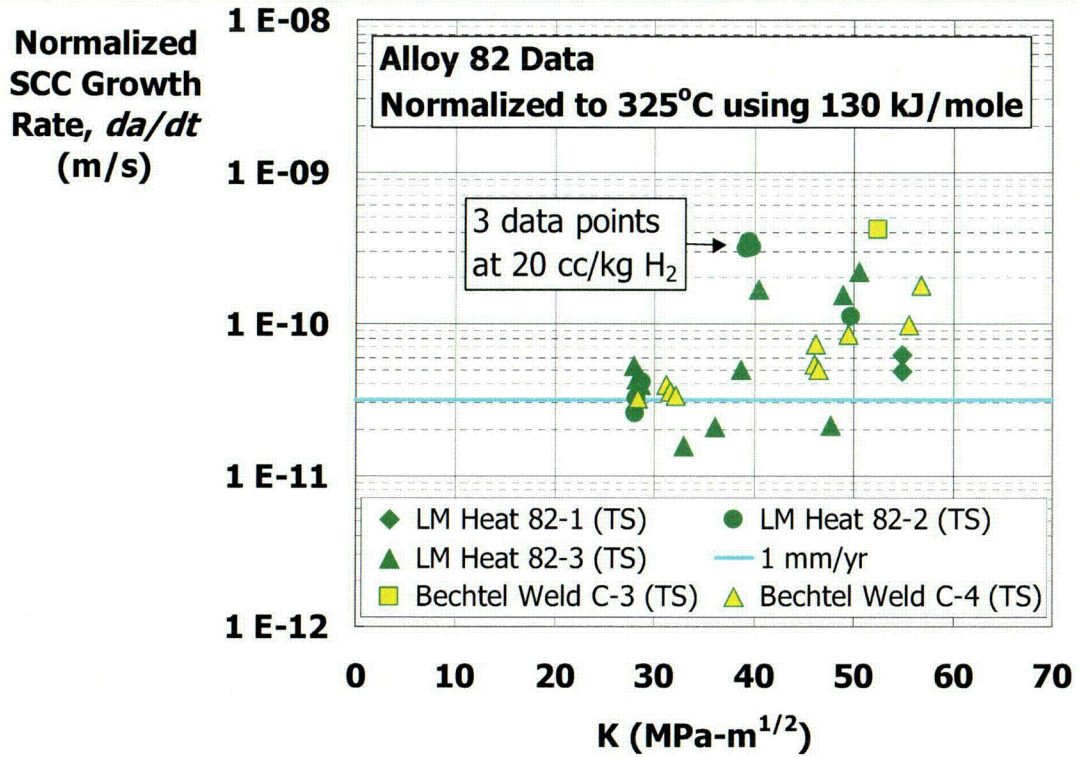

- Compare to published data where *average* SCCGR was reported (fairest comparison)
- All root-to-crown growth; LM data 20 or 40 scc/kg H_2; Bechtel data 40 to 60 scc/kg H_2
- Some of the variability in heat LM82-2 caused by H_2 (highest SCCGRs at 20 scc/kg H_2)

LOCKHEED MARTIN

C14

Comparison of Alloy 182 and Alloy 82 - SCCGRs

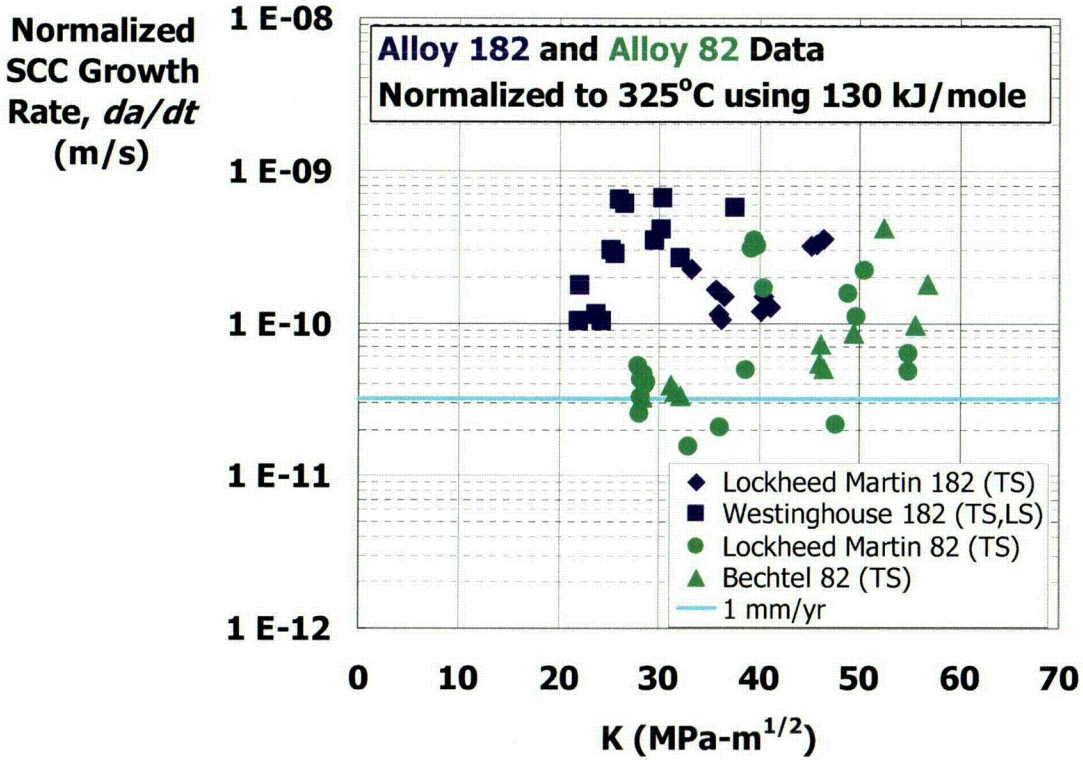

- Alloy 182 SCCGRs are faster on average (~15 *vs.* 20 %Cr, weld process, carbon levels)
  - May be appropriate to model 182 and 82 using an offset
- Insufficient data to identify and/or quantify an SCCGR threshold

LOCKHEED MARTIN

C15

Empirical Modeling - Evaluate Three Model Forms

- All three forms are exponential in temperature, power law in K_I
- Use data from both 182 and 82 to determine K_I, 1/T dependencies
  - Not enough data to determine independently (most of 182 data at ~ 325°C)
  - Treat with an offset since the two weld metals appear to have different rates
- General model form:

$$\frac{da}{dt} = A \cdot B_{material} \cdot \left(\frac{K_I - K_{th}}{K_o} \right)^{\beta} \cdot exp\left[-\frac{Q}{R \cdot T} \right]$$

- Model 1: $K_{th} = 0$
- Model 2: $K_{th} = 9$
- Model 3: $K_{th} = 9$, β fixed at 1.16 (Scott form)
  - K_o is a normalizing value (1 MPa√m)

LOCKHEED MARTIN

Model 1: No Threshold, K Dependence not Fixed

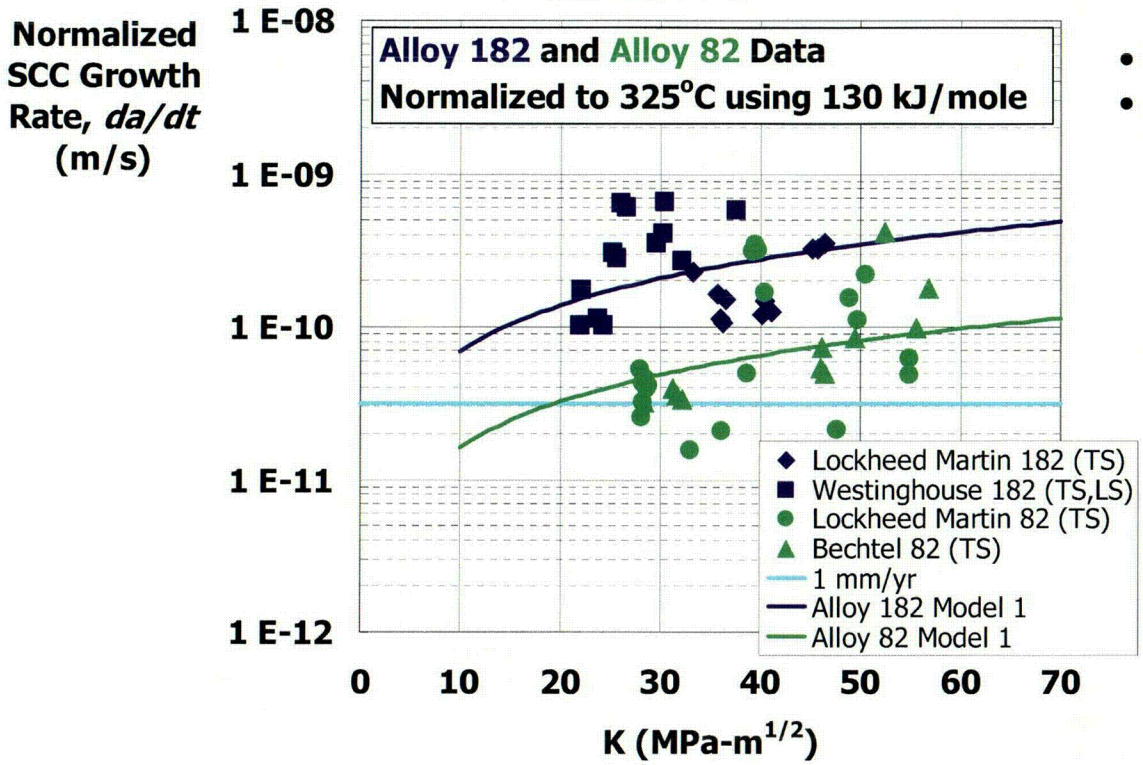

- $R^2 = 0.550$
- Std. Dev. = 0.760

$$\frac{da}{dt} = 14.76 \cdot \left\langle \begin{matrix} 4.272 & 182 \\ 1.000 & 82 \end{matrix} \right\rangle \cdot \left(\frac{K_I}{1} \right)^{0.999} \cdot exp\left[-\frac{148{,}300}{8.314 \cdot T} \right]$$

LOCKHEED MARTIN

C16

Model 2: Threshold (K_{th} = 9), K Dependence not Fixed

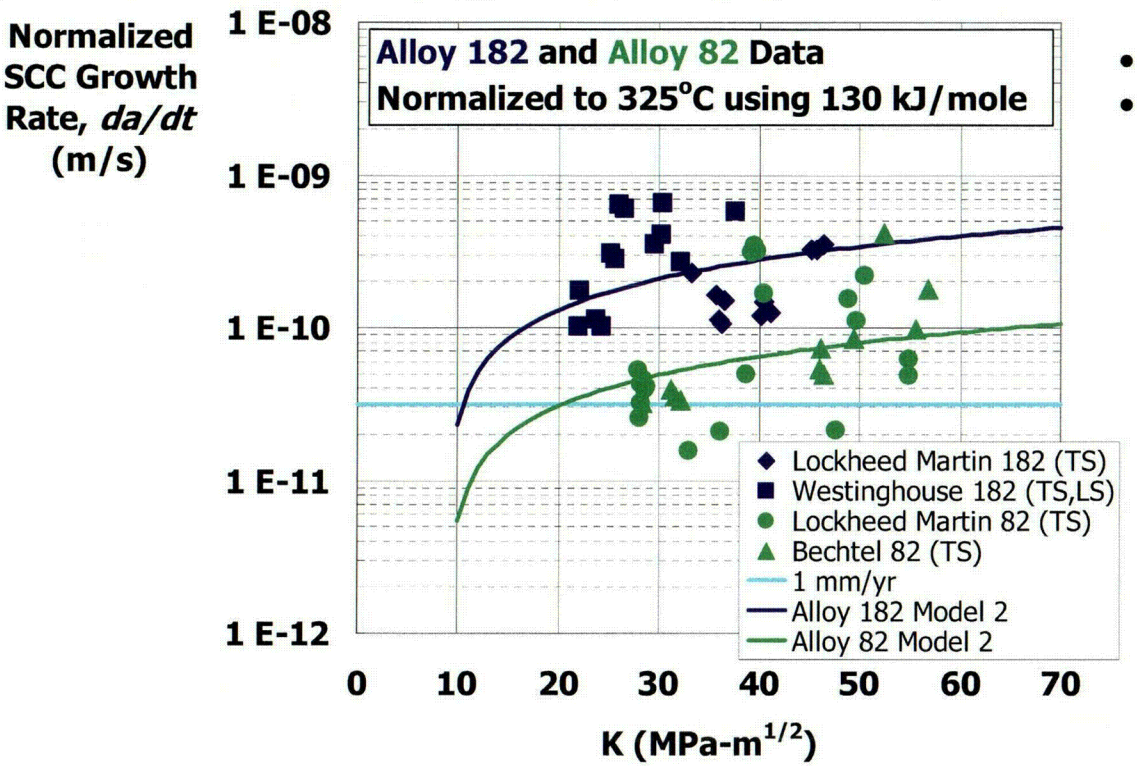

- R^2 = 0.549
- Std. Dev. = 0.760

$$\frac{da}{dt} = 71.24 \cdot \left\langle \begin{matrix} 4.267 \\ 1.000 \end{matrix} \middle| \begin{matrix} 182 \\ 82 \end{matrix} \right\rangle \cdot \left(\frac{K_I - 9}{1} \right)^{0.723} \cdot exp\left[-\frac{150{,}200}{8.314 \cdot T} \right]$$

LOCKHEED MARTIN

C17

Model 3: Threshold (K_{th} = 9), K Dependence = 1.16

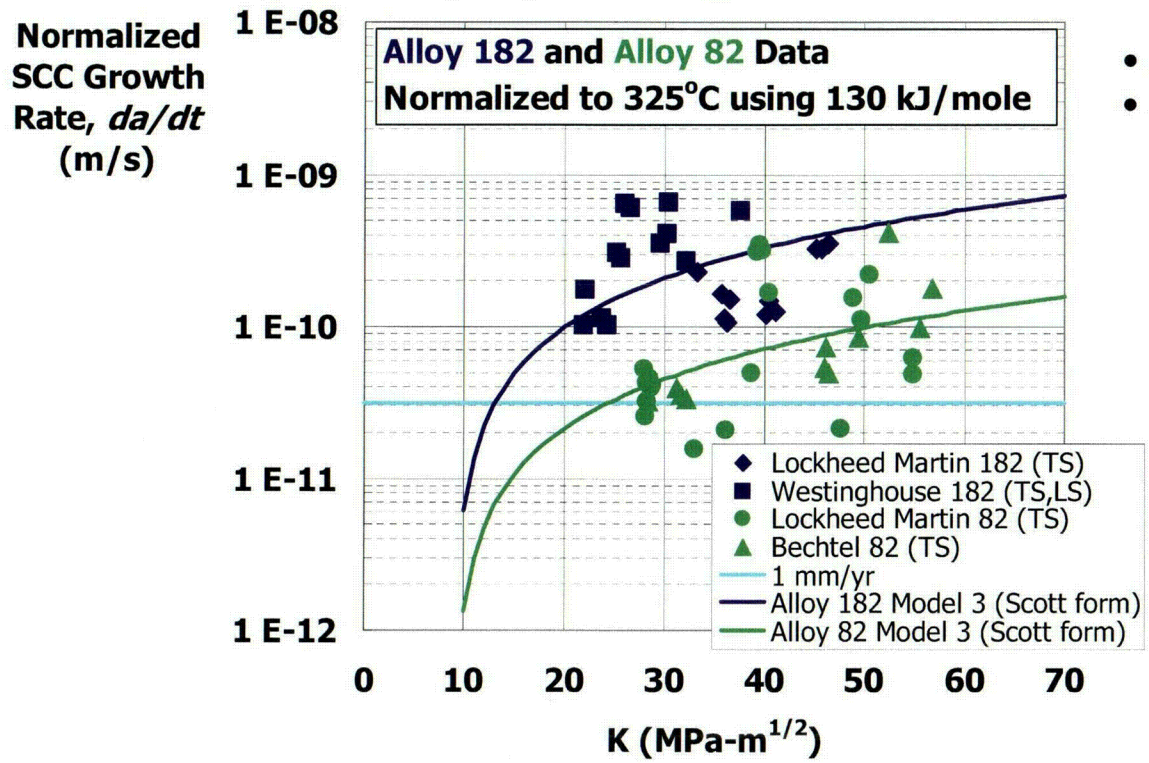

- R^2 = 0.520
- Std. Dev. = 0.764

$$\frac{da}{dt} = 5.028 \cdot \left\langle \begin{matrix} 4.618 \\ 1.000 \end{matrix} \middle| \begin{matrix} 182 \\ 82 \end{matrix} \right\rangle \cdot \left(\frac{K_I - 9}{1} \right)^{1.16} \cdot exp\left[-\frac{127{,}900}{8.314 \cdot T} \right]$$

LOCKHEED MARTIN

680

C18

Comparison of Models 1, 2, and 3

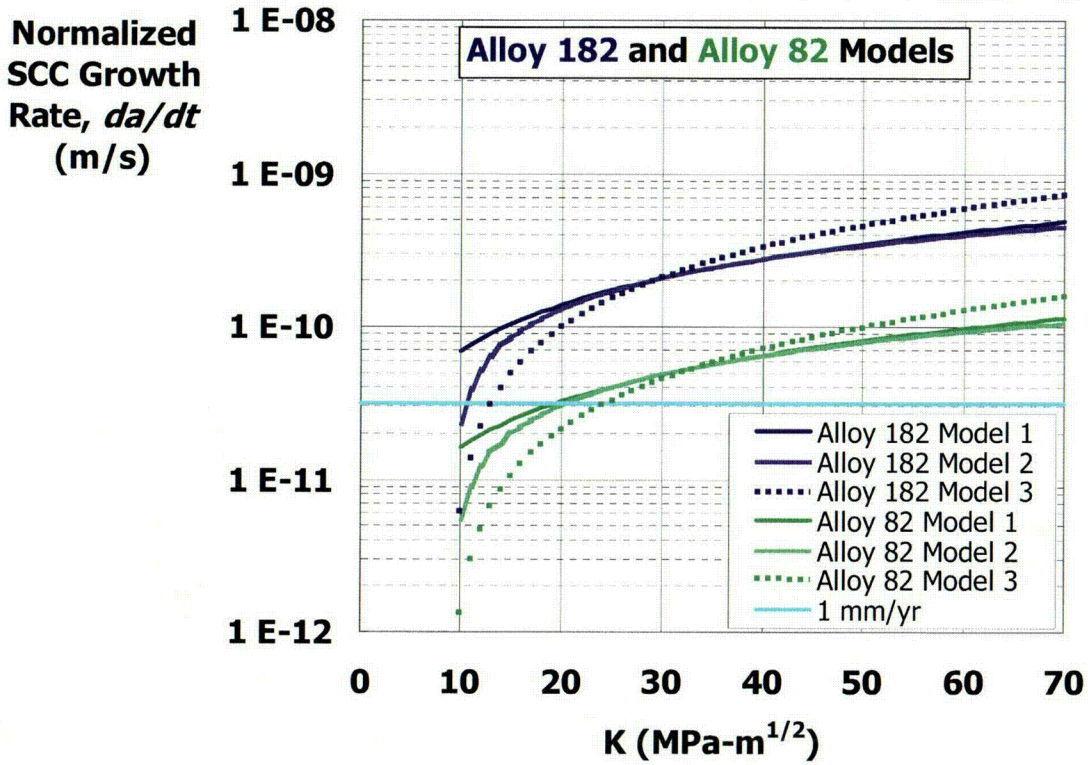

- Models 1 & 2 very similar for $K_I \geq 20$ MPa√m (important region for flaw disposition)
- Model 3 (Scott form) within ≤ 1.5X of other models for 20 MPa√m ≤ K_I ≤ 70 MPa√m

LOCKHEED MARTIN

C19

Model Summary

- Models 1 and 2 provide a viable approach for correlating the data
  - Model 3 is also reasonable
- Q_{SCCGR} values are 128 to 150 kJ/mol
- K dependencies are ~ 0.7 to 1.0 (when not forced to 1.16)
  - Somewhat lower than Scott model, but not very different than 1.16
  - K dependence of Alloy 182 may be lower than that of Alloy 82
    - EDF/ETH/CEA $SCCGR_{max}$ data for Alloy 182 suggest a low K-dependence ($K^{0.1}$)
- Weld variability is an issue for all three models (R^2 values ~ 0.55)
  - Attempted to collapse the data using a K-1/T interaction:

$$\frac{da}{dt} = A \cdot B_{material} \cdot \left(\frac{K_I - K_{th}}{K_o}\right)^{\beta} \cdot exp\left[-\frac{Q}{R \cdot T}\right] \cdot exp\left[\frac{C \cdot ((K - K_{th})/K_o)}{R \cdot T}\right]$$

    - No measureable improvement in either R^2 or standard deviation
    - Not the only possible equation form to describe K-1/T interactions
  - Normalizing the data for aqueous hydrogen may help reduce scatter

Effect of Aqueous H_2 Concentration - Prior Work

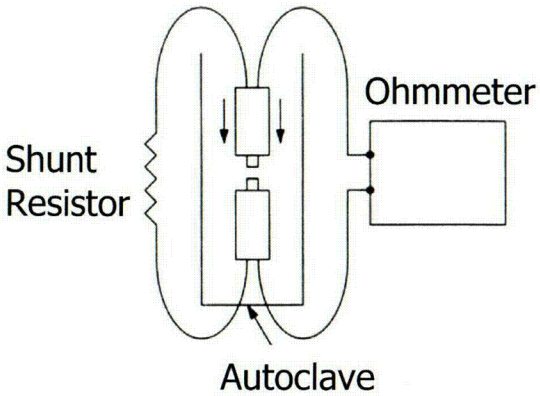

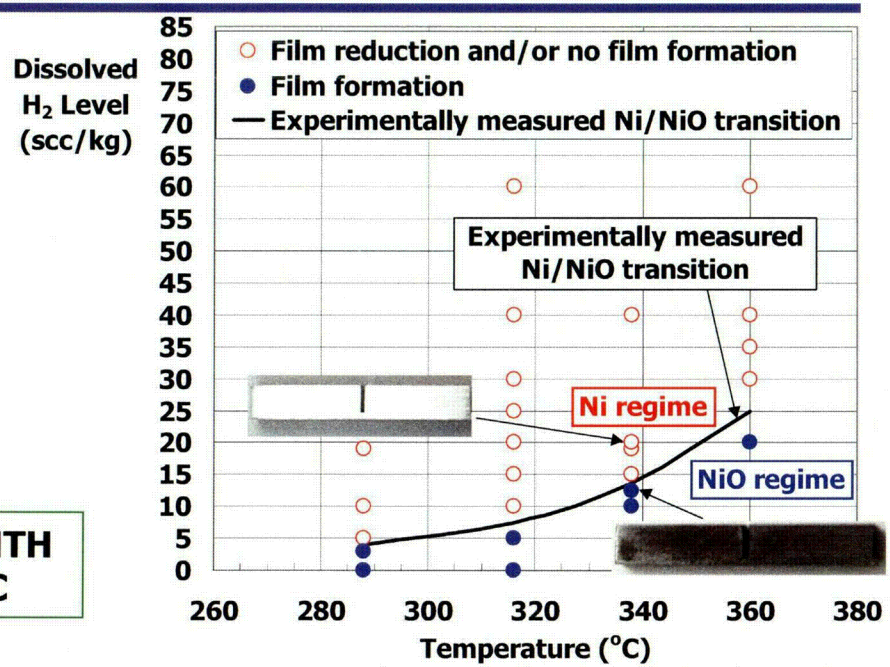

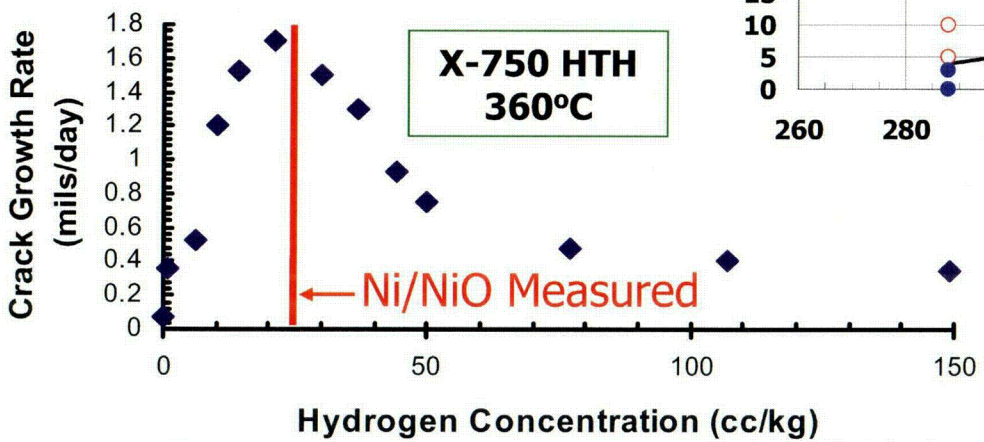

- Similar behavior noted for A600, X-750 AH (Morton, Attanasio)
- Also studied by Scott, Cassagne, Economy, Totsuka, Andresen, *etc.*

Effect of Aqueous H_2 Concentration - Prior Work

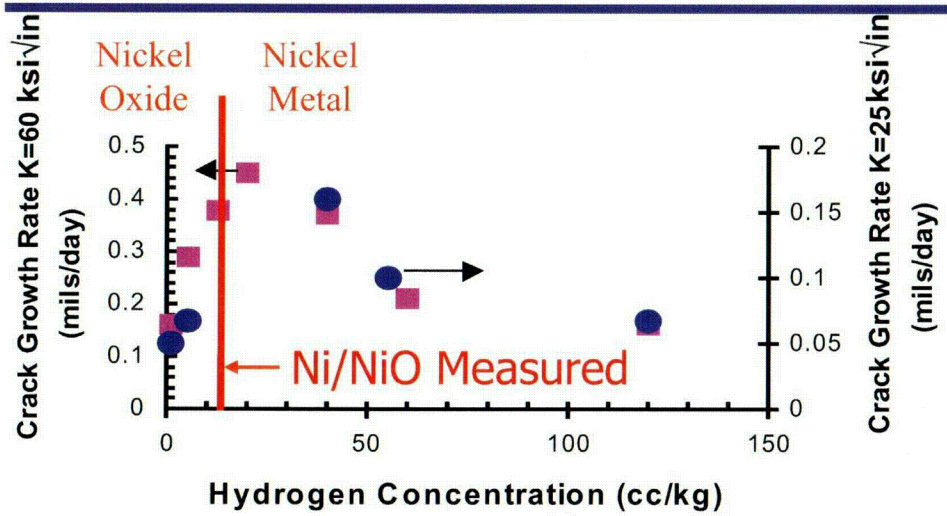

Wrought Alloy 600
K=66 & 27 MPa√m
(K=60 & 25 ksi√in)
338°C

- Correlations for H_2 effects on SCCGR have been presented for A600, X-750 AH, X-750 AH (Morton)
  - Use EcP *vs.* $EcP_{Ni/NiO}$ as correlating parameter
  - Measure EcP via Pt or YSZ/Fe-Fe_3O_4 electrode

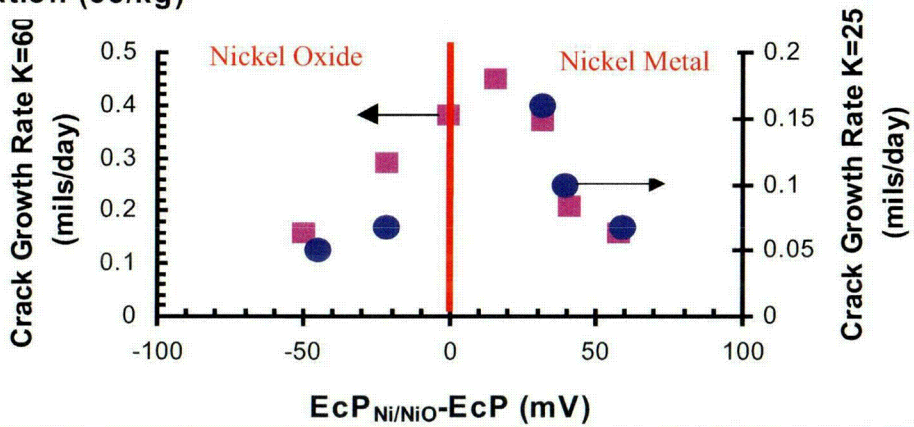

LOCKHEED MARTIN

C21

Effect of Aqueous H_2 Concentration - Alloy 82

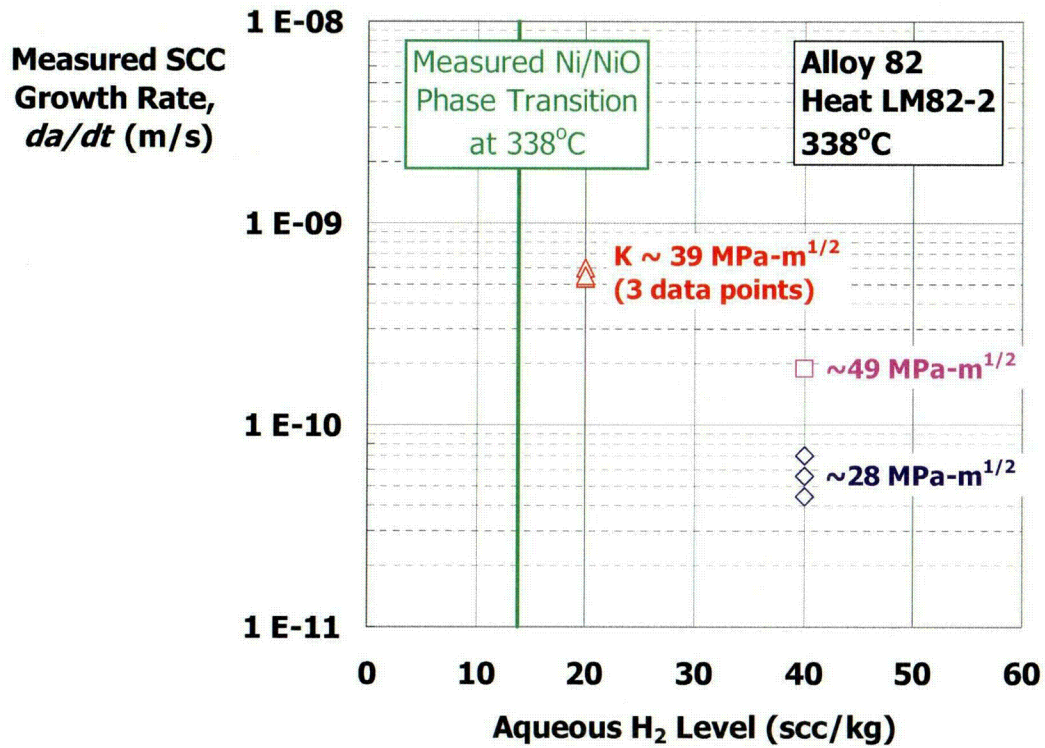

- SCCGRs increase as measured Ni/NiO phase transition is approached
- 20 cc/kg H_2 specimens are bolt loaded - H_2 effect confirmed using active load specimens
- Developing a weld metal correlation so that data can be normalized for H_2 effects

LOCKHEED MARTIN

C22

Conclusions

- Ring-loaded specimens can generate efficient, viable SCCGR data
- Crack shape evolution well-described by the maximum/average ratio
- SCCGR data can be reasonably reported using $SCCGR_{ave}$ + RATIO
- LM data are consistent with $SCCGR_{ave}$ data from other researchers
- Three empirical model forms were evaluated - all seem reasonable
  - Data scatter leads to an appreciable standard deviation in all 3 cases
- Aqueous H_2 level influences SCCGR - more quantification is desirable

Acknowledgements

- Maureen Schurman, Brian Gain, John Schisano
- Norm Perazzo Kerry Cotterell, Bruce Furbeck (CSLCT specimens)
- Bill Mills (Bechtel)
- Glenn White (DEI) and John Hickling (EPRI)

References

- G White, EPRI Report MRP-55, August 12, 2002.
- N Totsuka, S Sakai, N Nakajima and J Mitsuda, CORROSION/2000.
- PM Scott, Research Topical Symposium at CORROSION/96, 1996.
- DS Morton, SA Attanasio and MA Ando, 10th Environmental Degradation Conference, August 2001.
- WJ Mills and CM Brown, Bechtel report B-T-3435, March 2002.
- S Le Hong, JM Boursier, C Amzallag and J Daret, 10th Environmental Degradation Conference, August 2001.
- G Economy, RJ Jacko and FW Pement, *Corrosion*, 43, 1987.
- T Cassagne, B Fleury, F Vaillant, O de Bouvier & P Combrade, 8th Environmental Degradation Conference, August 1997.
- W Bamford and J Foster, EPRI Report MRP-21, June 2000.
- SA Attanasio, DS Morton, MA Ando, NF Panayotou & CD Thompson, 10th Environmental Degradation Conference, August 2001.

Appendix - Measured SCCGR Data (Not Normalized)

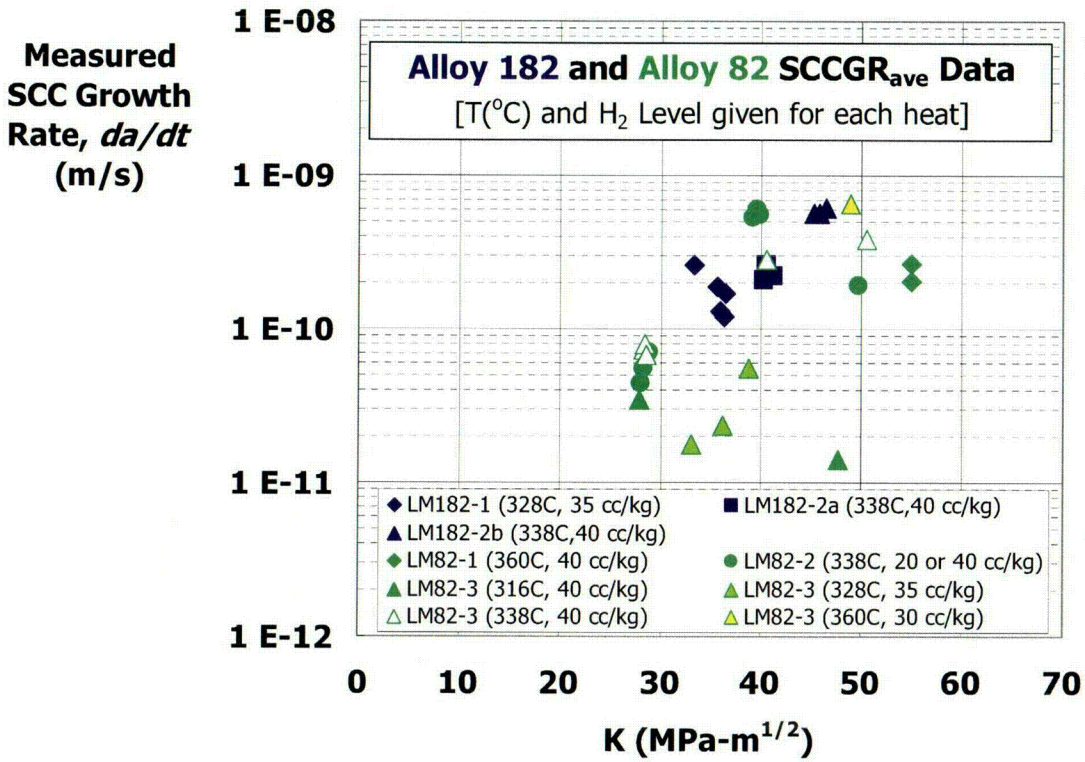

- TS orientation (all data)
- K is reported as the average K value during a test
- No unload-reload cycles
- LM (Lockheed Martin) heats 182-2a and -2b have a different yield strength (YS)
  - 454 and 530 MPa, respectively - due to differences in processing
- Room temperature YS for other heats:
  - 182-1: 503 MPa
  - 82-1: 439 MPa
  - 82-2: 465 MPa
  - 82-3: 460 MPa

LOCKHEED MARTIN

C23

Appendix - Compare LM Data to Screening Criteria

- All data conform to the following:
  - Single condition tests
  - Data based on post-test destructive examination
  - Careful autoclave chemistry control
  - No periodic unload-reload
- ASTM E647 Specimen Size Criteria
  - 4 data points rejected
- Reject if percent engagement is <50% or if SCC extent < 0.2 mm
  - 14 data points rejected
- Focus on the data that pass the screening criteria

Appendix - Material Composition

Heat	Ni	Cr	Fe	C	Mn	Cu	Si	Co	S	P	Ti	Nb +Ta
LM182-1	Bal	15.0	7.2	0.03	5.9	0.00	0.7	0.03	0.005	N/A	0.5	2.0
LM182-2	68.7	15.1	7.0	0.02	6.0	0.00	0.8	0.03	0.005	0.01	0.5	1.9
LM82-1	73.4	17.5	1.7	0.047	3.14	0.05	0.26	0.04	0.005	N/A	0.17	3.64
LM82-2	73.5	19.0	1.46	0.045	2.80	0.05	0.12	0.04	0.001	0.013	0.30	2.32
LM82-3	71.5	20.6	1.27	0.045	2.81	0.31	0.14	0.04	0.002	0.012	0.35	2.44

Influence of temperature on Primary Water Stress Corrosion Cracking of Alloy 600 Weld Metals

Yoshito Nishikawa, Nobuo Totsuka and Koji Arioka

Institute of Nuclear Safety System, Inc.

Background

- PWSCC were found in Alloy 182 in PWR nuclear power plants.
- There are some studies on Alloys 82 and 182. But a few studies about influence of temperature and susceptibility of heat affected zone (HAZ).

Purpose

- To clarify the difference of the susceptibility on PWSCC between Alloys 82 and 132 (modified metal of 182).
- To clarify the difference of the susceptibility on PWSCC between weld metal and HAZ.

Chemical Compositions and Mechanical Properties of Weld Metals and Base Metal

Composition (wt%)	C	Si	Mn	P	S	Ni	Cr	Fe	Cu	Nb
82	0.017	0.26	2.54	0.006	0.001	72.9	17.95	3.72	0.01	1.93
132	0.030	0.30	2.10	0.009	0.002	71.5	15.40	8.50	0.01	1.88
600 (Base Metal)	0.030	0.27	0.29	0.010	0.001	72.9	16.20	-	0.05	-
182	≤ 0.10	≤ 1.0	5.0~ 9.5	≤ 0.03	≤ 0.015	≥ 59.0	13.0~ 17.0	≤ 10.0	≤ 0.50	1.0~ 2.5

Mechanical Properties	0.2% YS (N/mm^2)	TS (N/mm^2)	Elongation Rate (%)	Contraction of Area (%)
82	306	625	26.6	20.2
132	291	625	27.3	26.6
600	287	675	43.3	31.8

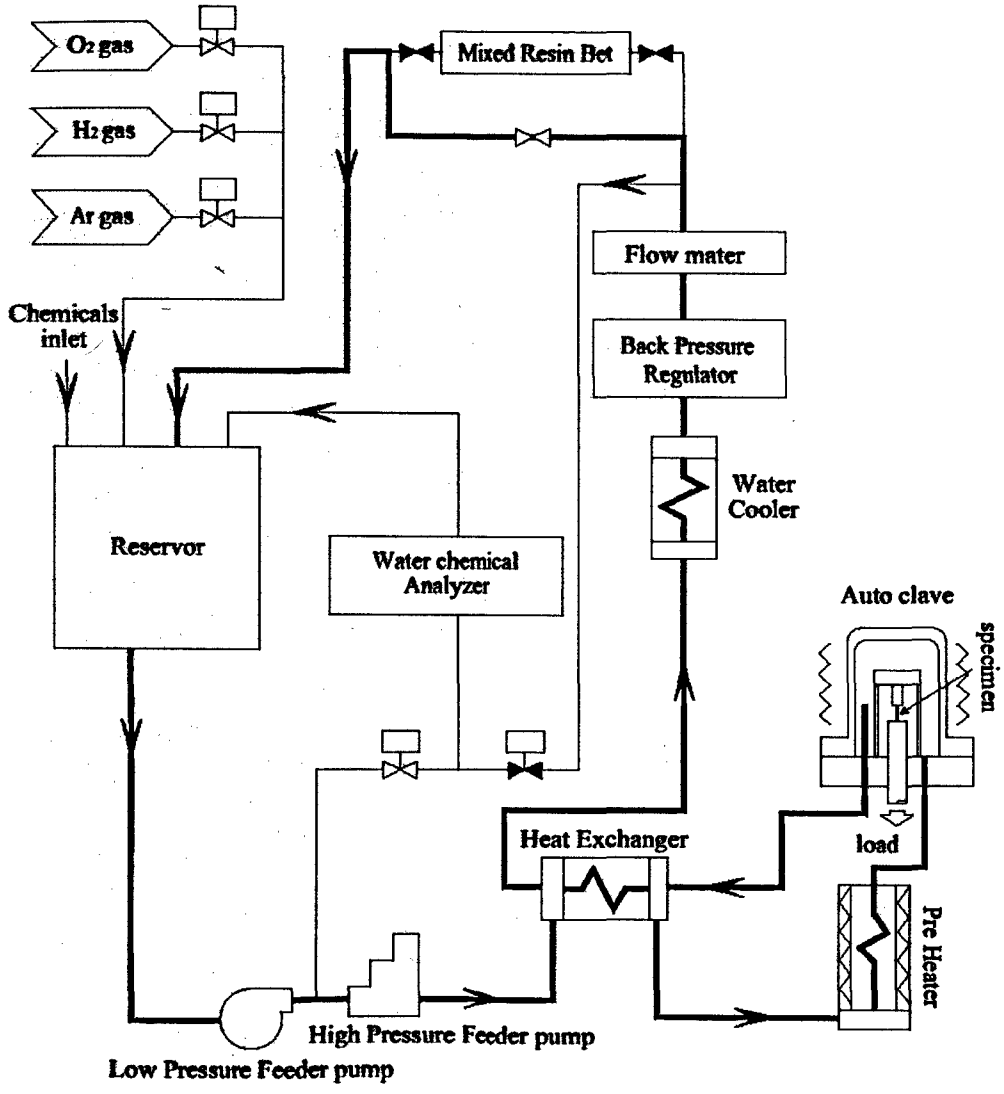

Solution
500 ppm B
2 ppm Li
2.75 ppm H_2

Temperature
360 ~ 330 °C

Strain Rate
5×10^{-7} /s
as 20 mm gauge length

Test System and Environment

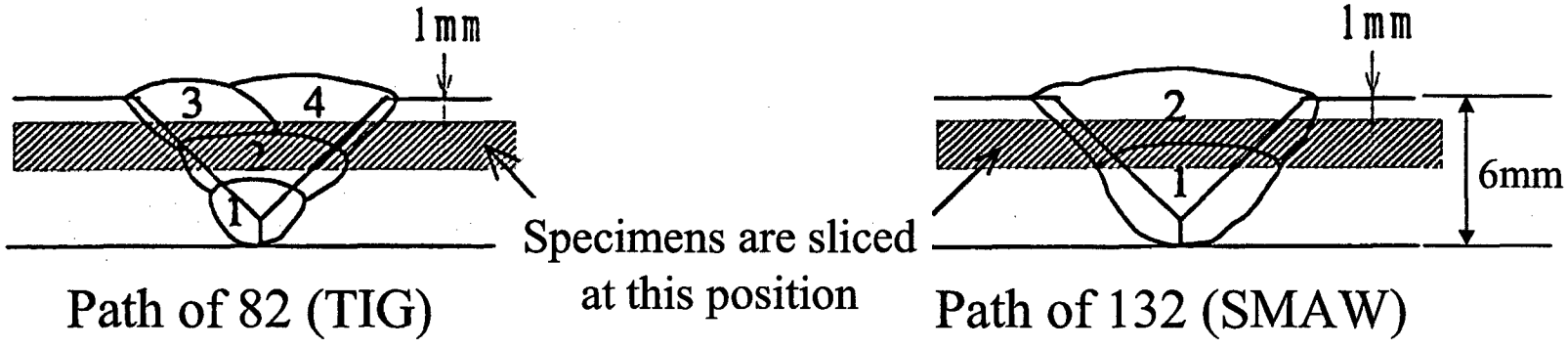

Welding heat

about 10 kJ/cm (both TIG and SMAW)

Welding conditions

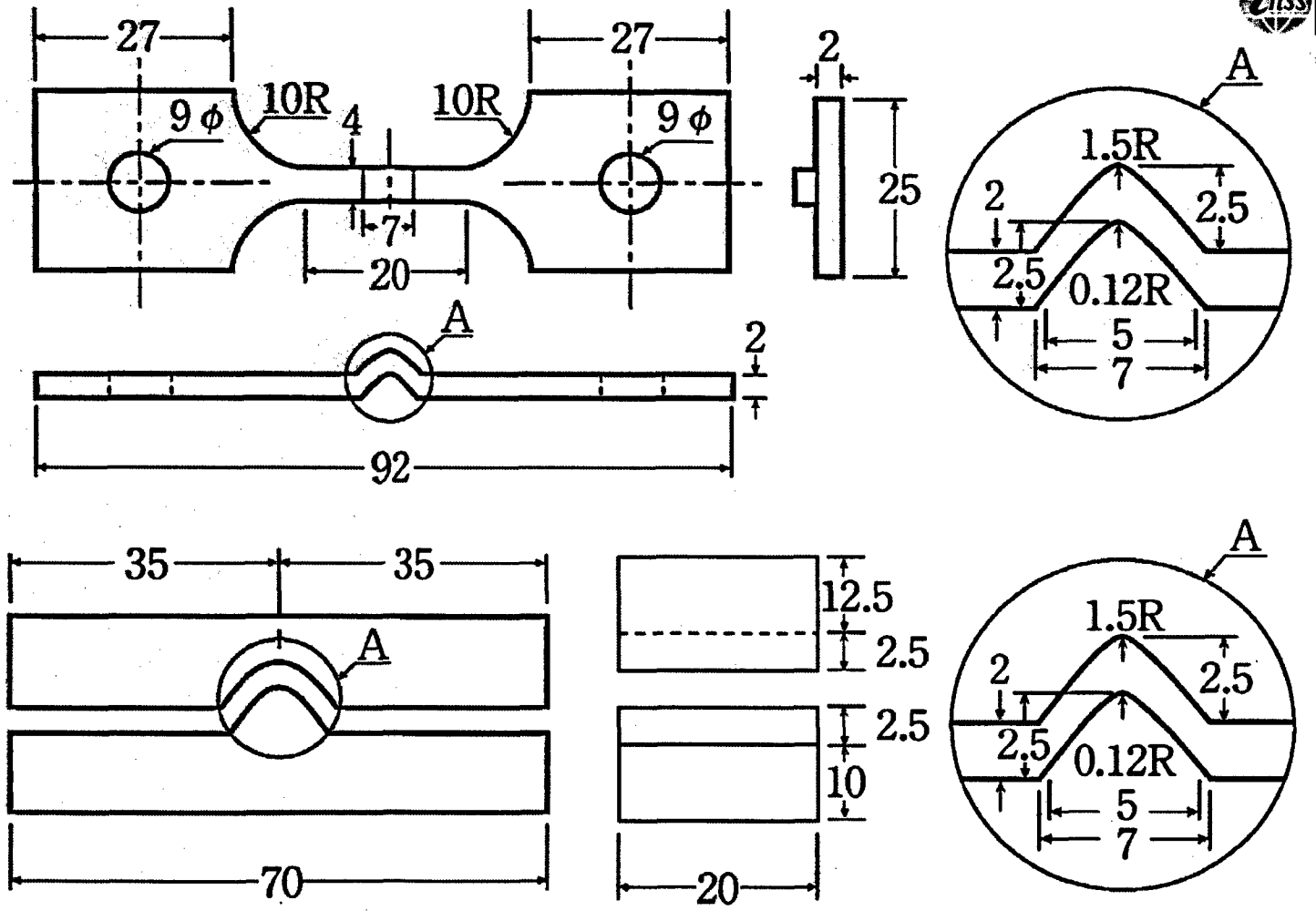

Specimens Used in the Accelerated SSRT Method

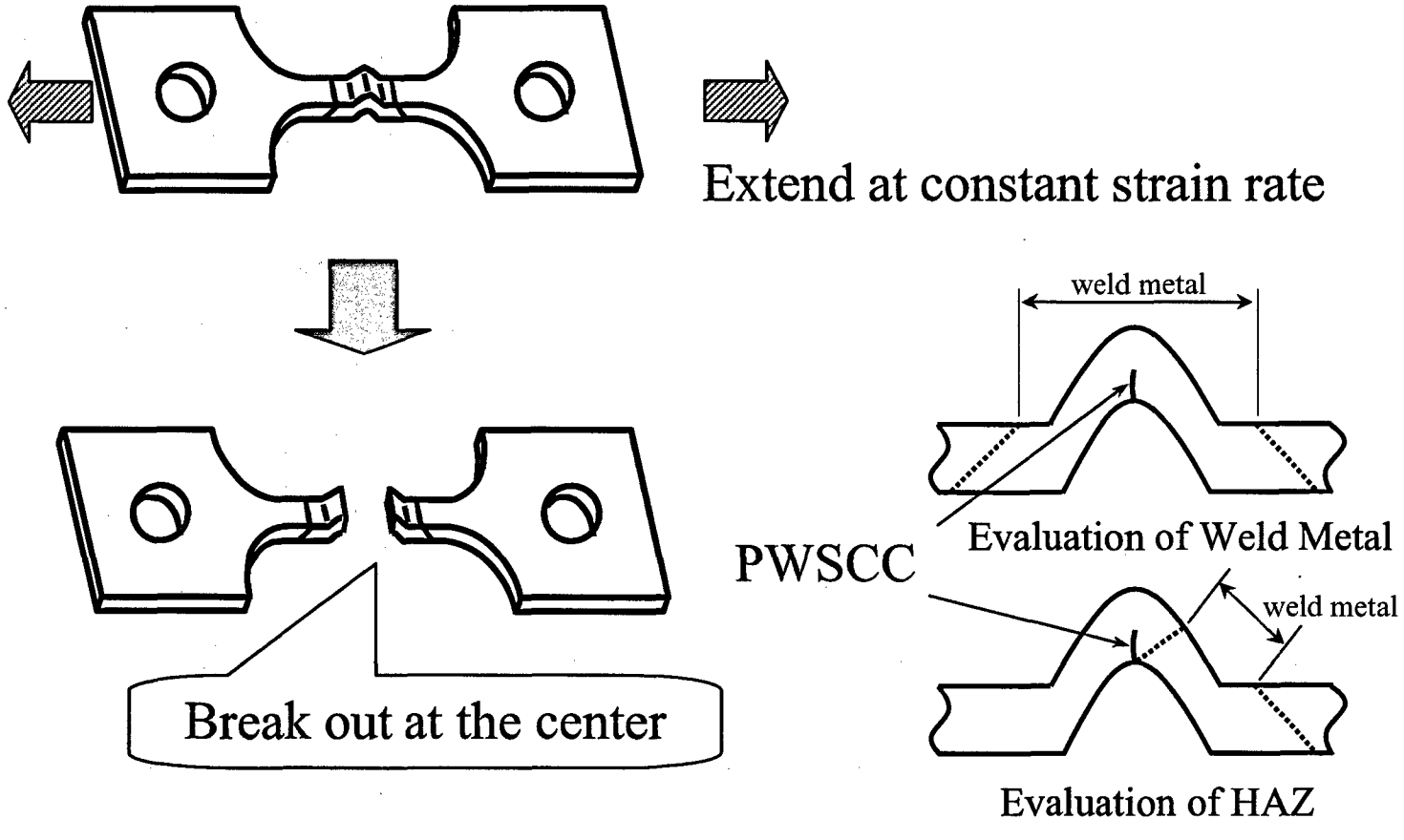

Specimen with hump

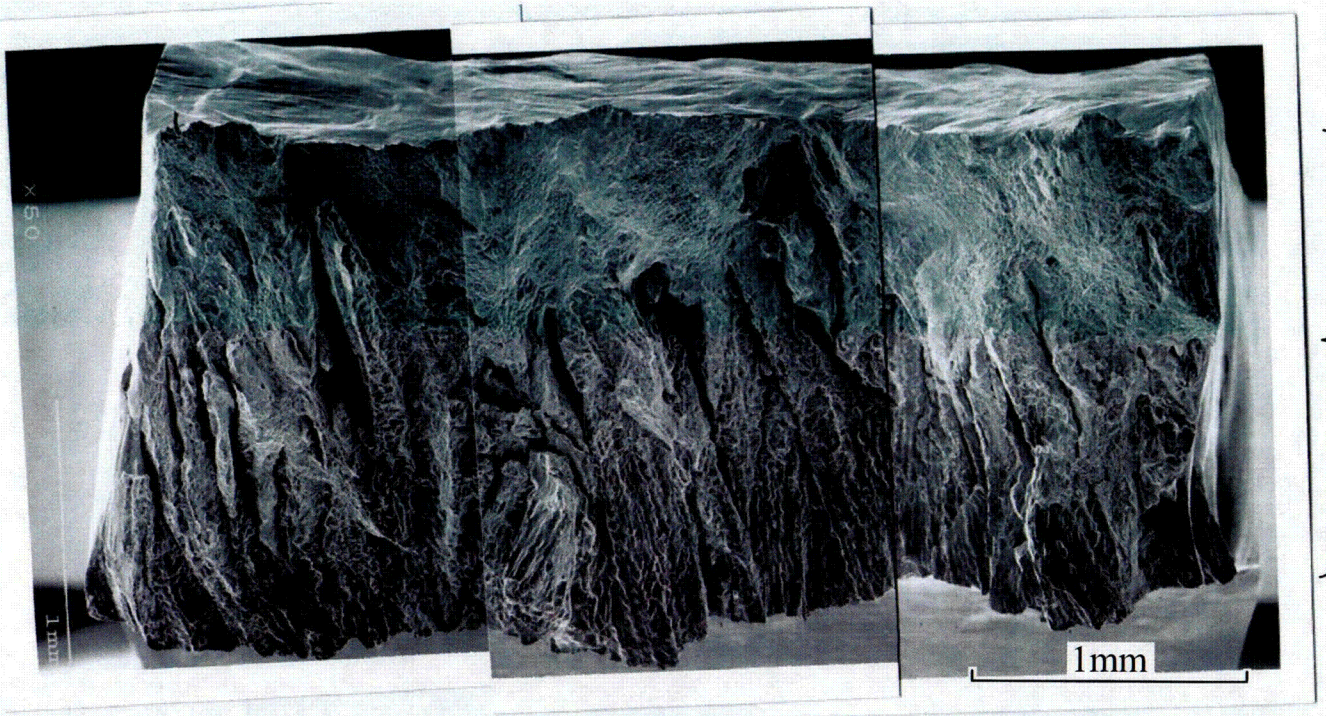

Ductile

Dendritic

Temperature	: 360 °C
Strain Rate	: $5\times10^{-7}s^{-1}$
Time to Failure	: 67.4 hr
SCC%	: 52.6 %

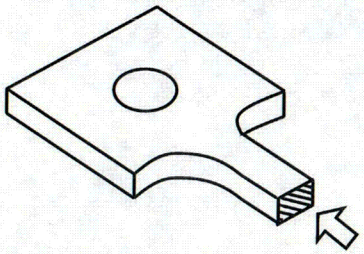

SEM photo of alloy 82

C24

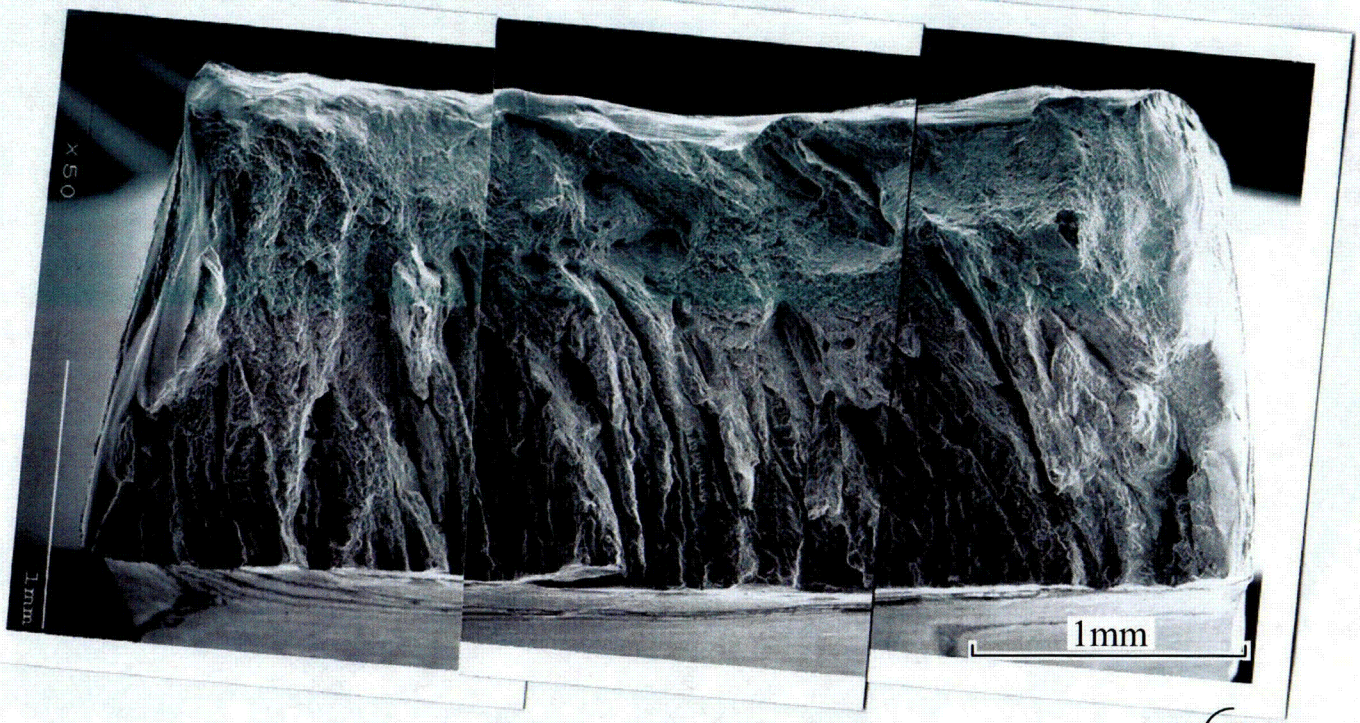

Ductile

Dendritic

Temperature : 360 °C
Strain Rate : $5\times10^{-7}s^{-1}$
Time to Failure: 73.6 hr
SCC% : 33.0 %

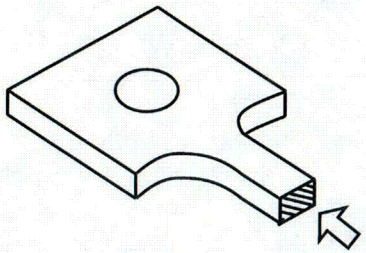

SEM photo of alloy 132

C25

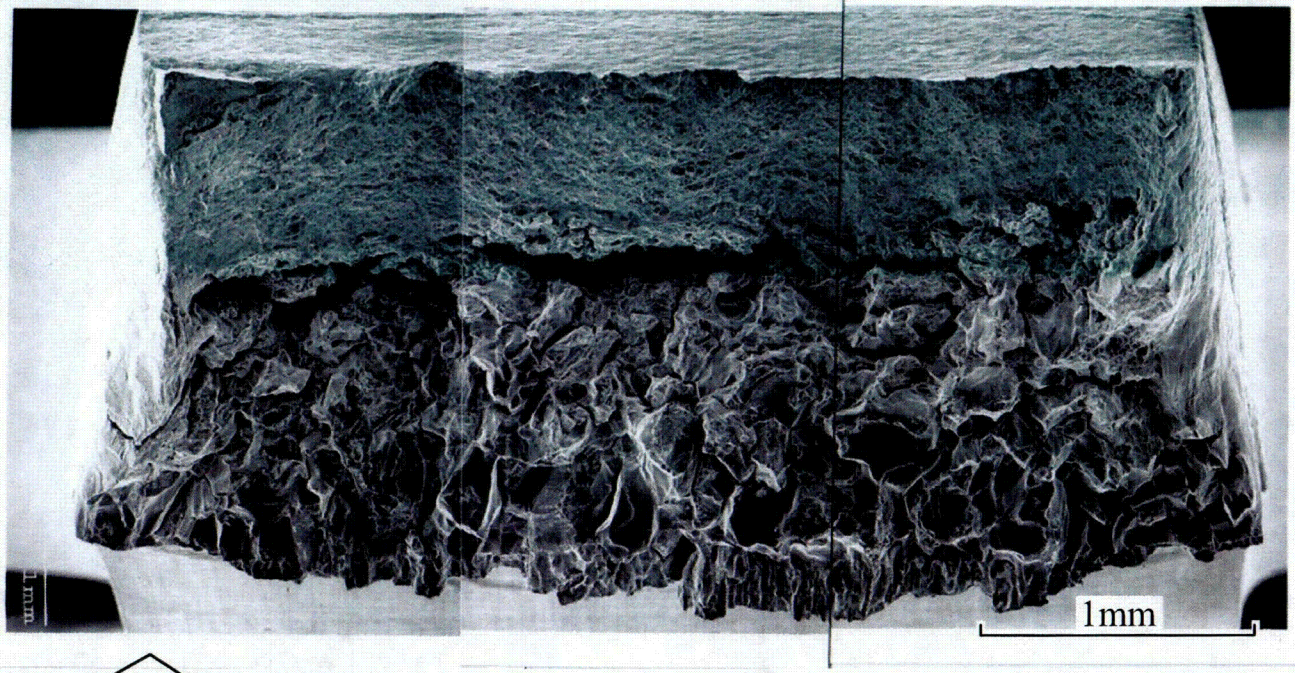

Ductile

Intergranular Cracking

Dendritic

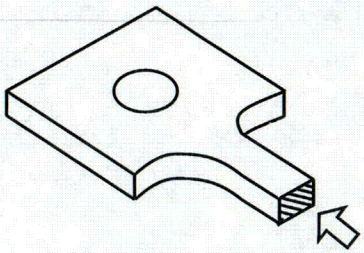

Temperature : 360 °C
Strain Rate : $5\times10^{-7}s^{-1}$
Time to Failure: 64.3 hr
SCC% : 55.9 %

SEM photo of HAZ welded by alloy 82

C26

Ductile

Intergranular Cracking

Dendritic

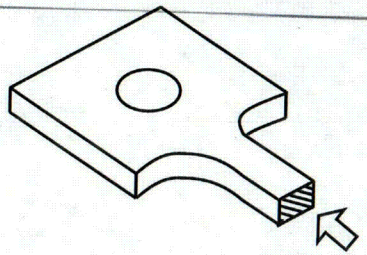

Temperature : 360 °C
Strain Rate : $5\times10^{-7}s^{-1}$
Time to Failure: 82.3 hr
SCC% : 61.8 %

SEM photo of HAZ welded by alloy 132

C27

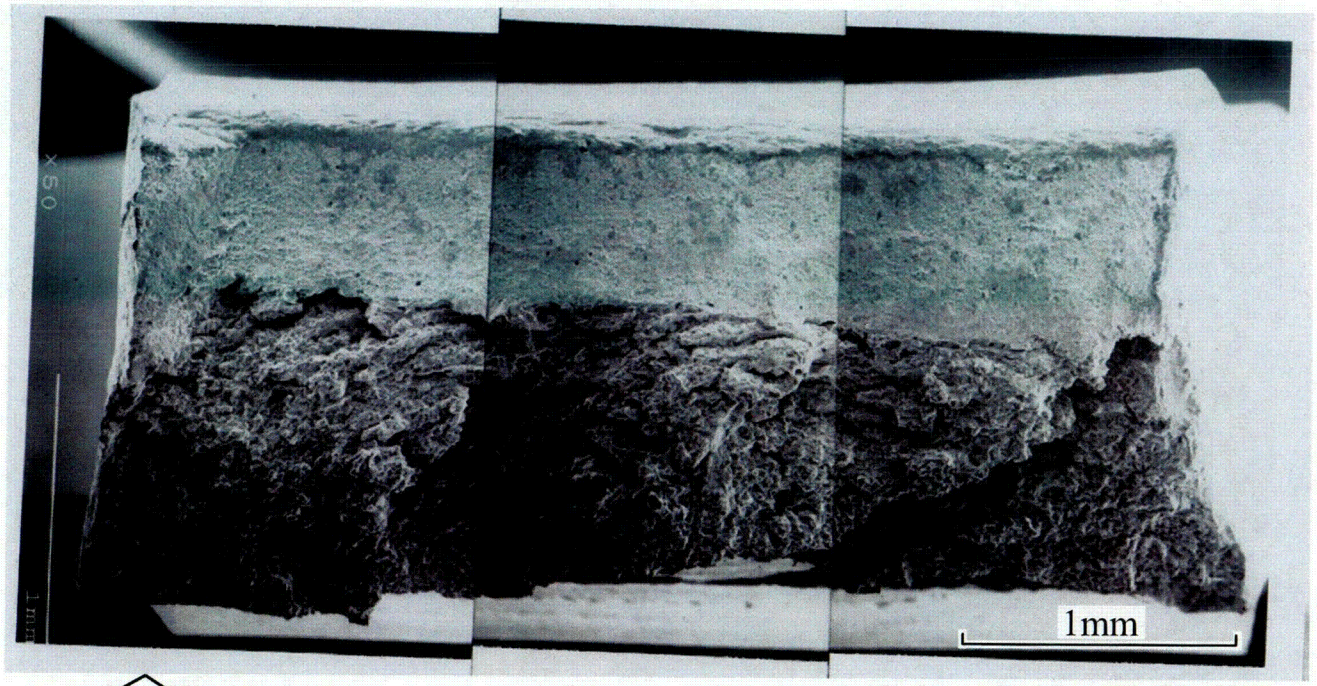

Ductile

Intergranular Cracking

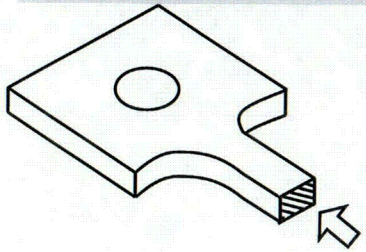

Temperature : 360 °C
Strain Rate : $5\times10^{-7}s^{-1}$
Time to Failure: 101.9 hr
SCC% : 60.8 %

SEM photo of alloy 600 base metal

C28

Crack Growth Rate (v)
= Plate Thickness × SCC % / Time to failure

$$Ea = - R \ln(v_1 / v_0) / (1/T_1 - 1/T_0)$$

where

Ea : Apparent activation energy

R : Gas constant = 8.3145×10^{-3} kJ/(mol·K)
= 1.9862×10^{-3} kcal/(mol·K)

T_0 , T_1 : Absolute temperature

v_0 : Rate at temperature T_0

v_1 : Rate at temperature T_1

Calculation of Apparent Activation Energy by Arrhenius' Equation

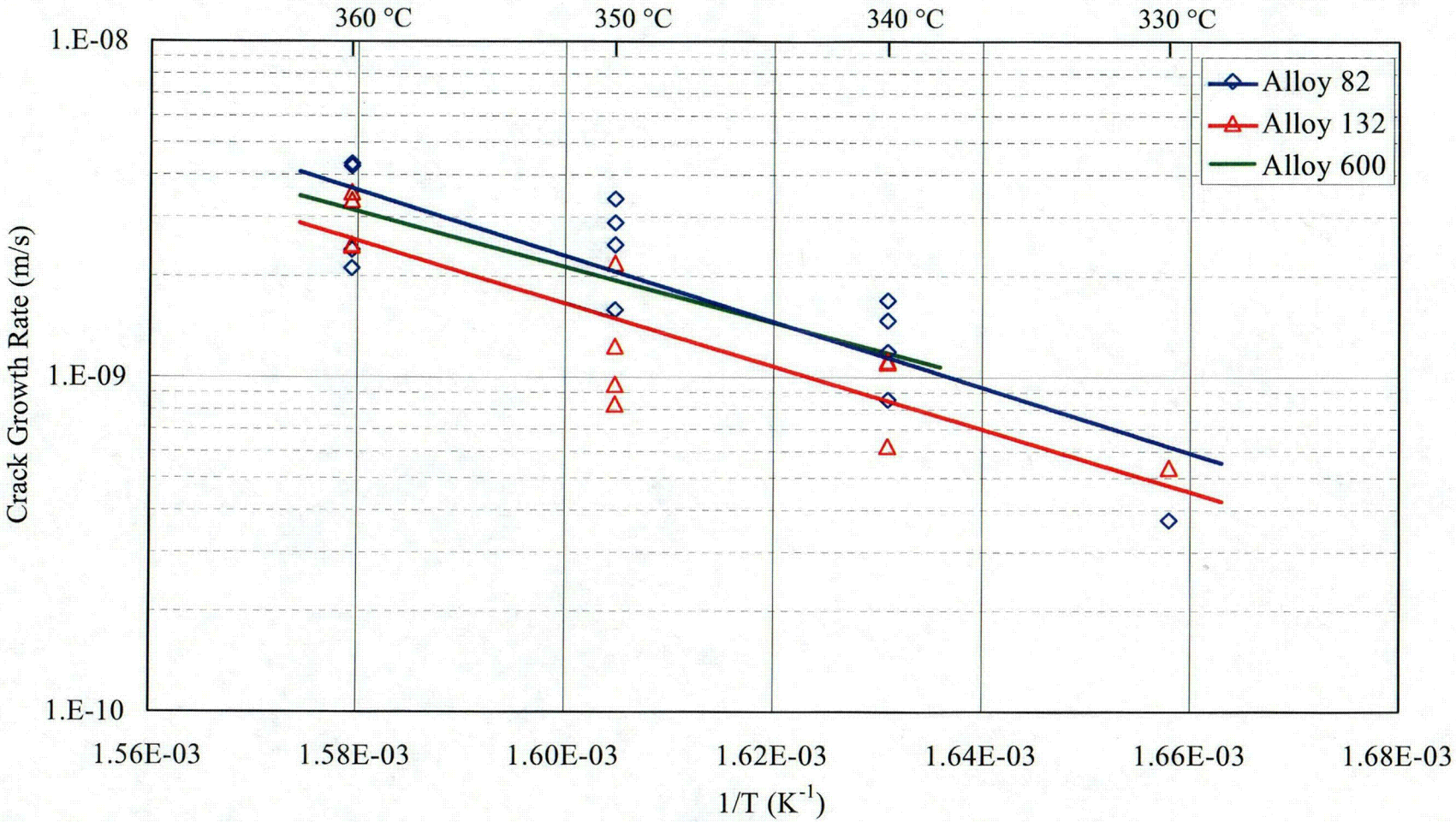

Relationship between Temperature and Crack Growth Rate of Weld Metal in SSRT

C29

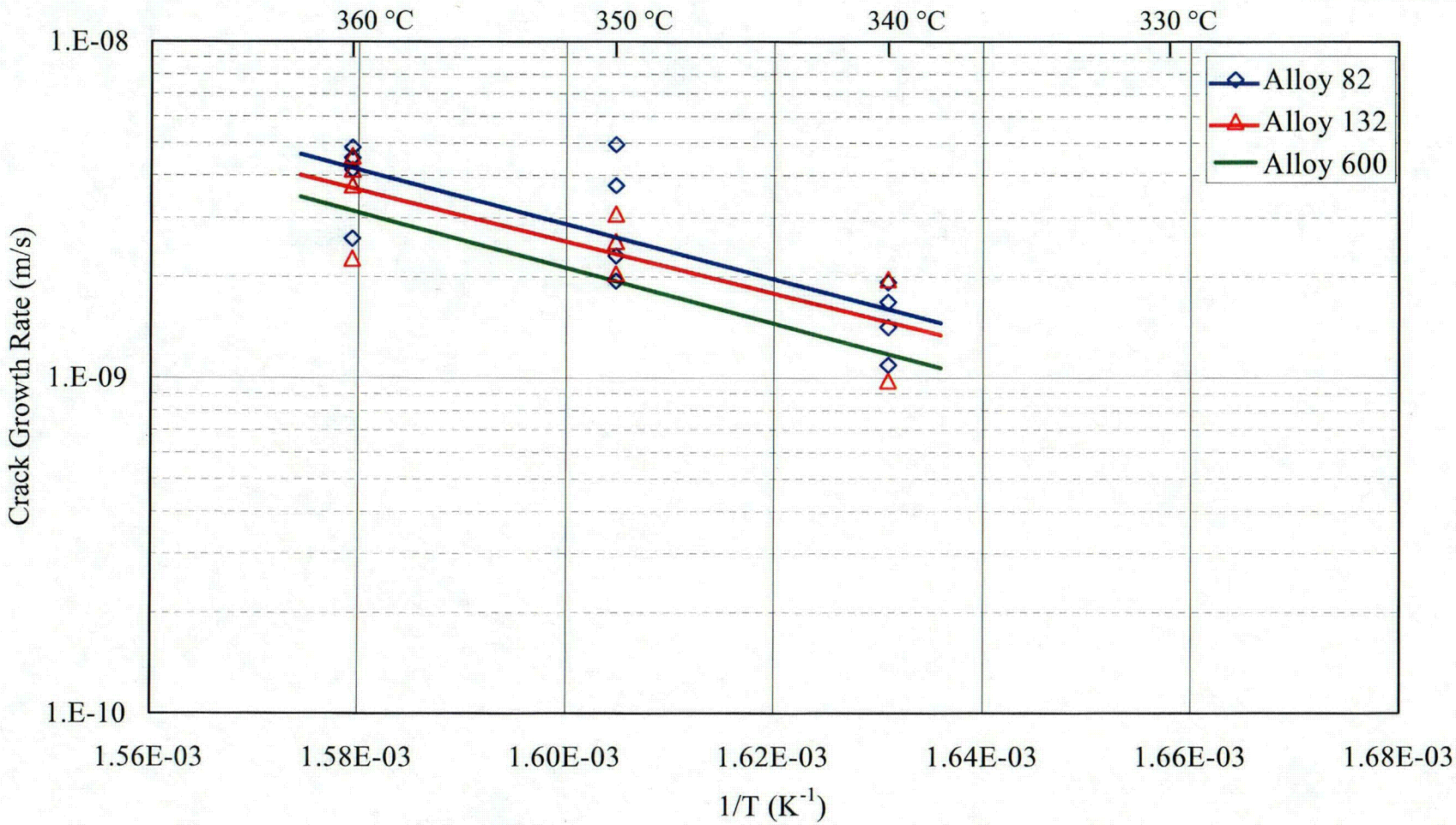

Relationship between Temperature and Crack Growth Rate of HAZ in SSRT

C30

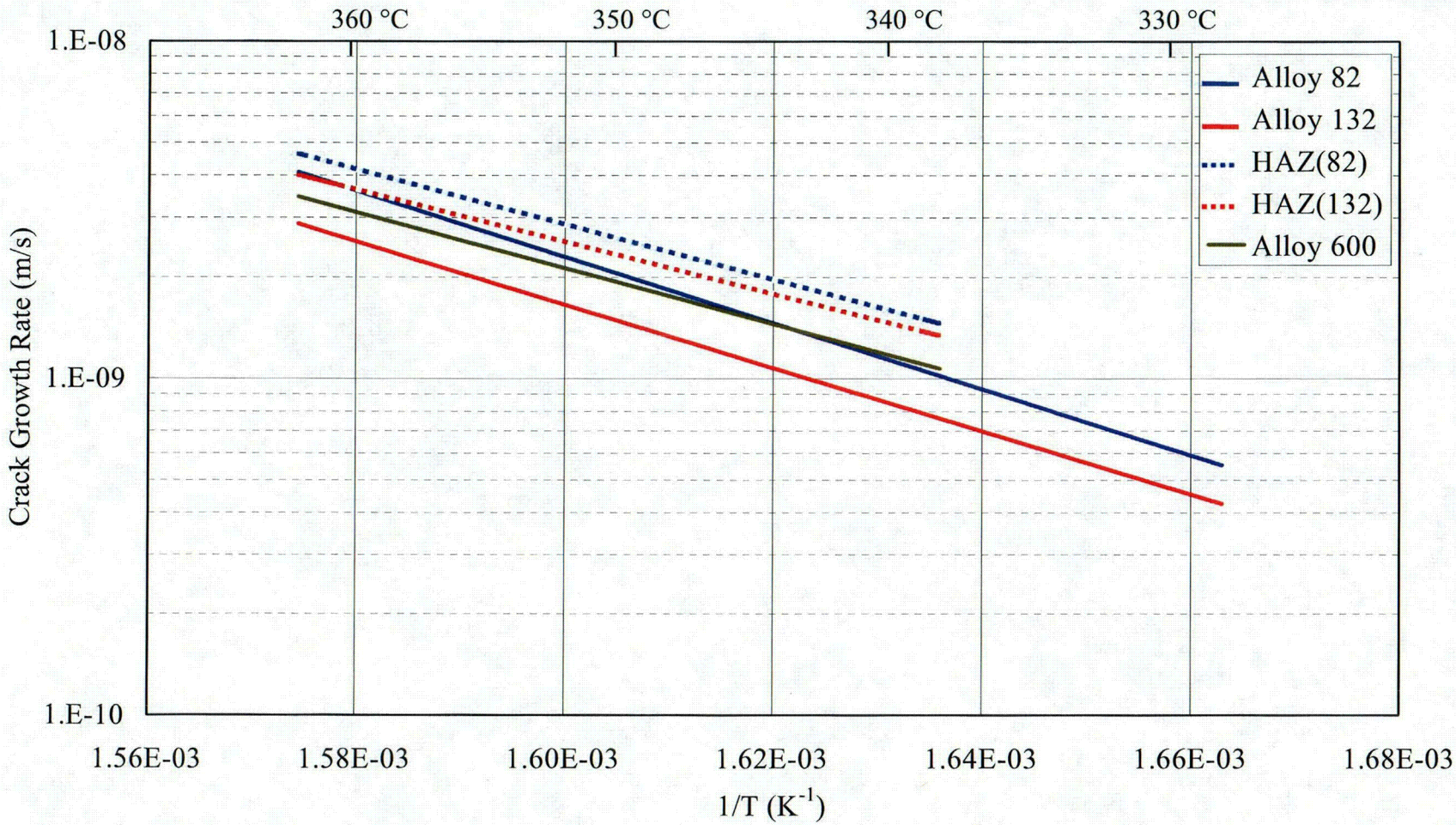

Relationship between Weld Metal, HAZ and Base Metal in SSRT

C31

Results

Alloy	Weld Metal or HAZ	Apparent Activation Energy
82	Weld Metal	188 kJ/mol (45 kcal/mol)
132		179 kJ/mol (43 kcal/mol)
82	Heat Affected Zone	156 kJ/mol (37 kcal/mol)
132		148 kJ/mol (35 kcal/mol)

Alloy 600 Base Metal	167kJ/mol (40 kcal/mol)

Conclusions

- The effects of temperature on PWSCC are similar between Alloys 82 and 132.

- The apparent activation energy of weld metal is a little higher than that of heat affected zone (HAZ). It seems that PWSCC on weld metal is more rarely than on heat affected zone at lower temperature.

Reference-1

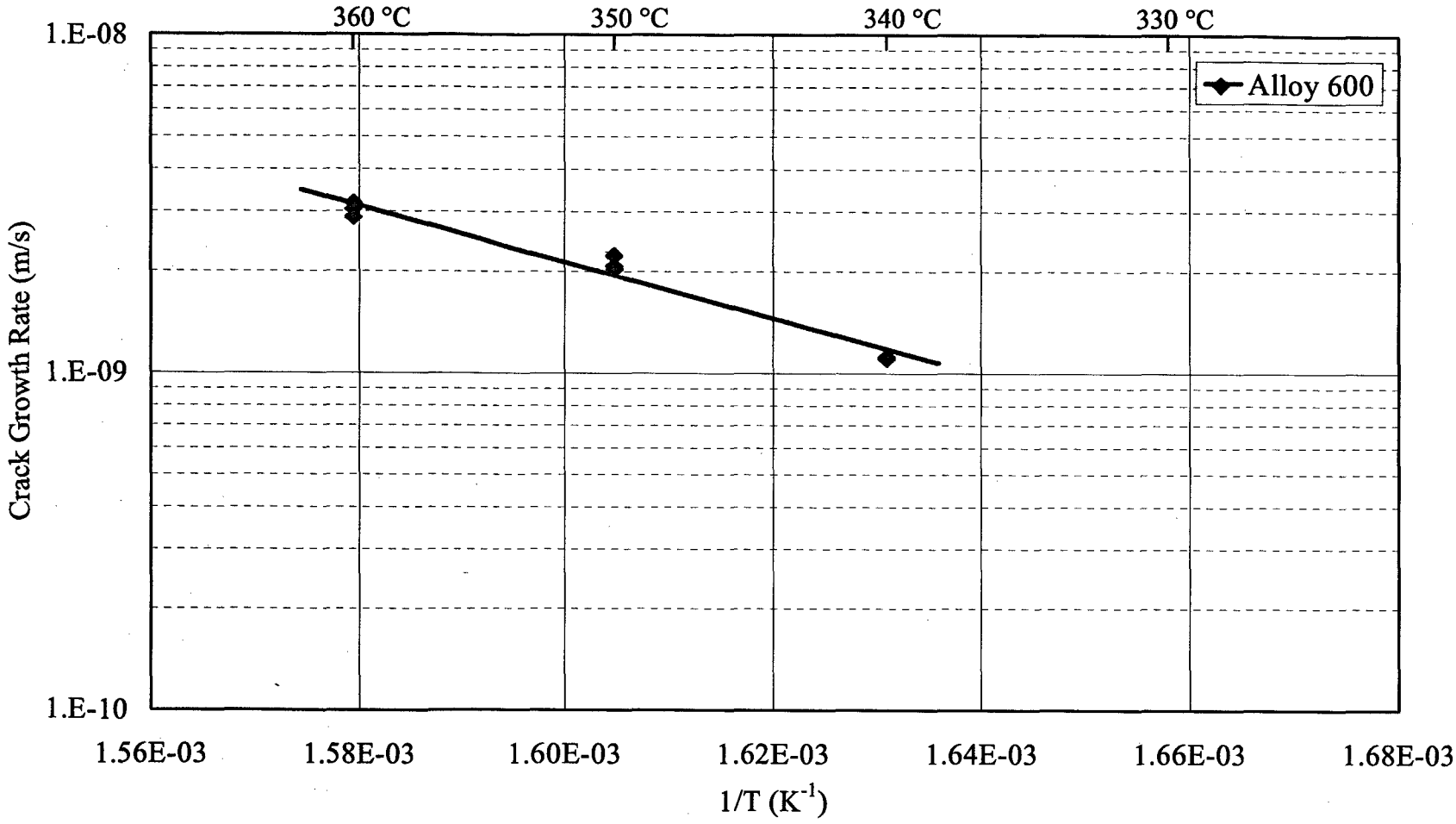

Crack Growth Rate and its approximately curve of Alloy 600 base metal

Evaluation of Scattering

Alloy	Weld Metal or HAZ	Deviations*	total
82	Weld Metal	1.43	1.44
132		1.38	
82	Heat Affected Zone	1.37	
132		1.33	
600	Base Metal	1.20	

* Deviations: Index numbers of standard deviations of logarithms of deviance of each crack growth rate from the approximated curve

FRI

Experimental and Numerical Approaches for Characterizing the Crack Growth Behavior of Alloy 600 in PWR Primary Water, and Lifetime Predictions for Welded Structures

Tetsuo Shoji, Zhanpeng Lu and Qunjia Peng

Fracture Research Institute
Tohoku University
Sendai 980-8579, JAPAN

Outline (1)

FRI

- Introduction
- Literature Survey

  -Existing Crack Growth Data and Significant Parameters
- FRI Generalized Crack Growth Rate Formulation
- Numerical Analysis

  – K dependence

  – Effects of yield strength

  – Effects of dK/dt

Outline (2)

FRI

- Prediction of Crack Growth Behavior in Weld Residual Stress Field
  - -Core Shroud Cracking
  - -VHP behavior
- Disposition of Flaws
- Conclusions
- Acknowledgements

Introduction (1)

FRI

- More concerns on PWSCC of alloy 600 and weld metals such as 182 in PWR Vessel Penetrations.

- Need Quantitative Evaluation of the remaining lifetime of the vessel penetration (VP) in PWR

- Need fully understanding of the crack growth behavior of Ni-based alloys from a view point of Disposition of Flaw.

Introduction (2)

FRI

- Special emphasis should placed on the K dependence of crack growth rate as a function of metallurgical variables, mechanical properties, temperature and dK/dt.

- Therefore, multiple factors, such as material, environmental, and mechanical are involved in EAC processes and their synergy effects are complex.

- Prediction of nickel base alloy components in real PWR plants based on PWSCC mechanism and CGR modeling is highly demanded

Literature Survey(1)

-Existing CGR Data-Laboratories & Plants

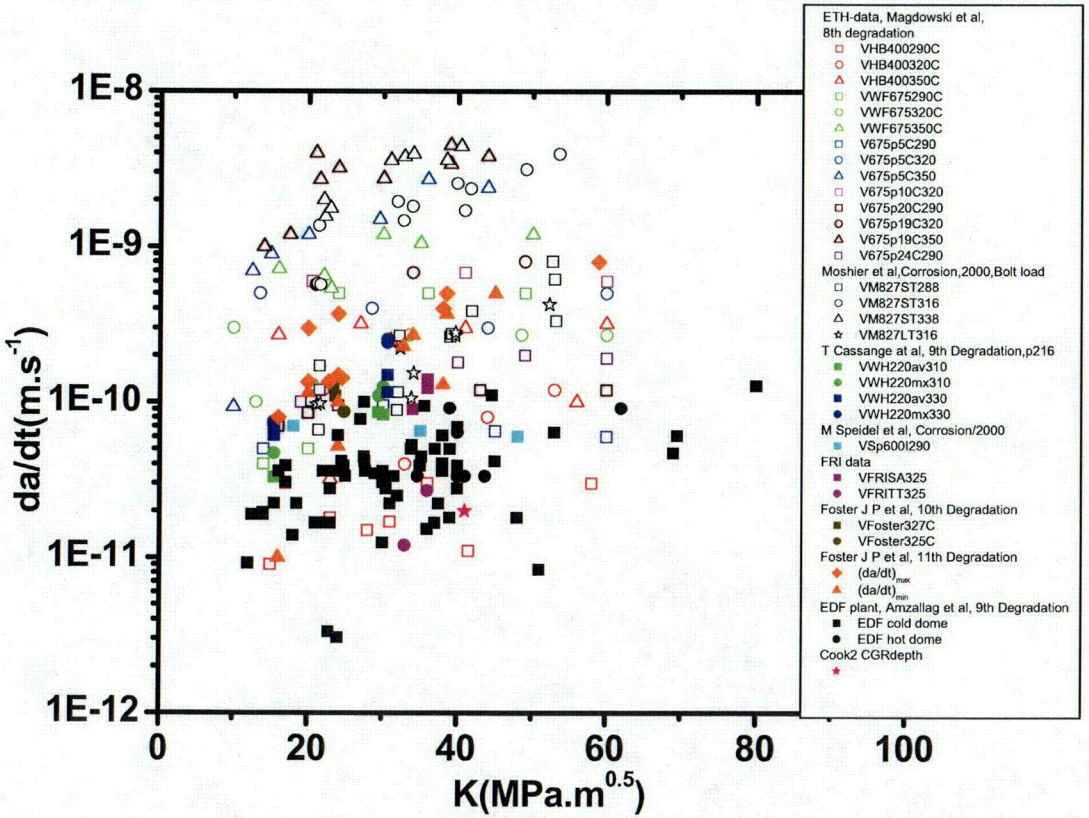

CGRs of Alloy 600 in PWR environments

- Lab. data:

-thick plate material

-fracture mechanics specimen

- Plant data: EDF & Cook 2

>Huge scatter of the data in da/dt vs K

C32

Literature Survey(2)
-Significant Parameters for CGR

FRI

- Material Chemistry and Microstructure

  -Carbide content and distribution
  (Grain boundary carbides improve SCC resistance)
  -Fraction of Coincidence Site Lattice Boundaries (CSLB)
  (High CSLBs-low IGSCC susceptibility)

- Temperature effects

  CGR increase follows Arrhenius law
  ~180kJ/mol for component failure time(including initiation)
  ~130kJ/mol for crack growth rate

- DH effects

  ~da/dt(max) near the Ni/NiO equilibrium potential line

Literature Survey(3)
-Significant Parameters for CGR

FRI

- K effects
  - -CGR plateau region at high K level(ETH data, EDF data, et c.)
  - -CGR monotonically increase-(Westinghouse data, EDF data, etc.)

Most CGR models are based on K effect

- YS effects

  High YS from material chemistry or cold/warm rolling
  - -significantly raise CGR

In empirical equations, a coefficient is used to introduce CW effect

- Loading and dK/dt effects
  - -Loading mode effect
  - -dK/dt effect for weldments with residual stress/strain

etc.,

FRI Generalized CGR formulation (5)

-CTSR formulation - Gao & Hwang's equation

FRI

- Gao and Hwang's definition of work hardening exponent, n,

$$\varepsilon = \begin{cases} \left(\frac{\sigma}{E}\right) & for \quad \sigma \le \sigma_y \\ \left(\frac{\sigma}{E}\right) + c \cdot (\sigma - \sigma_y)^n & for \quad \sigma > \sigma_y \end{cases}$$

- Gao & Huang's equation for the crack tip strain of a growing crack for constant K and da/dt.

$$\varepsilon_{ct} = \beta\left(\frac{\sigma_y}{E}\right)\left[\ln\left(\frac{A}{r}\right)\right]^{\frac{n}{n-1}} \qquad \varepsilon_{ct} = \beta\left(\frac{\sigma_y}{E}\right)\left\{\ln\left[\left(\frac{\lambda}{r}\right)\left(\frac{K}{\sigma_y}\right)^2\right]\right\}^{\frac{n}{n-1}}$$

Derived under the condition of plain strain and small scale yield

FRI Generalized CGR formulation (6)

-CTSR formulation - Validity Confirmed by 3D-FEM

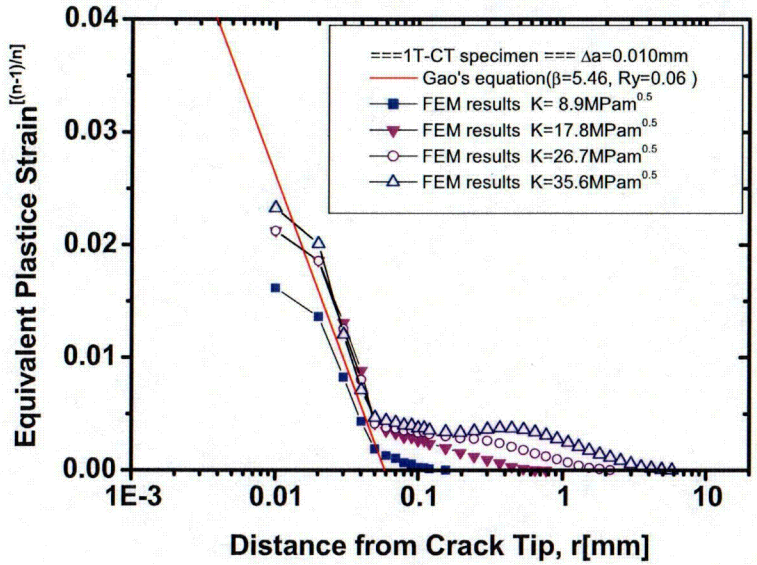

Equivalent plastic strain distribution at crack tip under constant load conditions, n (Gao's definition) is 10.

- 3D-FEM results match well with the theoretical calculation at different values of stress intensity factor, K.
- Although Gao's equation was derived for a steady growing crack under quasi-static loading (constant K), the 3D-FEM analyses indicate that Gao's equation may still be applicable even under the loading conditions without constant crack growth and/or constant K.

FRI Generalized CGR formulation (9)

-Shoji's model based on Slip/Oxidation mechanism

FRI

- FRI theoretical CGR formulation, based on the crack tip reaction kinetics and the theoretical CTSR formulation

$$\frac{da}{dt} = \left[\frac{M \cdot i_0}{z \cdot \rho \cdot F \cdot (1-m)}\right]\left(\frac{t_0}{\varepsilon_f}\right)^m \left\{ \beta \cdot \left(\frac{\sigma_y}{E}\right) \cdot \left(\frac{n}{n-1}\right) \cdot \left[2 \cdot \frac{\dot{K}}{K} + \frac{\dot{a}}{r}\right] \cdot \left\{ \ln\left[\lambda \cdot \frac{\left(\frac{K}{\sigma_y}\right)^2}{r}\right] \right\}^{\frac{1}{n-1}} \right\}^m$$

- *A unique expression for CGR as a function of K- combining a mechanism of crack growth with the mechanics of a crack tip stress/strain field.*
- *Synergistic terms among the material parameters, mechanical properties, electrochemical properties and crack tip mechanics in terms of K and dK/dt*

FRI Generalized CGR Formulation (10)

-CGR equation

FRI

A generalized CGR formulation can be obtained by combining the general oxidation mechanism and the theoretical CTSR equation,

$$\frac{da}{dt} = \kappa_a \cdot \left\{ \beta \cdot \left(\frac{\sigma_y}{E}\right) \cdot \left(\frac{n}{n-1}\right) \cdot \left[2 \cdot \frac{\dot{K}}{K} + \frac{\dot{a}}{r}\right] \cdot \left\{ \ln\left[\lambda \cdot \frac{\left(\frac{K}{\sigma_y}\right)^2}{r}\right] \right\}^{\frac{1}{n-1}} \right\}^m$$

where κ_a is a crack tip oxidation rate constant, which is a function of local material chemistry, local environmental chemistry, transient interfacial rate kinetic law, and the stress/strain state.

FRI Generalized CGR Formulation (12)

-Possible Accelerated CGR testing based on mechanism (1) YS& κ_a effect

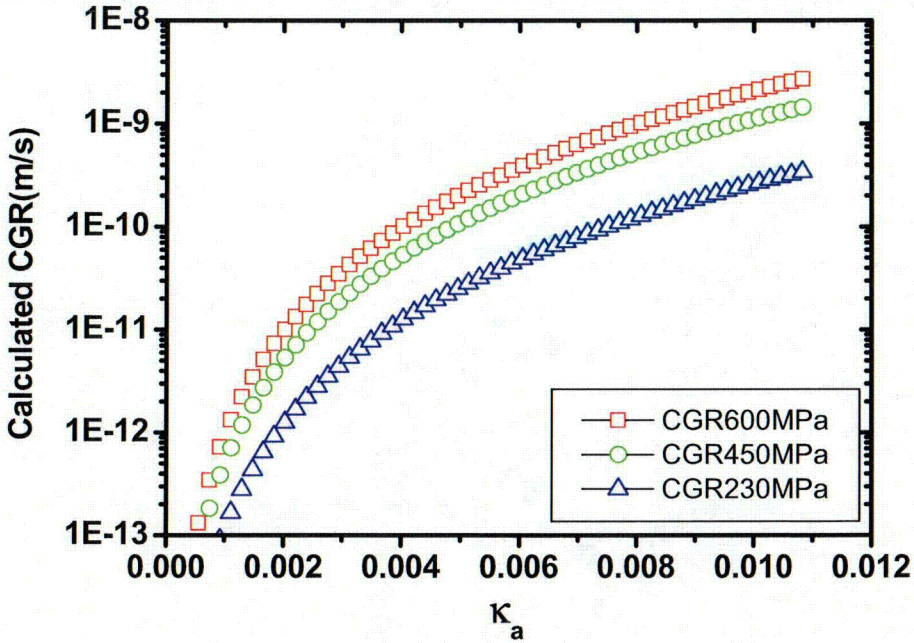

Sensitivity analysis of YS effect at different κ_a levels (m= constant)

- **At each YS level, CGR increases with increasing of κ_a value**
- **A non-linear relationship between CGR and κ_a**
- **CGR increases with YS**

C34

FRI Generalized CGR Formulation (13)

-Possible Accelerated CGR testing based on mechanism (2) YS & m effect

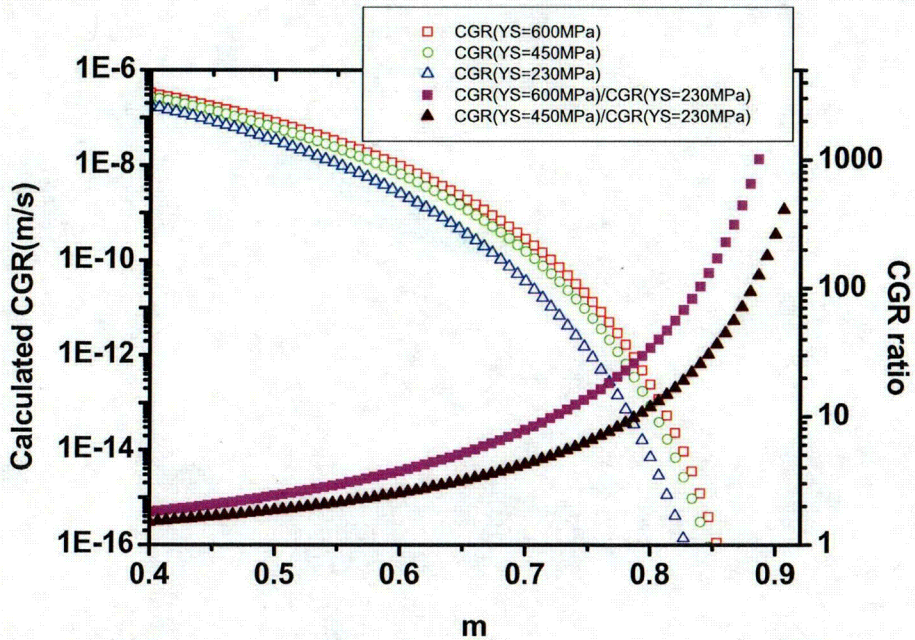

Sensitivity analysis of the effect of YS on CGR for different values of m (κ_a =constant)

CGR ratio= CGR(YS)/CGR(230MPa)

- CGR decreases with an increase of m
- Effect of YS increases with an increasing m,

-implying that the effect of YS is more significant for materials with a faster repassivation (or fast film recovery) process

FRI Generalized CGR Formulation (14)

- Possible Accelerated CGR testing (3)YS & κ_a & m effect

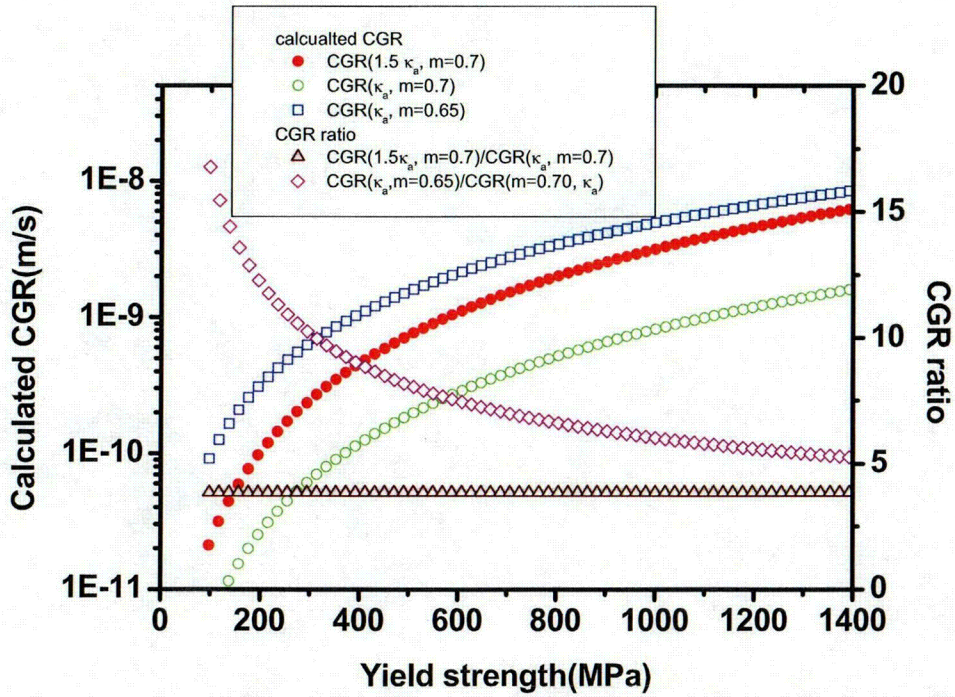

- The enhancement factor by decreasing m is less with an increase of YS.

-CGR enhancement by decreasing *m* (slower film recovery process) could be more significant for materials of lower YSs

FRI Generalized CGR Formulation (16)

- Possible Accelerated CGR testing based on mechanism (5) K&dK/dt effect

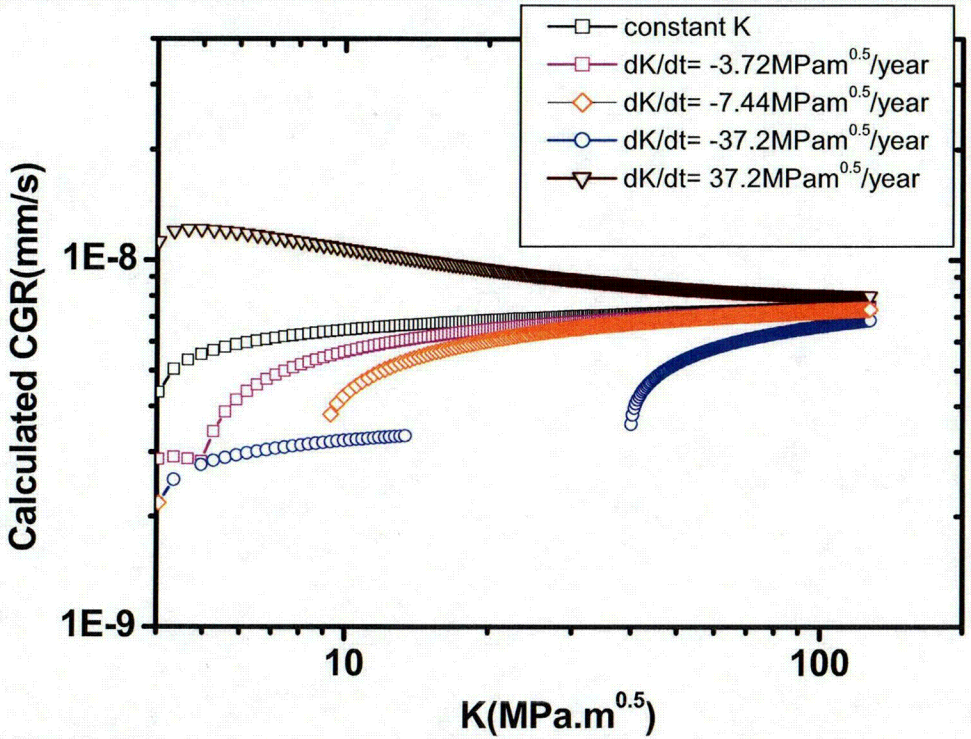

n=9
m=0.5
YS=200MPa
Different dK/dt

- Significant effect of dK/dt on CGR
- Negative dK/dt results in lower CGR and higher threshold
- CGR testing at higher dK/dt accelerates CGR-specimen design

C37

Numerical Analysis of experimental CGR(1)
-K dependence - Moderate K effect

FRI

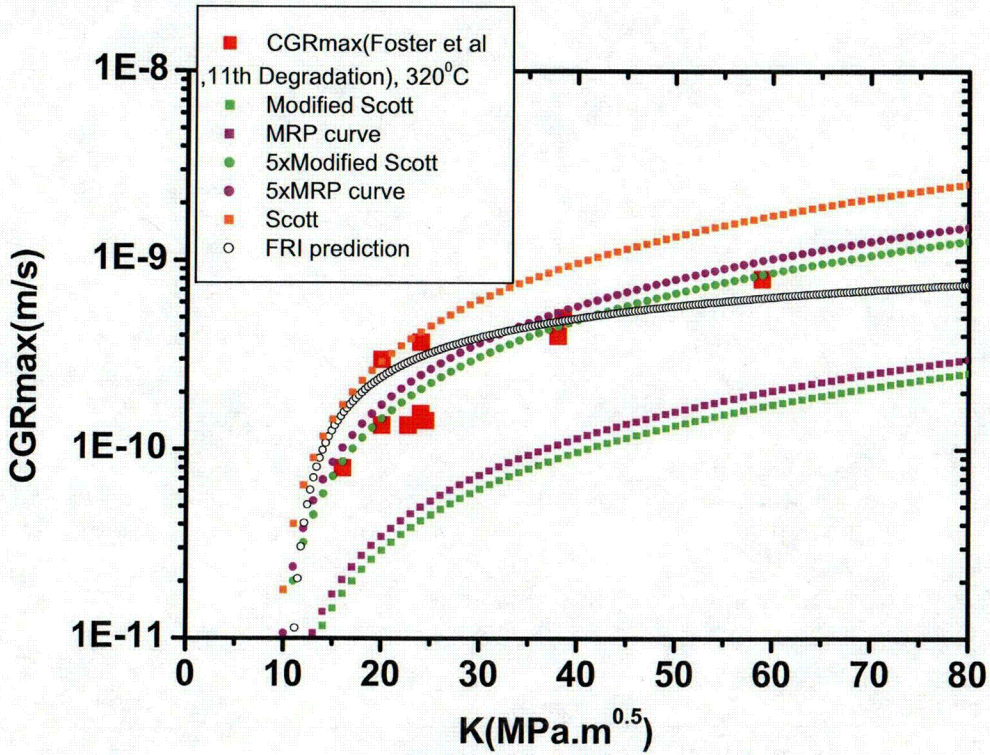

Alloy 600, heat 69
Material of low YS,
YS=274MPa
n=3

Parameter used in the model:
m=0.77

- FRI prediction on the material with YS=274MPa
- Comparison with modified Scott model & MRP model.

Numerical Analysis of experimental CGR(4) -YS effect (1)

FRI

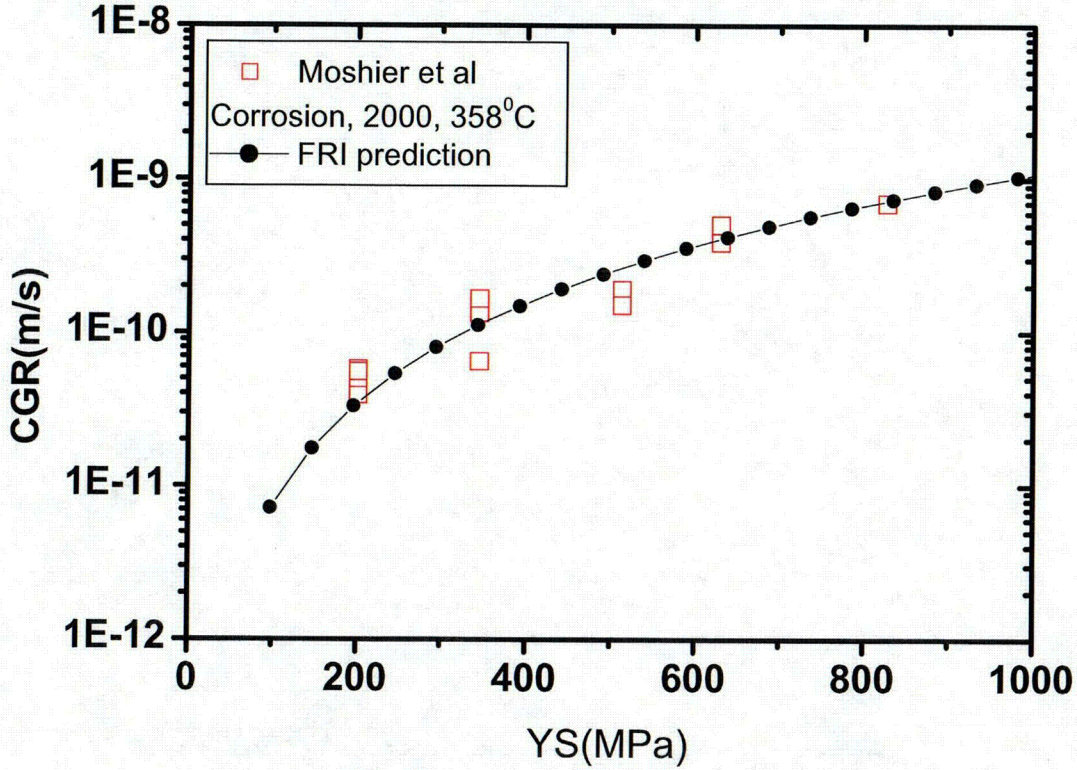

Parameters used in the model: m=0.70 and n=6

The effect of YS on CGR can be predicted by FRI generalized model

Numerical Analysis of experimental CGR(5)
-YS effect (2) YS & T effect

FRI

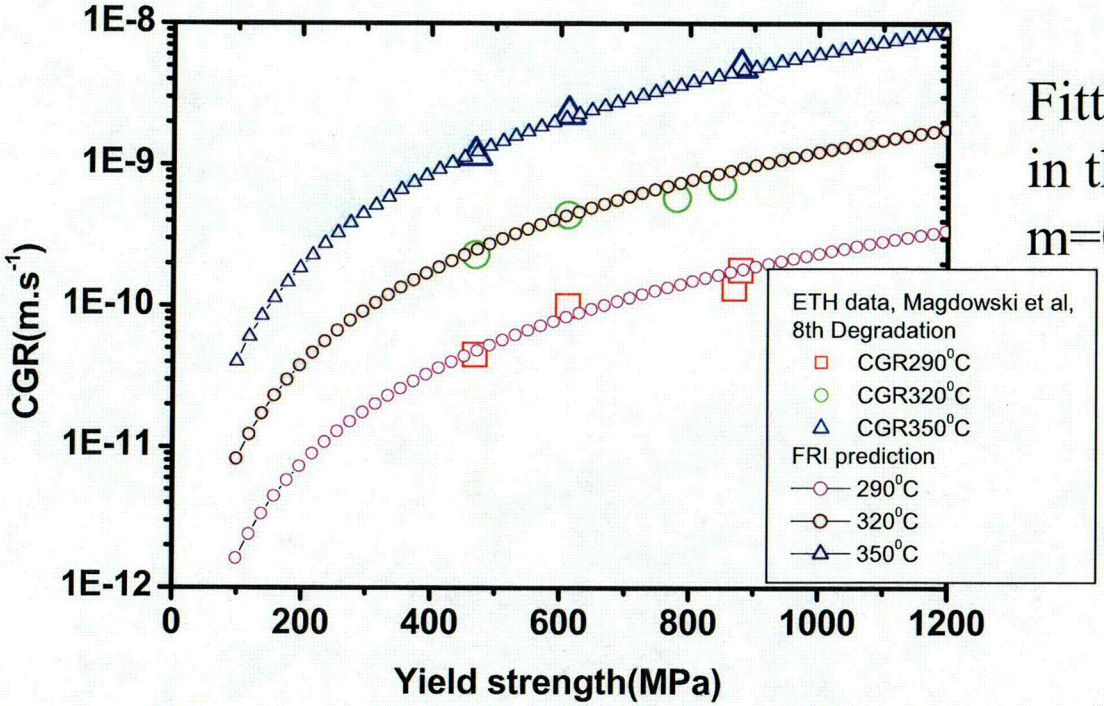

Fitting parameters in the model: m=0.70 and n=6

- Again, effect of YS can be formulated with the FRI generalized model
- CGRs at different can be calculated by only changing values of κ_a

Numerical Analysis of experimental CGR(7) -dK/dt effect

FRI

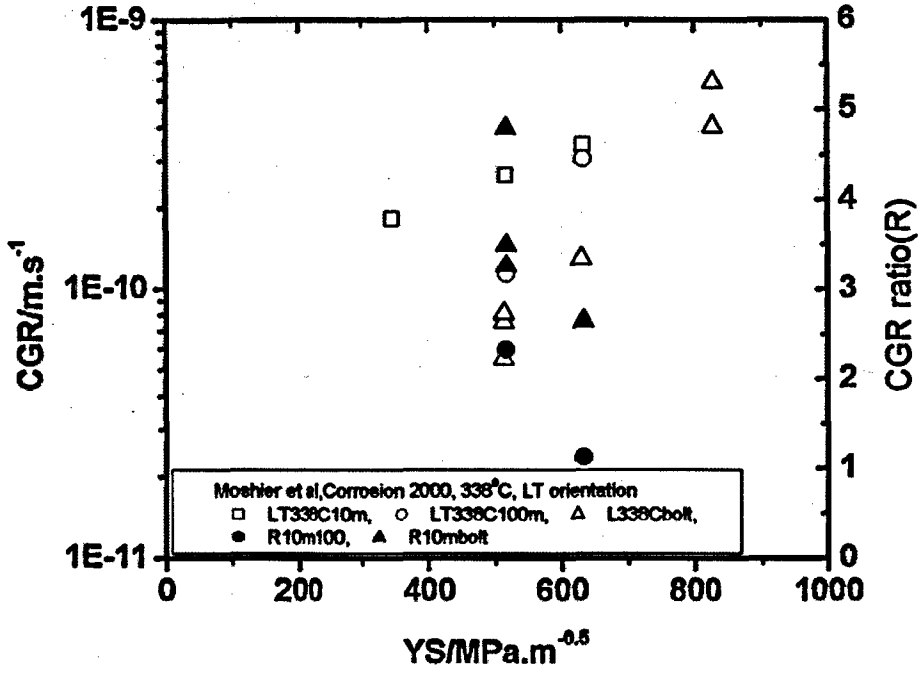

- CGR(bolt)<CGR(active load) in this data set, can be explained by the sensitivity analysis of dK/dt effect by FRI mode

Prediction of CGR in Weld Residual Stress Field(1)
-Core Shroud Cracking(1)Residual Stress distribution

FRI

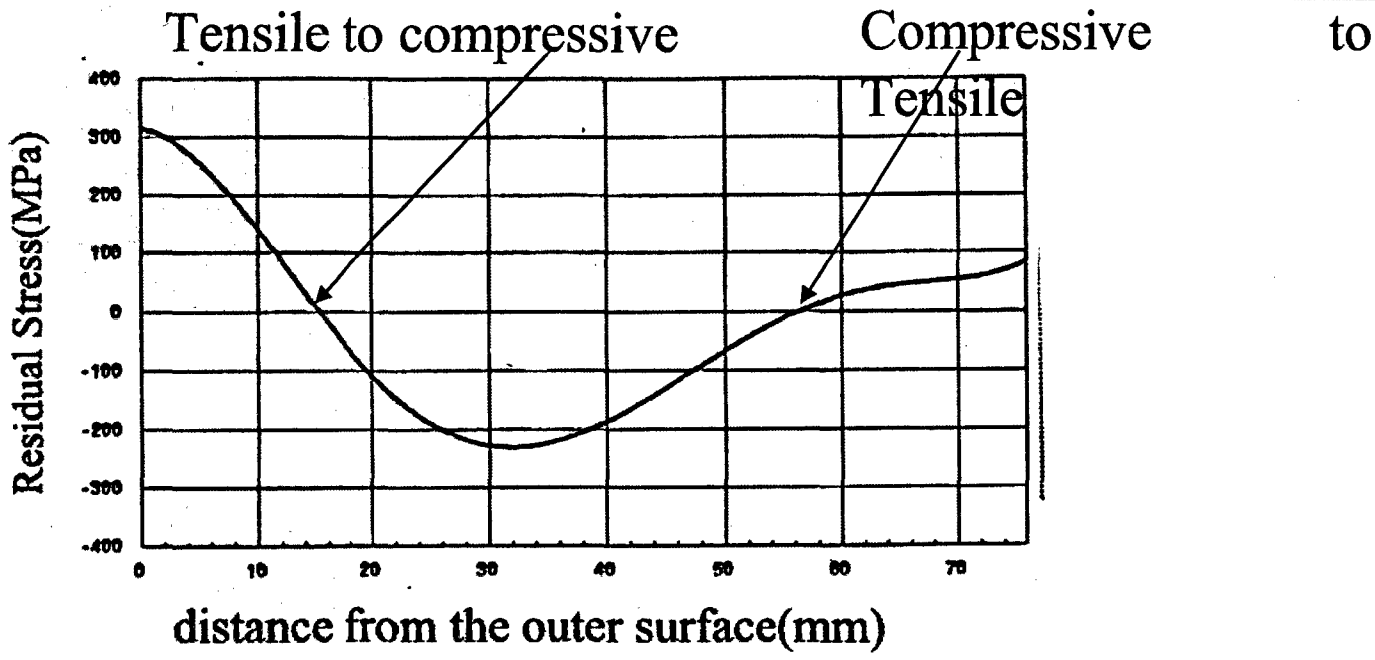

Distribution of the axial residual stress in H6a in a BWR core Shroud

- The residual stress changes from tensile to compressive or vise versa at certain depths of the weldment

Prediction of CGR in Weld Residual Stress Field(2)

-Core Shroud Cracking(2) K distribution

FRI

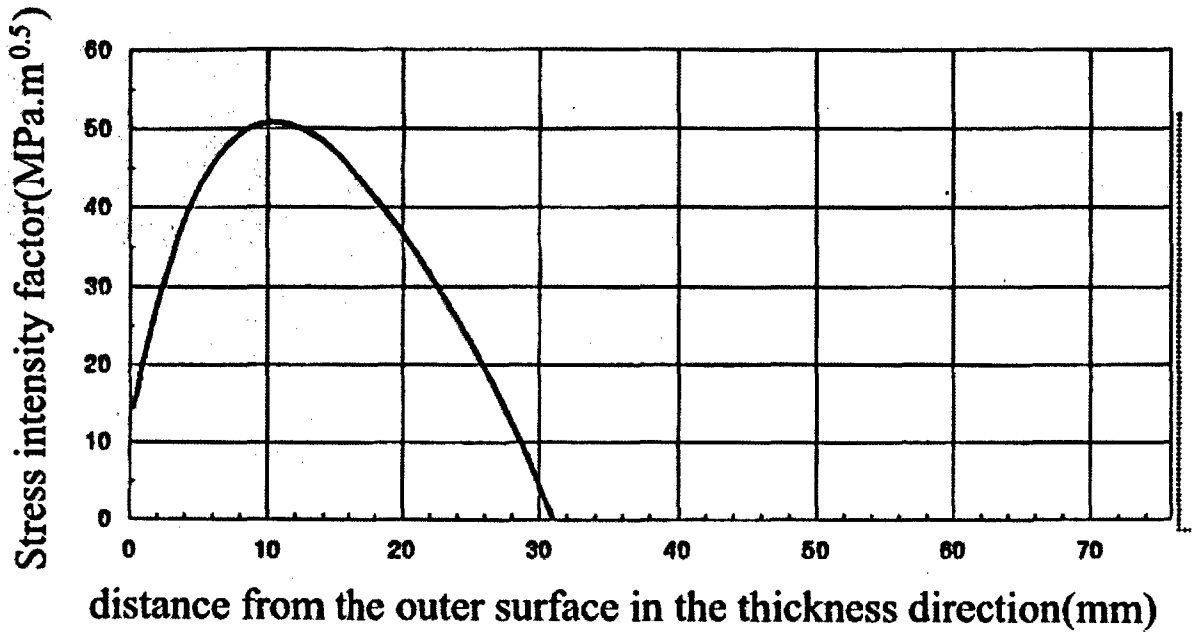

Estimated distribution of K in H6a in a BWR Core Shroud

- K increases to a maximum value and then decreases in the through-thickness direction of the weldment.

Prediction of CGR in Weld Residual Stress Field(4)

-Core Shroud Cracking (4) Crack depth prediction

FRI

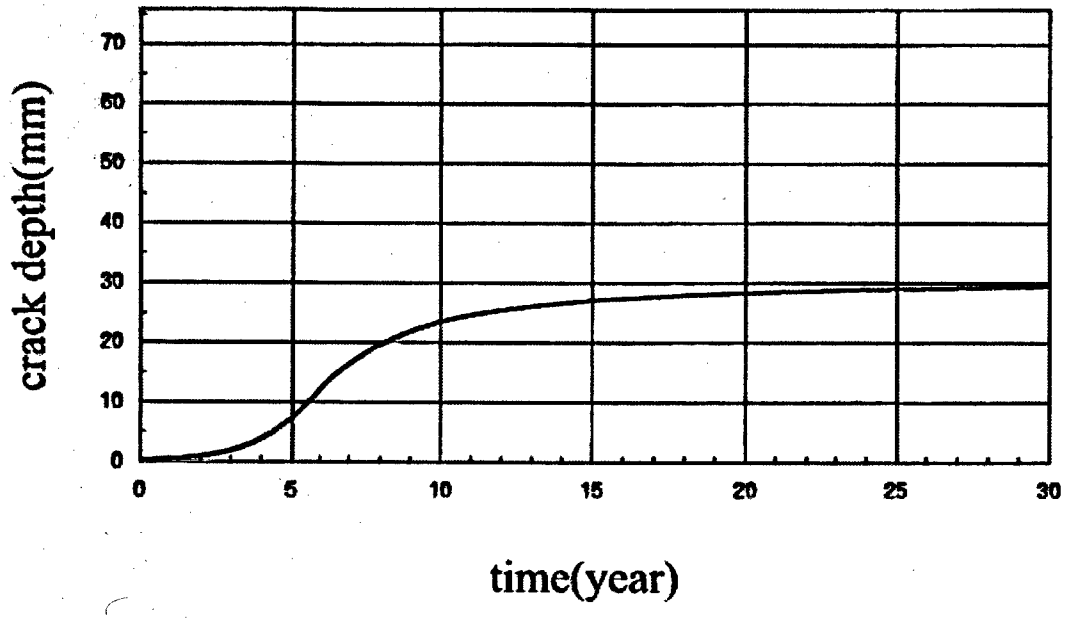

Relationship between the crack depth and time

- High crack growth rate is expected for the period of 4-9years
- After ca. 9 years, CGR decreases with time

Prediction of CGR in Weld Residual Stress Field (6)
-Details of a PWR VHP & an Inside-reactor Instrument tube

FRI

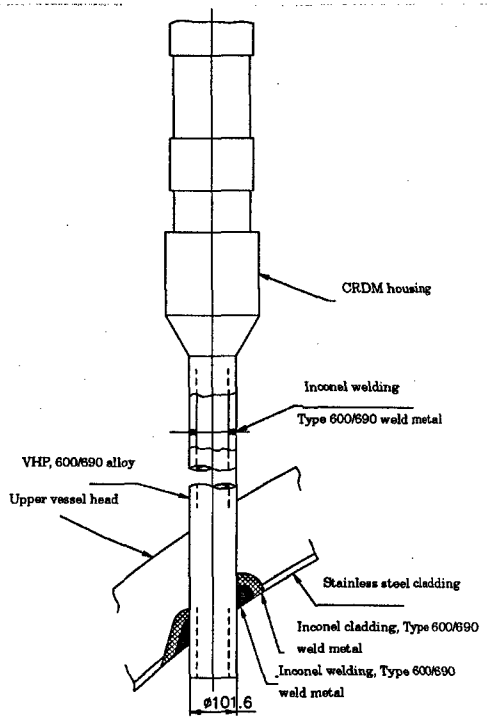

Structure of the VHP

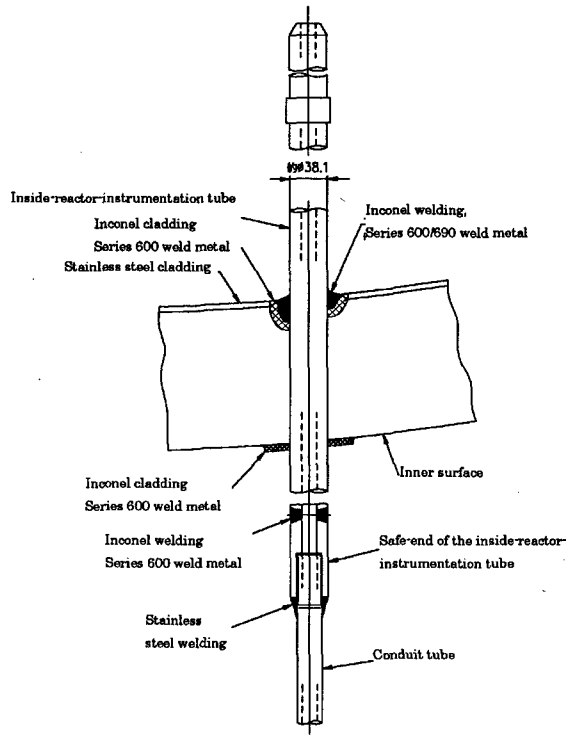

Structure of the inside-reactor-instrumentation tube

Illustration of a PWR VHP(left) and an inside-reactor instrument tube(right)

Prediction of CGR in Weld Residual Stress Field (7)

-PWR VHP(3) Crack growth behavior of PWR VHPs

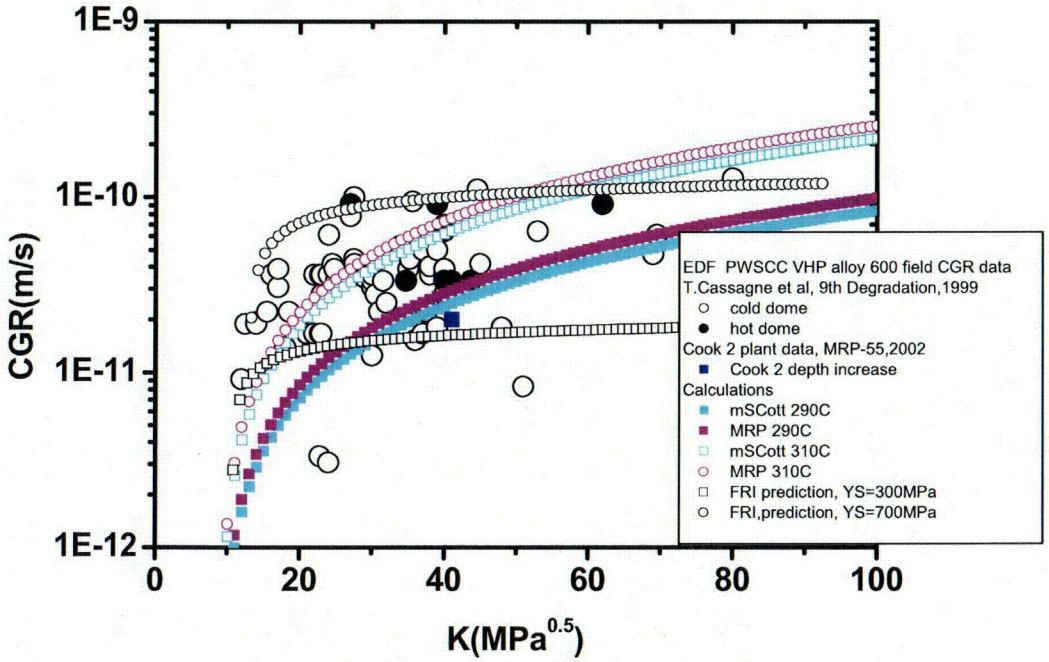

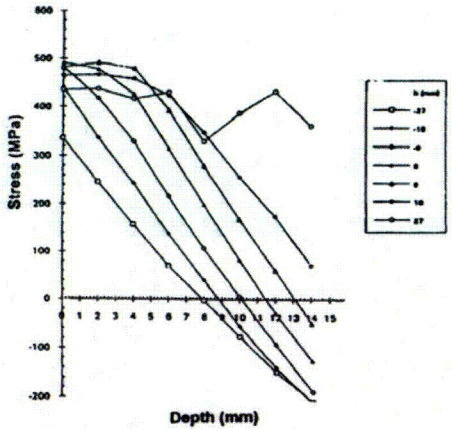

Weld Residual stress analysis of a PWR VHP (EDF data)

CGR prediction of Plant CGRs(from EDF & MRP) due to variations of YS may partly explain the scattered CGR data in the CGR-K diagram

Disposition of flaws (6)

- PWR environments (5) FRI generalized CGR model

FRI

-CGR is very sensitive to YS and this effect could be one of the factor of the scattered CGR in the data base.

-The shape of the CGR-K curve is important for developing the disposition line. **Variability in strain hardening ability may contribute to different types of CGR-K relationship**.

-Time variation of K(dK/dt) with crack growth can significantly affect the CGR of structural materials either in BWR or in PWR

Disposition of flaws (7)

- PWR environments (6) FRI generalized CGR model

FRI

-**This dK/dt variation** with crack growth can be more important in crack growth under the real plant condition where crack grows **in welded component**.

-**Loading condition and residual stress/stain analysis** is necessary for the crack growth rate formulation and for lifetime prediction of NPP components, especially for weldments.

FRI Generalized CGR Formulation

FRI

A generalized CGR formulation can be obtained by combining the general oxidation mechanism and the theoretical CTSR equation,

$$\frac{da}{dt} = \kappa_a \cdot \left\{ \beta \cdot \left(\frac{\sigma_y}{E}\right) \cdot \left(\frac{n}{n-1}\right) \cdot \left[2 \cdot \frac{\dot{K}}{K} + \frac{\dot{a}}{r}\right] \cdot \left\{ \ln\left[\lambda \cdot \frac{\left(\frac{K}{\sigma_y}\right)^2}{r}\right] \right\}^{\frac{1}{n-1}} \right\}^m$$

where κ_a is a crack tip oxidation rate constant, which is a function of local material chemistry, local environmental chemistry, transient interfacial rate kinetic law, and the stress/strain state.

Conclusions (1)

FRI

- FRI Model and CGR formulation can predict experimental and field CGR data with a good agreement, taking into account the effects of K, yield strength, strain hardening, temperature and dK/dt on CGRs

- Based upon the FRI model, CGR should have K dependence in the form of $\underline{\{\ln K\}^{m/n-1}}$ in principle where m is oxidation kinetic parameter and n strain hardening coefficient.

Conclusions (2)

FRI

- The significance of K, yield strength and strain hardening coefficient on CGR was demonstrated by numerical analysis.

- Particularly, numerical calculation showed that CGR under negative dK/dt condition can be much lower than those obtained under constant K or positive dK/dt condition.

Conclusions (3)

FRI

- The effect of dK/dt on CGR can be critical in lifetime prediction of NPP welded components such as VHPs and BMIs in PWR

- Experimental verification of the crack growth behavior under the condition of positive and negative dK/dt would be highly recommended for better lifetime prediction of NPP welded components. Disposition line for flaw evaluation may take into account of these effects on CGR

Hydrogen Assisted Fracture Model Predictions for Alloy 600 PWSCC

Sensitivities of Crack Growth Rate to Applied Stress Intensity Factor, Temperature, Carbon Concentration, Yield Stress and Crack Growth Orientation and coolant-borne hydrogen

M. M. Hall, Jr., W. C. Moshier and D. J. Paraventi

Conference on Vessel Head Penetration
Inspection, Cracking, Repairs

Sponsored by the US NRC and ANL
September 29 – October 2, 2003
Gaithersburg, MD, USA

OUTLINE

- SCC Variables
- HAF Model Concepts and Equation Development
- Experimental
- SCC Data
- Comparisons to Model

Variables Potentially Affecting NiCrFe Alloy PWSCC CGR*

- Alloy and Corrosion Film Composition and Structure
  - chromium and carbon concentrations, carbide morphology and distribution, grain size (Alloy X-750)
  - cold work (yield stress, strain hardening, strain rate sensitivity)
  - crack growth orientation for cold worked material
- Crack Tip Environment
  - $[H^+] = 10^{-pH}$
  - hydrogen over potential $\eta = E - E_r$ where E_r is the reversible H_2 / H^+ potential determined by coolant-borne hydrogen, DH_2
  - temperature
  - other ionic species
- Stress Intensity Factor

* Variables in red are currently included in HAF Model

Hydrogen Assisted Fracture (HAF) Model*
- Concepts -

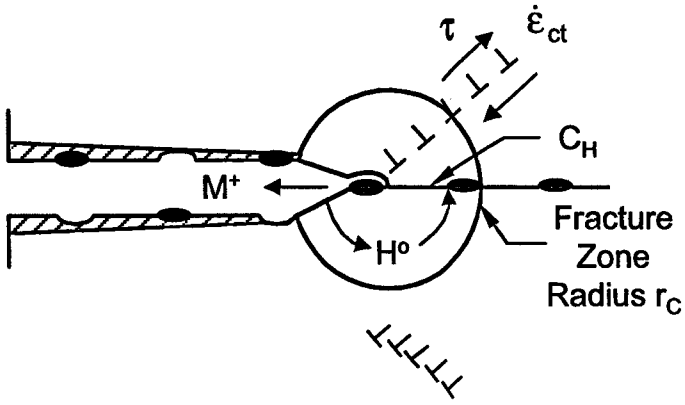

$$\dot{a} = \frac{r_c \dot{\varepsilon}_{ct}}{\varepsilon_f} = \frac{r_c \dot{\varepsilon}_{ct}}{\varepsilon_{fo}} \left(\frac{C_{gb}}{C_o} \right)^{\frac{1}{2}}$$

- Hydrogen evolves at crack tip due to cathodic reduction of water
- Hydrogen absorbs, permeates, diffusively segregates and is trapped at grain boundaries
- Cracks advance due to hydrogen-assisted-creep fracture of hydrogen embrittled grain boundaries
- Rate limiting step potentially may be any of the hydrogen and crack tip strain rate processes

*M. M. Hall, Jr. and D. M. Symons, "Hydrogen Assisted Creep Fracture Model for Low Potential Stress Corrosion Cracking of Ni-Cr-Fe Alloys", Chemistry and Electrochemistry of Stress Corrosion Cracking: A Symposium Honoring the Contributions of R. W. Staehle, R. H. Jones, Ed. TMS, 2001, 447 - 466.

HAF Model Equations

Alloy Composition and Structure

HER/HAR Rate Constant

Coolant Borne H Fugacity

Sievert's Law Constant

H Over Potential, η

~ pH

Strain Hardening $F(\sigma_Y, \text{w/o C})$

Activation Enthalpy for dislocation glide $F(C, \text{orientation})$

H Heat of Solution

Stress Effect on H Solubility

Reversible H_2 Potential $F(DH_2)$

Corrosion Generated Hydrogen Fugacity

gb Trapping Energy

H Diffusivity

$$\dot{a} = \frac{r_c \dot{\varepsilon}_{ct}}{\varepsilon_f} = \frac{r_c \dot{\varepsilon}_o}{\varepsilon_{fo}} \left(\frac{c_{gb}}{c_o}\right)^{\frac{1}{2}} \left(\frac{K - K_{th}}{K_{IC} - K_{th}}\right)^{\frac{2N}{N+1}\frac{\Delta H}{RT}}$$

$$\frac{c_{gb}}{c_o} = \frac{S}{c_o}\left[f_{DH_2} + \kappa[H^+]^2 \exp\left(-\frac{\alpha(E - E_r)F}{RT}\right)\right]^{\frac{1}{2}} \exp\left(\frac{-\Delta H_s + 2\sigma_y \overline{V}_H + \Delta H_b}{RT}\right) \operatorname{erfc}\left(\sqrt{\frac{r_c \dot{a}}{4D_H}}\right)$$

For $T > 250°C$ $\quad f_{DH_2} << f_{CorH_2}$, $\quad \frac{4D_H}{r_c} >> \dot{a} \Rightarrow \operatorname{erfc}\left(\sqrt{\frac{r_c \dot{a}}{4D_H}}\right) \approx 1$

Q_{cor} $\quad Q_{mech}$

$$\dot{a}_{\dot{\varepsilon}} = \frac{r_c \dot{\varepsilon}_o}{\varepsilon_{fo}} \gamma e^{-\frac{\Delta \tilde{H}}{RT}} \left(\frac{K - K_{th}}{K_{IC} - K_{th}}\right)^{\frac{2N}{N+1}\frac{\Delta H}{RT}} = \dot{a}_o \exp\left\{-\frac{\Delta \tilde{H}}{RT} - \frac{2N}{N+1}\frac{\Delta H}{RT} \ln\left(\frac{K_{IC} - K_{th}}{K - K_{th}}\right)\right\}$$

BETTIS ATOMIC POWER LABORATOR

BECHTEL

Slide 5

Modeling Dynamic Strain Aging Effects* on Alloy 600 Crack Growth Rate

Mobile ⊥ x o Interaction Energy

Drag-free Activation Energy

$$\dot{a}_{\dot{\varepsilon}} = \dot{a}_o e^{-\frac{\Delta\tilde{H}}{RT}} \left(\frac{K - K_{th}}{K_{IC} - K_{th}} \right)^{\frac{2N}{N+1}\frac{\Delta H}{RT}}$$

Activation Enthalpy for dislocation glide F(C, orientation)

$$\Delta H = \Delta H^o(C) + U(\bar{n}) = \Delta H^o \left\{ 1 - \alpha \exp\left[-\beta \left(\ln\left(\frac{T}{T_o} \right) \right)^2 \right] \right\} \cong \Delta H^o \left| 1 - \frac{T}{T_o} \right|$$

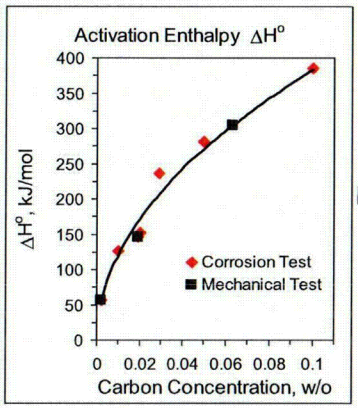

Interaction Strength Factor $F(\sigma_Y, C) \cong 1$ for σ_Y = 826 MPa and 0.063 w/o C

Temperature @ Which Dislocation Wait Time = Solute Diffusion Time

$$T_o \approx \frac{U(\bar{n})/R}{\ln(1/C)}$$

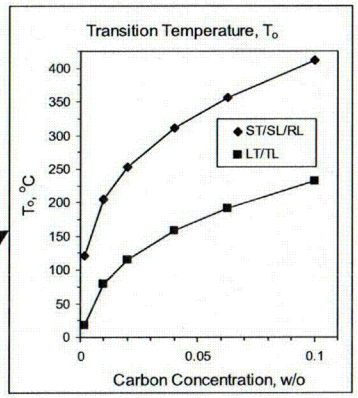

*M. M. Hall and D. M. Symons, "Constitutive Deformation Model for Analysis of Stress Corrosion Crack Tip Strain-Rates in Ni-Cr-Fe Alloy 600", International Conference on Hydrogen Effects on Material Behavior and Corrosion Deformation Interactions, R. Jones, N. Moody, A. Thompson, T. Magnin, R. Ricker and G. Was, Ed., TMS, 2002

C42

Linearized HAF Model Equations

Better Suited for Data Analysis

$$\ln \dot{a} = A_o - A_1 \frac{T_o}{T} \pm A_2 \frac{T_o}{T} \ln K_R \mp A_2 \ln K_R; \quad \pm \Rightarrow \text{orientation}$$

$$A_o = \ln \dot{a}_o \quad A_1 = \frac{\Delta \tilde{H}}{RT_o} \quad A_2 = \frac{2N}{N+1} \frac{\Delta H^o}{RT_o} \quad K_R = \frac{K - K_{th}}{K_{IC} - K_{th}}$$

Experimental

Bettis Data

- Alloy 600 plate given HTA – 1100°C/3600s/FC
- 0.063 w/o Carbon
- Extensive gb decoration with carbides
- 0% – 28% CW (YS 187 MPa – 826 MPa)
- 50 cc/kg dissolved hydrogen
- Conventional FM specimens and test methods
- LT and ST crack growth orientations

SCC Test Conditions

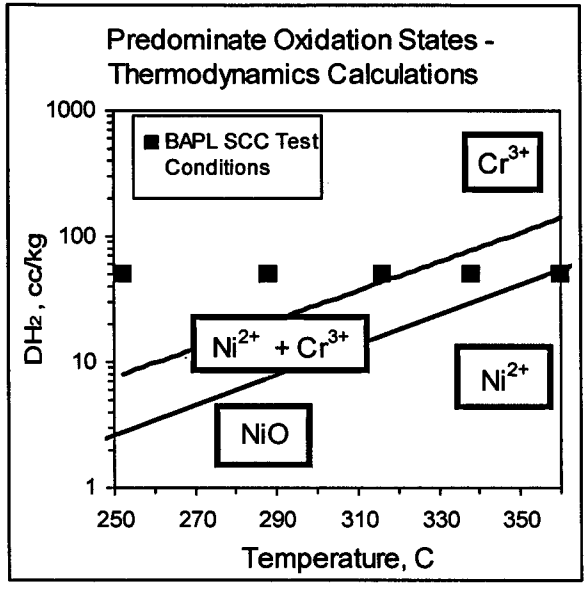

- SCC tests conducted at 252° C to 360° C at or on the Ni side of the Ni - NiO phase field boundary

Crack Growth Orientations for Plate and Bar

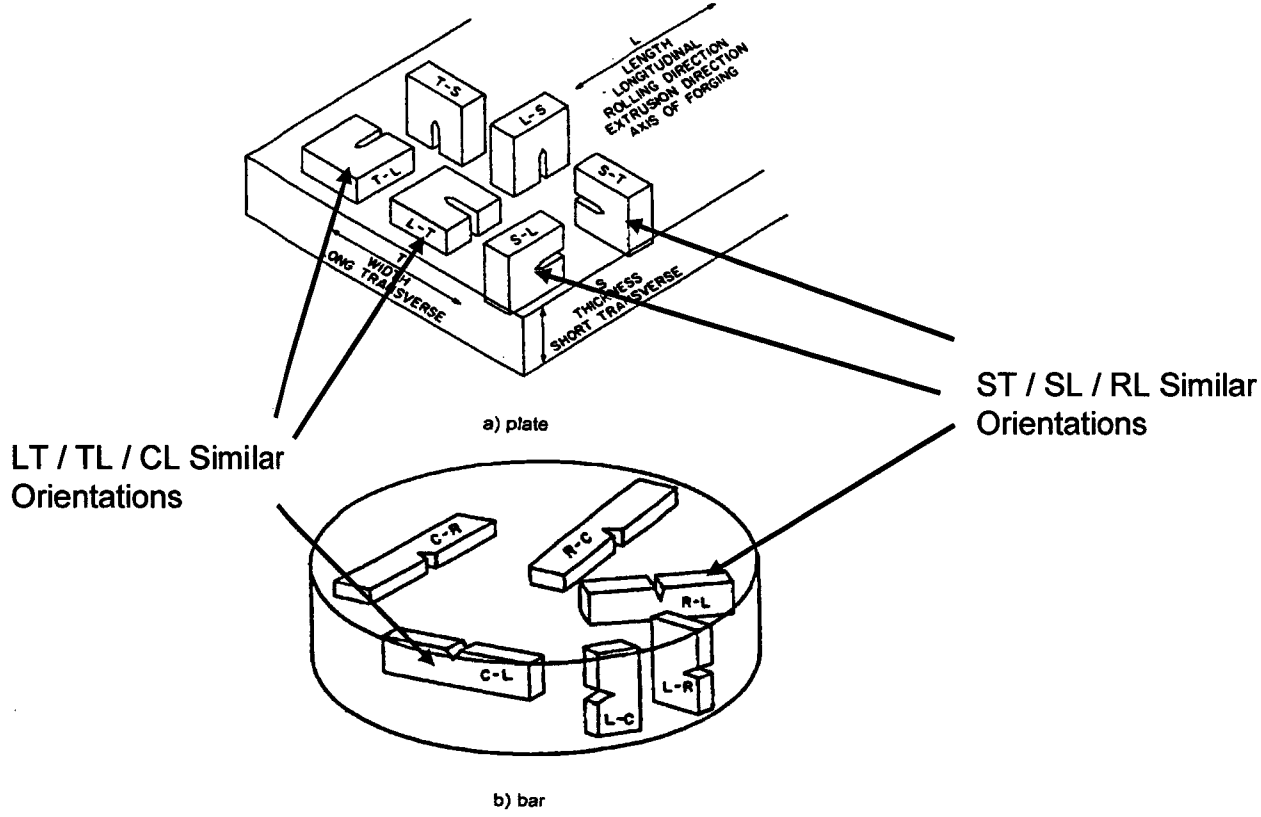

ST / LT orientation CGR data – single heat of Alloy 600

RL / CL orientation CGR data – different heats of Alloy 600

Stress Intensity Factor Exponent m Depends on Temperature and RT Yield Stress

Data Due to Moshier and Paraventi

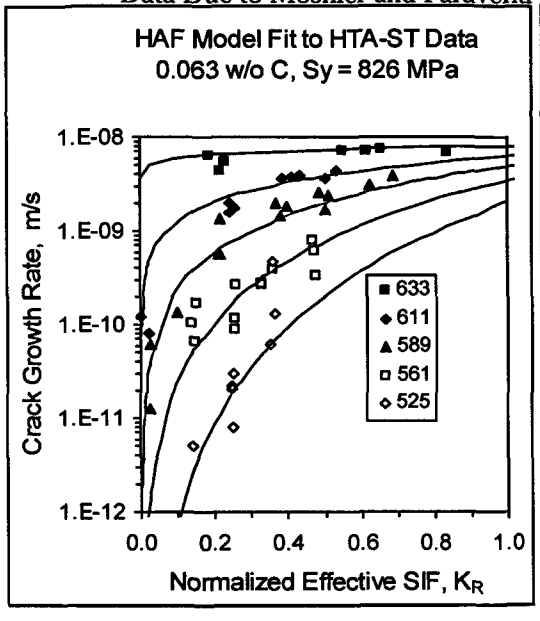

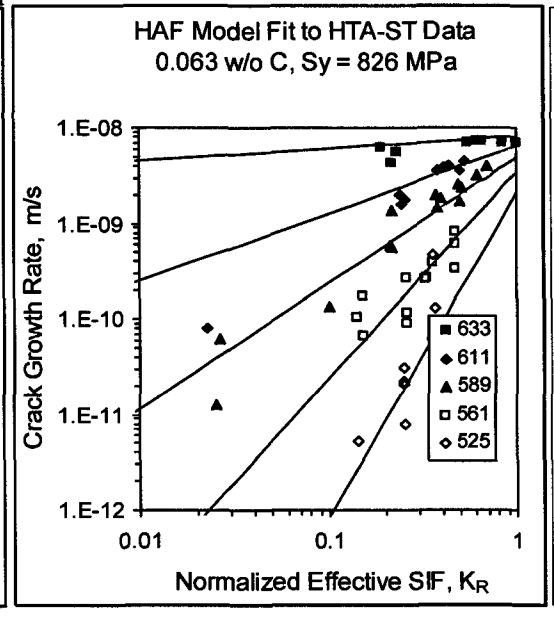

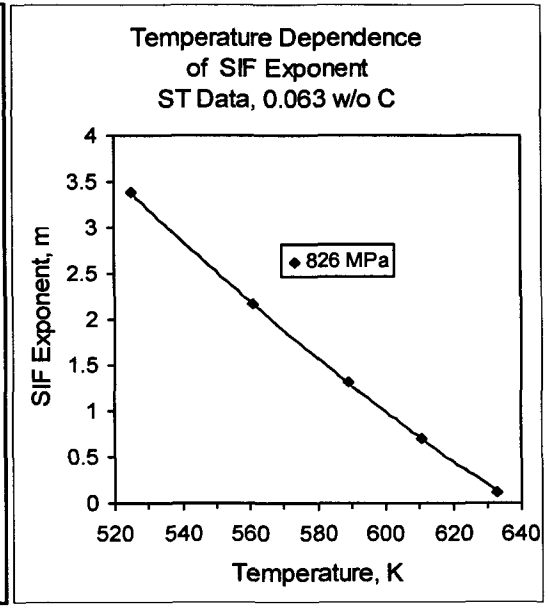

$$K_R \equiv \frac{K - K_{th}}{K_c - K_{th}} \qquad m \equiv \left.\frac{\partial \ln \dot{a}}{\partial \ln K_R}\right|_{T,\eta} \cong \frac{2N}{N+1}\frac{\Delta H^o}{RT}\left(1 - \frac{T}{T_o}\right); \quad T < T_o$$

ST orientation m value decreases with increasing temperature

LT Crack Growth Orientation Unlike ST

Data Due to Moshier and

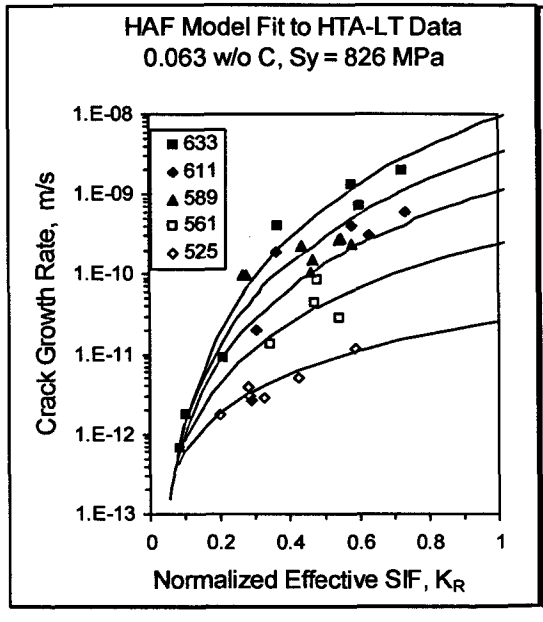

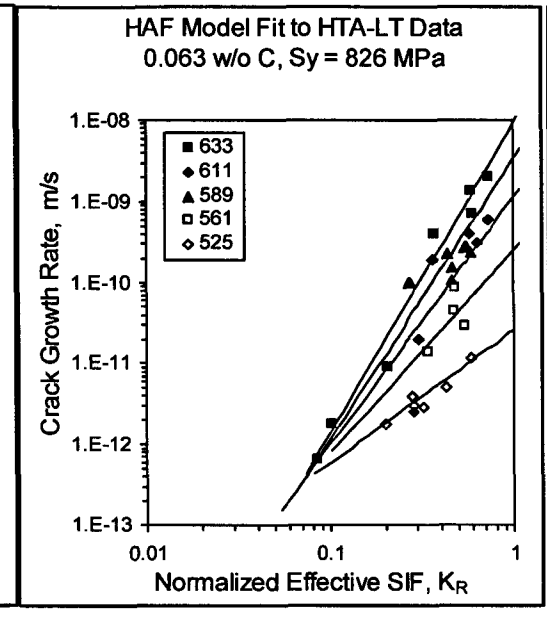

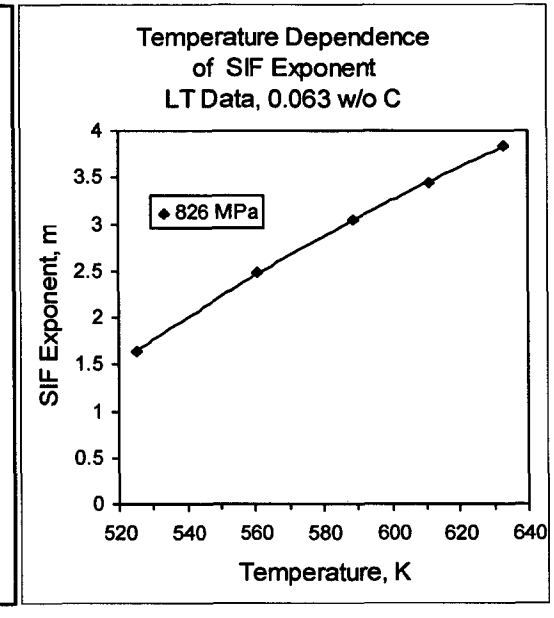

$$K_R \equiv \frac{K - K_{th}}{K_c - K_{th}}$$

$$m \equiv \left.\frac{\partial \ln \dot{a}}{\partial \ln K_R}\right|_{T,\eta} = \frac{2N}{N+1}\frac{\Delta H^o}{RT}\left(\frac{T}{T_o} - 1\right); \quad T > T_o$$

LT orientation m *increases* with increasing temperature

RL Crack Growth Orientation Similar to ST

Data due to Speidel and Magdowski

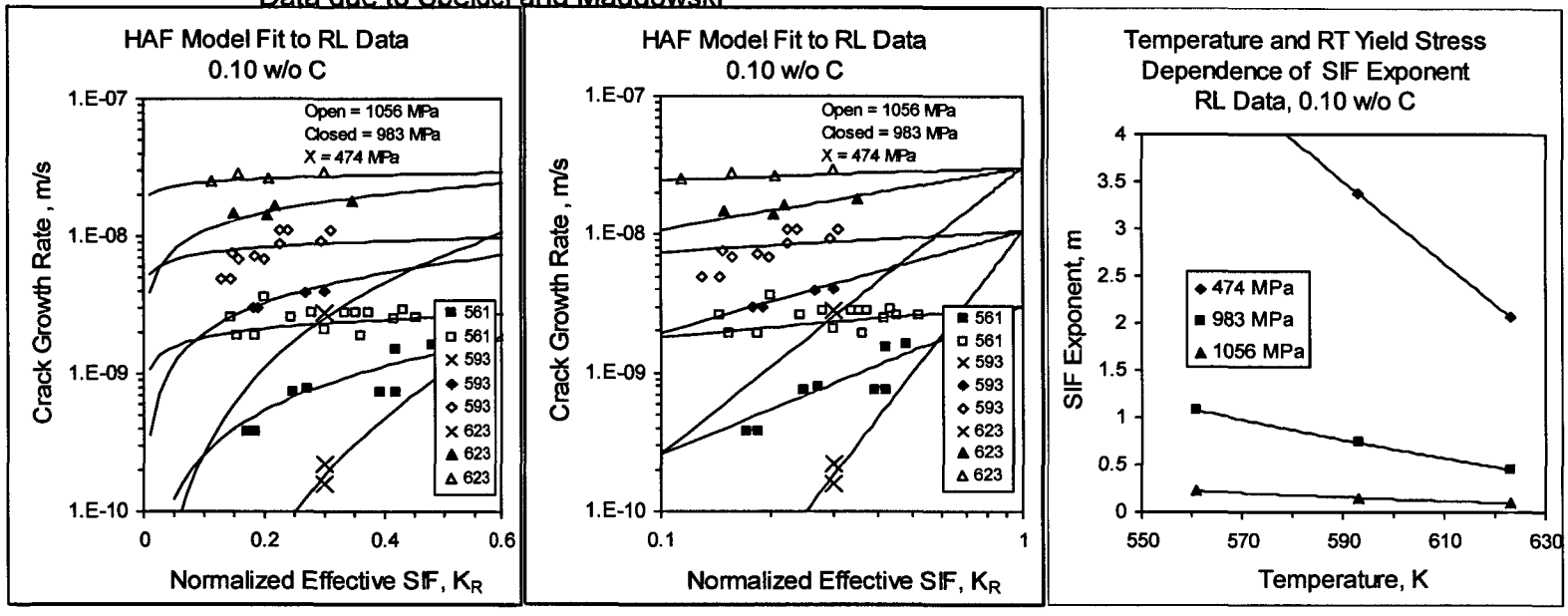

$$K_R \equiv \frac{K - K_{th}}{K_c - K_{th}}$$

$$m \equiv \left.\frac{\partial \ln \dot{a}}{\partial \ln K_R}\right|_{T,\eta} \cong \frac{2N}{N+1}\frac{\Delta H^o}{RT}\left(1 - \frac{T}{T_o}\right); \quad T < T_o$$

RL orientation m decreases with increasing temperature and RT yield stress (pre-strain or CW)

CL Crack Growth Orientation Similar to LT

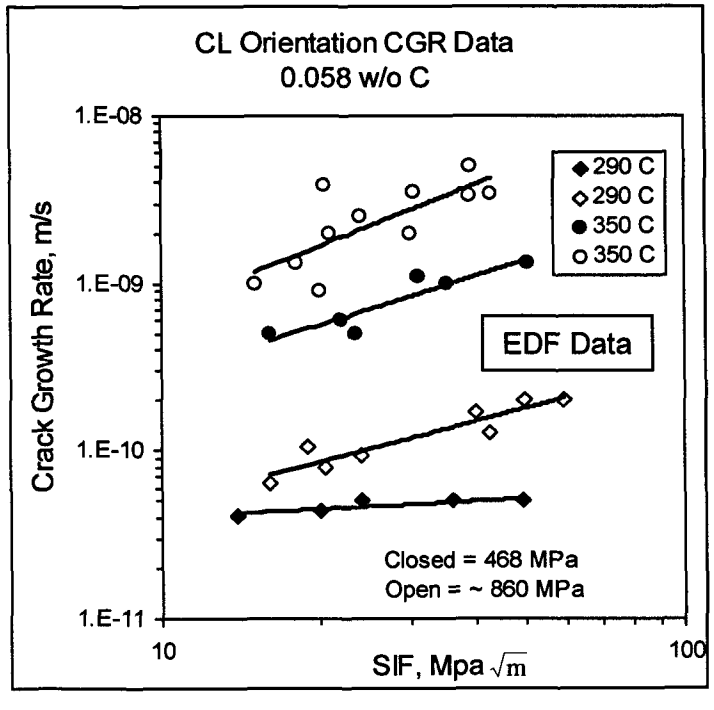

CL orientation m increases with increasing temperature and RT yield stress (pre-strain or CW)

ST Orientation Apparent Activation Energy Q is Decreasing Function of Stress Intensity Factor

Data Due to Moshier and Paraventi

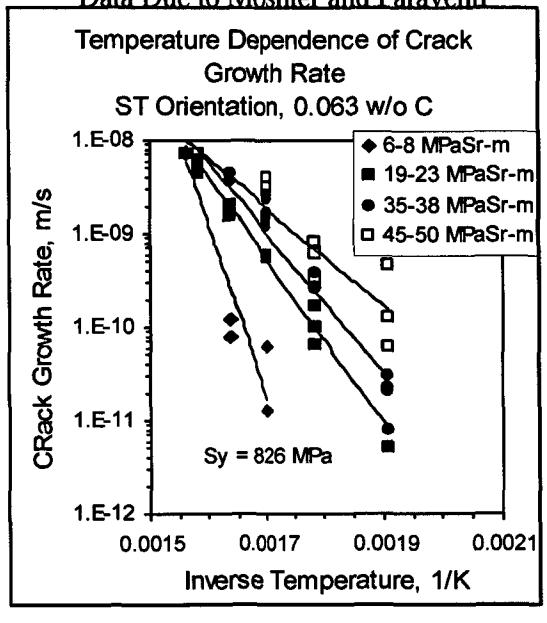

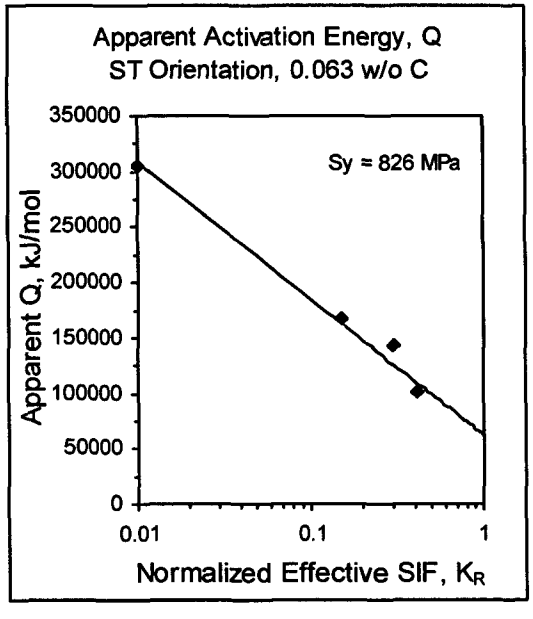

$$Q \equiv -R \left.\frac{\partial \ln \dot{a}}{\partial (1/T)}\right|_{K_R,\eta} = \Delta\tilde{H} - \frac{2N}{N+1}\Delta H^o \ln\left(\frac{K - K_{th}}{K_c - K_{th}}\right)$$

Apparent activation energy Q decreases with increasing Applied Stress Intensity Factor, K

RL Orientation Apparent Activation Energy Q is Decreasing Function of RT Yield Stress

Data due to Speidel and Magdowski

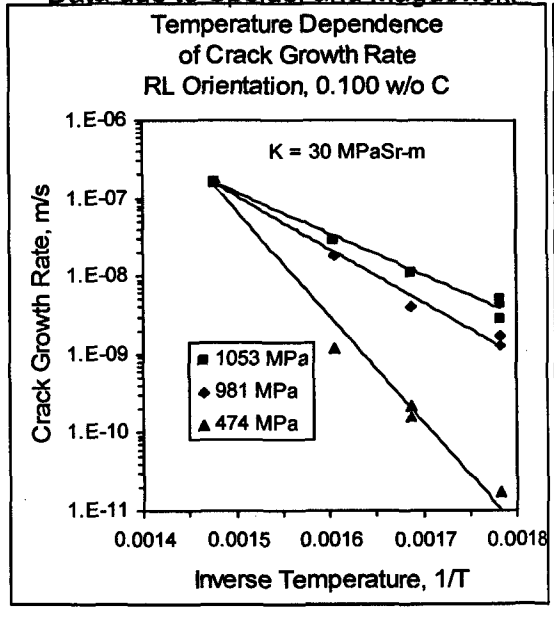

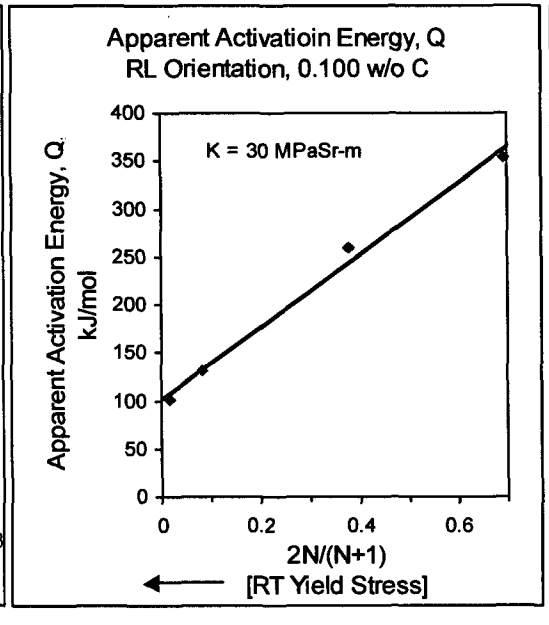

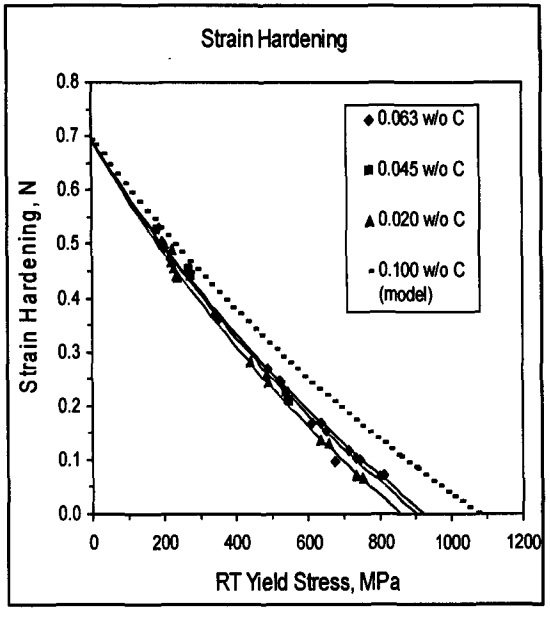

$$Q \equiv -R\left.\frac{\partial \ln \dot{a}}{\partial (1/T)}\right|_{K_R,\eta} = \Delta\tilde{H} - \frac{2N}{N+1}\Delta H^{o} \ln\left(\frac{K-K_{th}}{K_c-K_{th}}\right) \qquad N = \ln\left(\frac{2}{1-\sigma_y/\sigma_s}\right)$$

Apparent activation energy Q decreases with increasing RT yield stress (decreasing strain hardening)

LT Orientation Apparent Activation Energy Q Also is Decreasing Function of RT Yield Stress

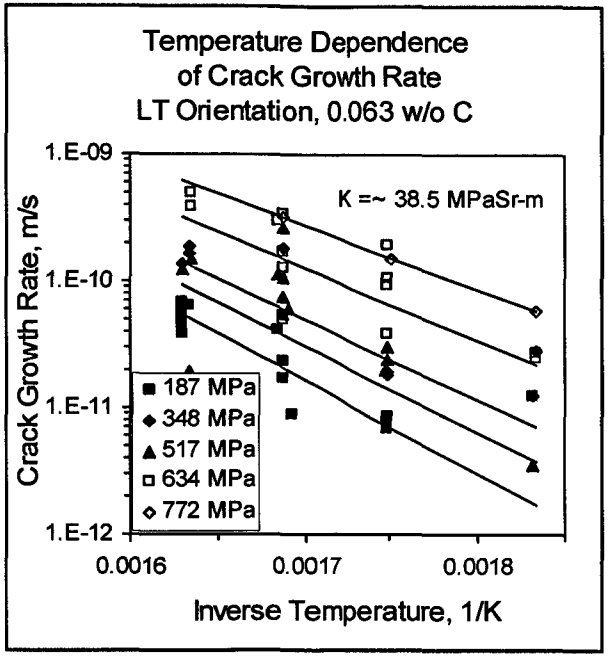

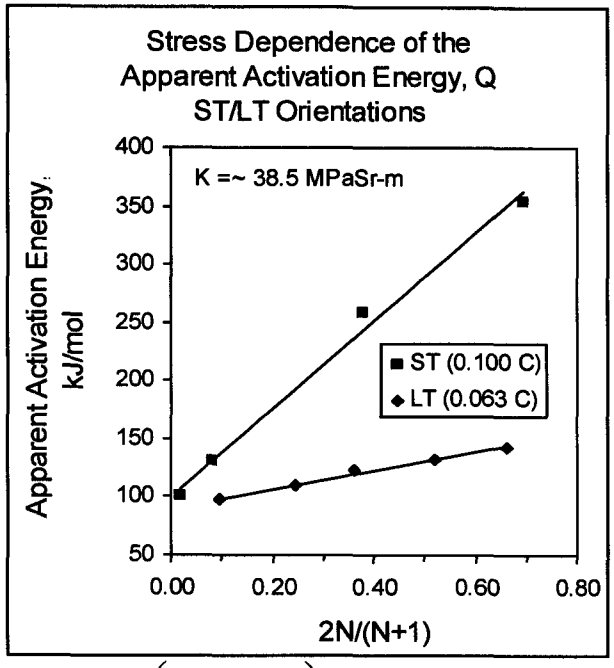

$$Q \equiv -R \left.\frac{\partial \ln \dot{a}}{\partial (1/T)}\right|_{K_R,\eta} = \Delta\tilde{H} - \frac{2N}{N+1}\Delta H^{o} \ln\left(\frac{K - K_{th}}{K_c - K_{th}}\right)$$

LT orientation Q decreases with increasing RT YS (decreasing N) but at a lesser rate than for ST orientation

Reality Checks

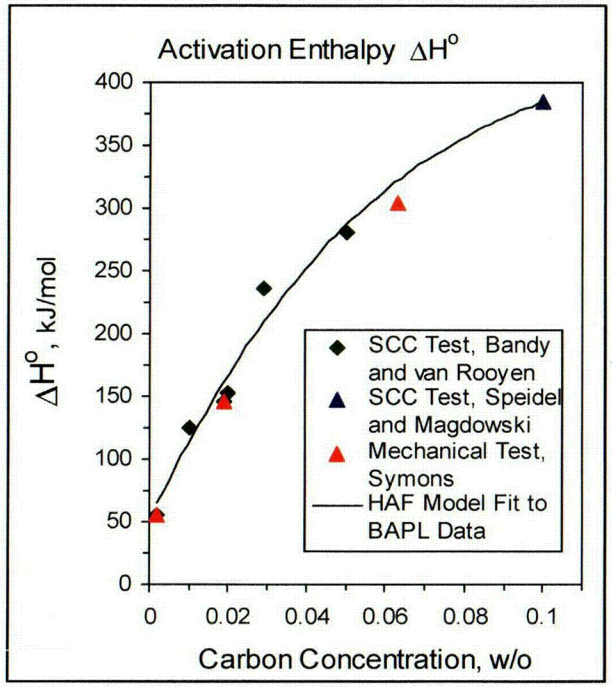

- Model fitting parameters must fall within physical bounds
- Parameter values, e.g, ΔH^o, obtained by fitting models to SCC data should be consistent with data obtained by separate effects tests

Conclusions

- A600 PWSCC is a complex function of the SCC variables
- To capture this complexity requires comprehensive data sets obtained on single heats of Alloy 600
- Physical models help in sorting out complex behaviors and provide higher confidence disposition curves

QUESTIONS?

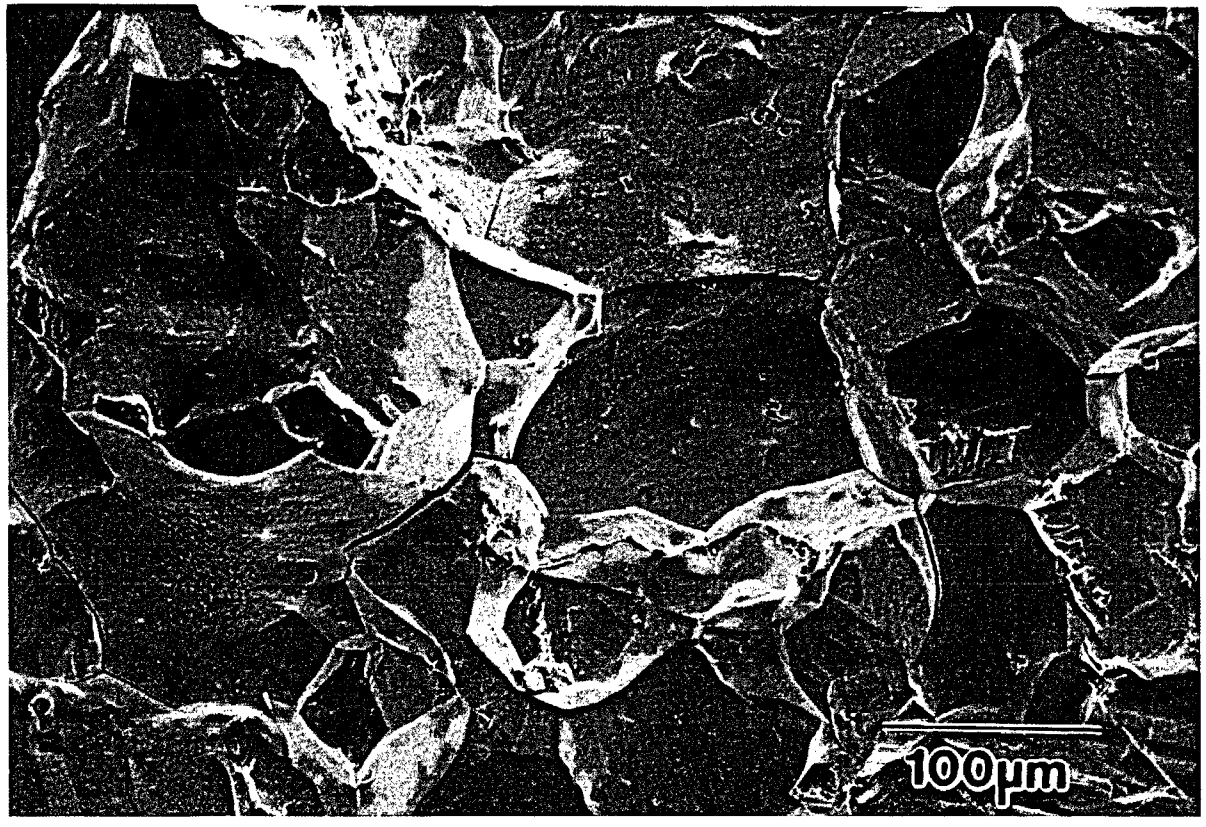

Orientation Dependence of CGR Established by Transition Temperature T_o

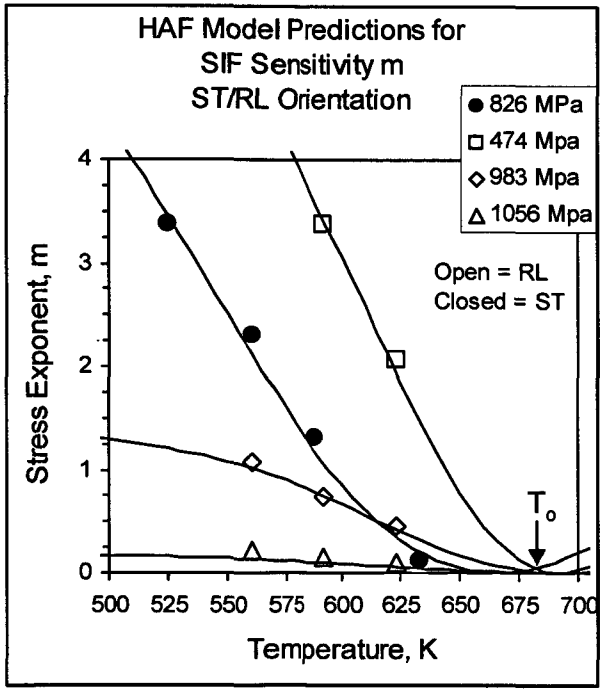

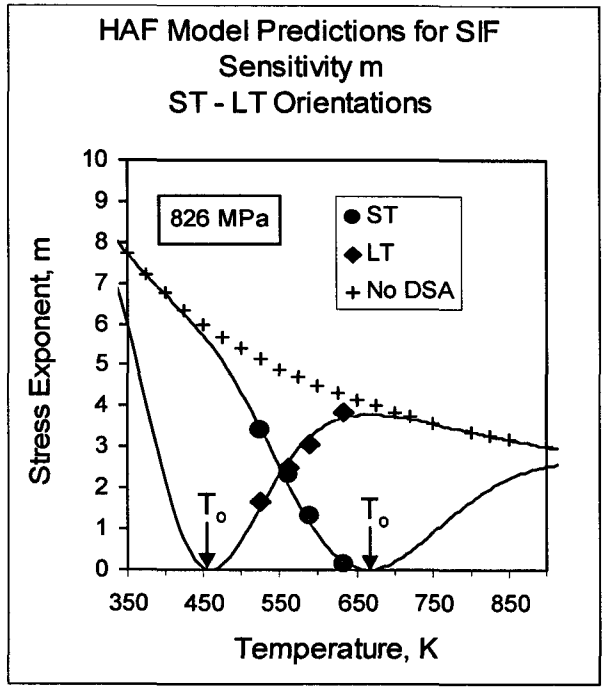

$$m = \frac{2N}{N+1}\frac{\Delta H^o(C) + U(\bar{n})}{RT} = \frac{2N}{N+1}\frac{\Delta H^o}{RT}\left\{1 - \alpha \exp\left[-\beta\left(\ln\left(\frac{T}{T_o}\right)\right)^2\right]\right\}$$

Modeling Coolant Borne Hydrogen Effects on Alloy 600 Crack Growth Rate

DH_2 establishes E_{rev} (H_2 / H^+)

Large DH_2 results in no Ni corrosion and no H_2(cor)

Anode : $Ni + H2O = NiO + 2H^+ + 2e^-$

Cathode : $H^+ + e^- = H^o$; $2H^o \Leftrightarrow H_2(cor)$

$$f_{H_2(cor)} = \kappa [H^+]^2 \exp\left(-\frac{\alpha \eta F}{RT}\right) \propto i_c$$

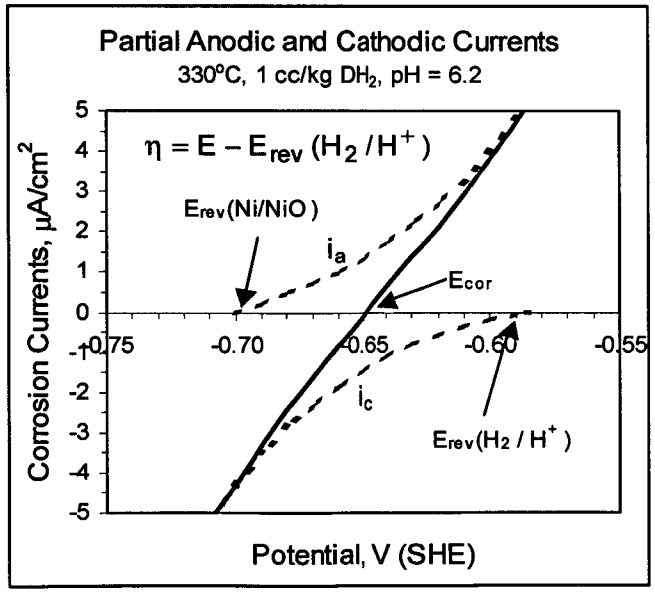

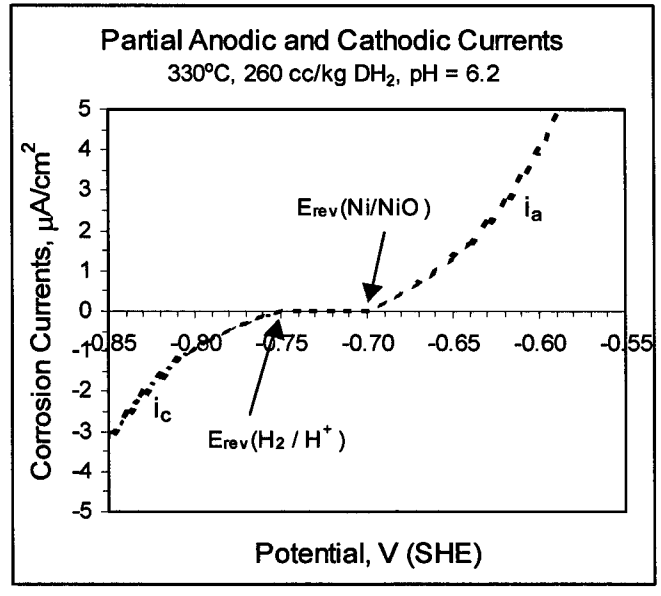

MITSUBISHI HEAVY INDUSTRIES, LTD.
TAKASAGO R&D CENTER

SCC Growth Rate of Nickel Based Alloy 132 Weld Metal

September 29- October 2, 2003
US NRC Conference on
Vessel Penetration Inspection, Cracking and Repairs

T.Yonezawa*, K.Tsutsumi, H.Kanasaki*, K.Yoshimoto*, Y.Nomura*, S.Asada****

*Takasago R & D Center, Mitsubishi Heavy Industries, LTD
**Kobe Shipyard & Machinery Works,
Mitsubishi Heavy Industries, LTD

MITSUBISHI HEAVY INDUSTRIES, LTD.
TAKASAGO R&D CENTER

CONTENTS

1. INTRODUCTION
2. EXPERIMENTAL PROCEDURES
3. RESULTS
4. DISCUSSIONS
5. SUMMARY

MITSUBISHI HEAVY INDUSTRIES, LTD.
TAKASAGO R&D CENTER

CONTENTS

1. INTRODUCTION
2. EXPERIMENTAL PROCEDURES
3. RESULTS
4. DISCUSSIONS
5. SUMMARY

INTRODUCTION

MITSUBISHI HEAVY INDUSTRIES, LTD. TAKASAGO R&D CENTER

In Japan, maintenance guide rule as ASME Sec.XI for allowable SCC flaw size is not established except austenitic stainless steels for BWRs.

In order to complete data base for the maintenance guide rule for allowable SCC flaw size, the Japanese national project on SCCGR measurement test program on the Alloy 600 and its weld metals of Ni based alloys for PWRs and BWRs has been started from April 2000.

Before starting this project, MHI has checked the propriety and applicability of periodic unloading method for PWSCC GR measurement test.

INTRODUCTION (Contd.)

MITSUBISHI HEAVY INDUSTRIES, LTD. TAKASAGO R&D CENTER

In western PWR plants, Alloy 182 is used for SMAW to Alloy 600. In Japanese PWR plants, Alloy 132 was used for different welding method (:alternating current as welding electric current) as the SMAW and consideration of resistance of hot cracking.

INTRODUCTION (Contd.)

MITSUBISHI HEAVY INDUSTRIES, LTD. TAKASAGO R&D CENTER

Japanese Status on Welding Materials for RV Nozzles

Table Difference of Welding Materials between Japan & Western Countries

	Japanese PWRs	Western PWRs
Welding Materials	Alloys 132 and 82	Alloys 182 and 82
Yield Strength of Base Metal (MPa)	200～350	300～500
Surface Finishing	Polished by Buff	Grinded

Alloy 132 : 70Ni-15Cr-9Fe-1Mn-2.5Nb
182 : 67Ni-15Cr-8Fe-7Mn-1.8Nb-0.5Ti
82 : 71Ni-20Cr-2Fe-3Mn-2.5Nb-0.5Ti

PWSCC CGR is affected by the material properties

INTRODUCTION (Contd.)

MITSUBISHI HEAVY INDUSTRIES, LTD. TAKASAGO R&D CENTER

The effect of Cr content on PWSCC susceptibility of Alloy 600.

- The PWSCC susceptibility of Alloy 600 decreases with increasing of Cr content.
- Alloy 132, 182 ; 15Cr
  82 ; 20Cr

↓

- The stress corrosion cracking resistance of Alloy 82 may be higher than that of Alloy 132 and 182.

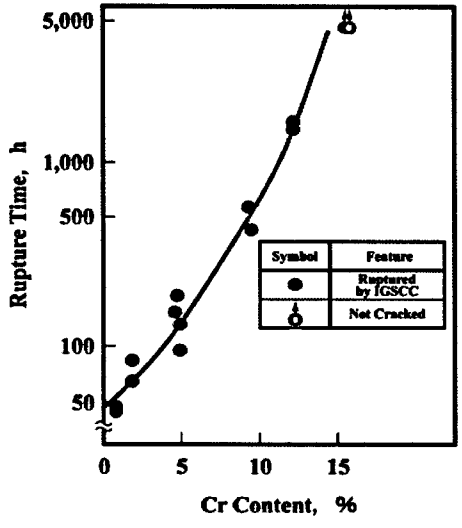

Fig 6. Effect of Cr content on the stress corrosion cracking resistance of solution annealed Ni base-Cr-Fe alloys in 360℃ high temperature water using by constant load stress corrosion cracking test (applied stress is 2.4 × 0.2% Proof stress)

INTRODUCTION (Contd.)

MITSUBISHI HEAVY INDUSTRIES, LTD. TAKASAGO R&D CENTER

The effect of Nb content on PWSCC susceptibility of Alloy 600.

- Nb and Ti addition increase PWSCC susceptibility of Alloy600, due to suppressing of IG carbides precipitation.

- Alloy 132 ; 2.5Nb
  182 ; 1.8Nb-0.5Ti
  82 ; 2.5Nb-0.5Ti

- The susceptibility of Alloy 132 may be same as that of Alloy 182.

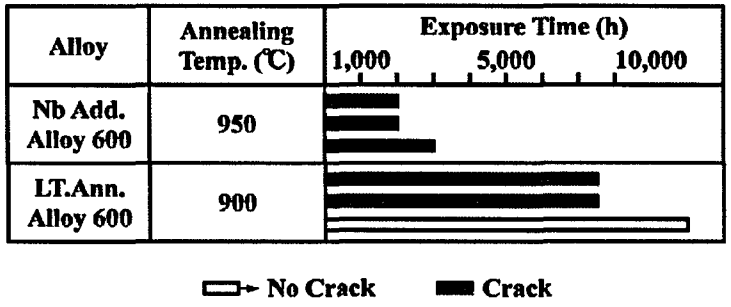

Fig7. Effect of Nb addition on the sress corrosion cracking resistance of annealed Alloy 600 in 360℃ high temperature water, using by prestrained U bent specimen.

INTRODUCTION (Contd.)

MITSUBISHI HEAVY INDUSTRIES, LTD. TAKASAGO R&D CENTER

In western PWR plants, Alloy 182 is used for SMAW to Alloy 600. In Japanese PWR plants, Alloy 132 was used for different welding method (:alternating current as welding electric current) as the SMAW and consideration of resistance of hot cracking.

⇩

In this study, we tested the PWSCC growth rate of Alloys 132 and 82 welded.

OBJECTIVES

MITSUBISHI HEAVY INDUSTRIES, LTD. TAKASAGO R&D CENTER

To compared the PWSCC growth rates of Alloys 132 and 82 with literature data on Alloy 182.

To recommend PWSCC GR measurement test techniques. (The propriety and applicability of periodic unloading method for PWSCC GR measurement test.)

MITSUBISHI HEAVY INDUSTRIES, LTD.
TAKASAGO R&D CENTER

CONTENTS

1. INTRODUCTION
2. EXPERIMENTAL PROCEDURES
3. RESULTS
4. DISCUSSIONS
5. SUMMARY

EXPERIMENTAL PROCEDURES

MITSUBISHI HEAVY INDUSTRIES, LTD.
TAKASAGO R&D CENTER

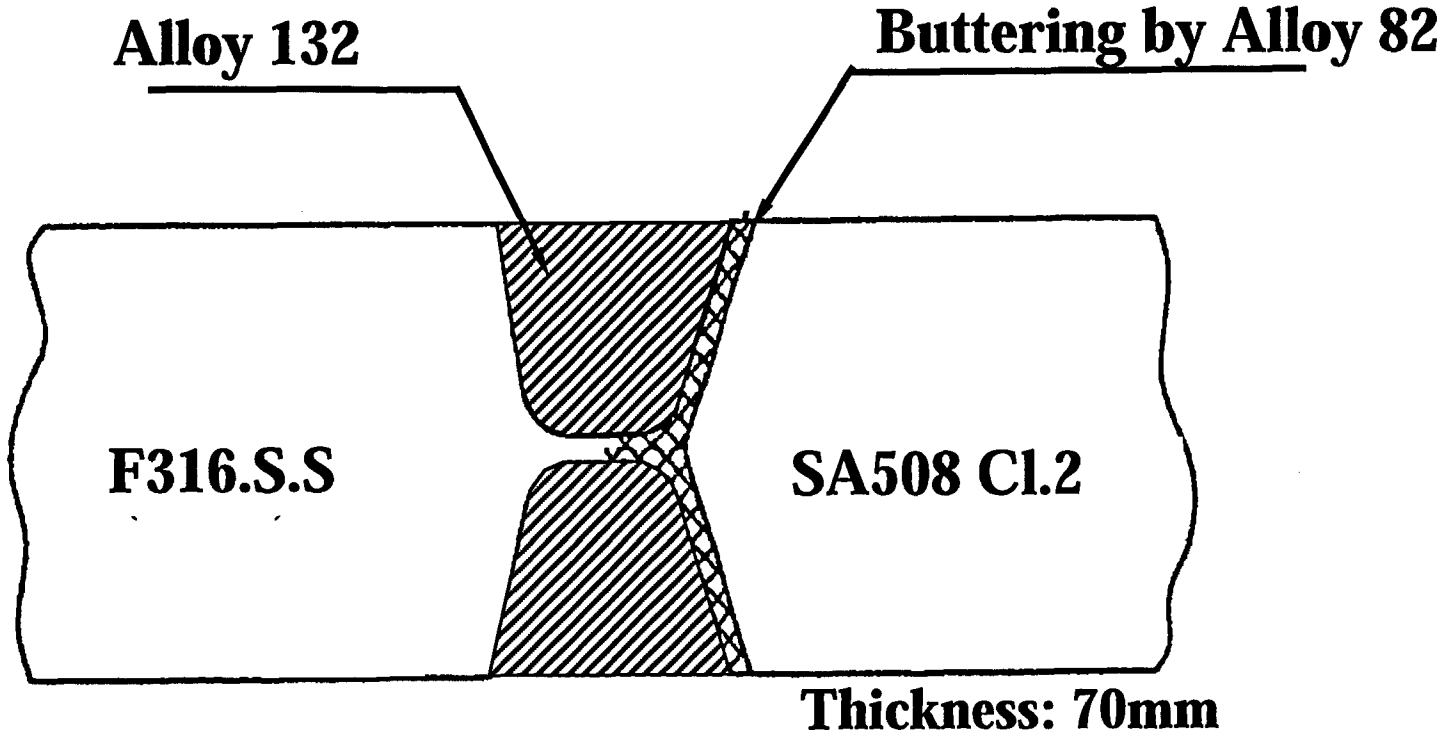

Figure Welding joint configuration of dissimilar metal arc welding model by Alloy 132

EXPERIMENTAL PROCEDURES

MITSUBISHI HEAVY INDUSTRIES, LTD.
TAKASAGO R&D CENTER

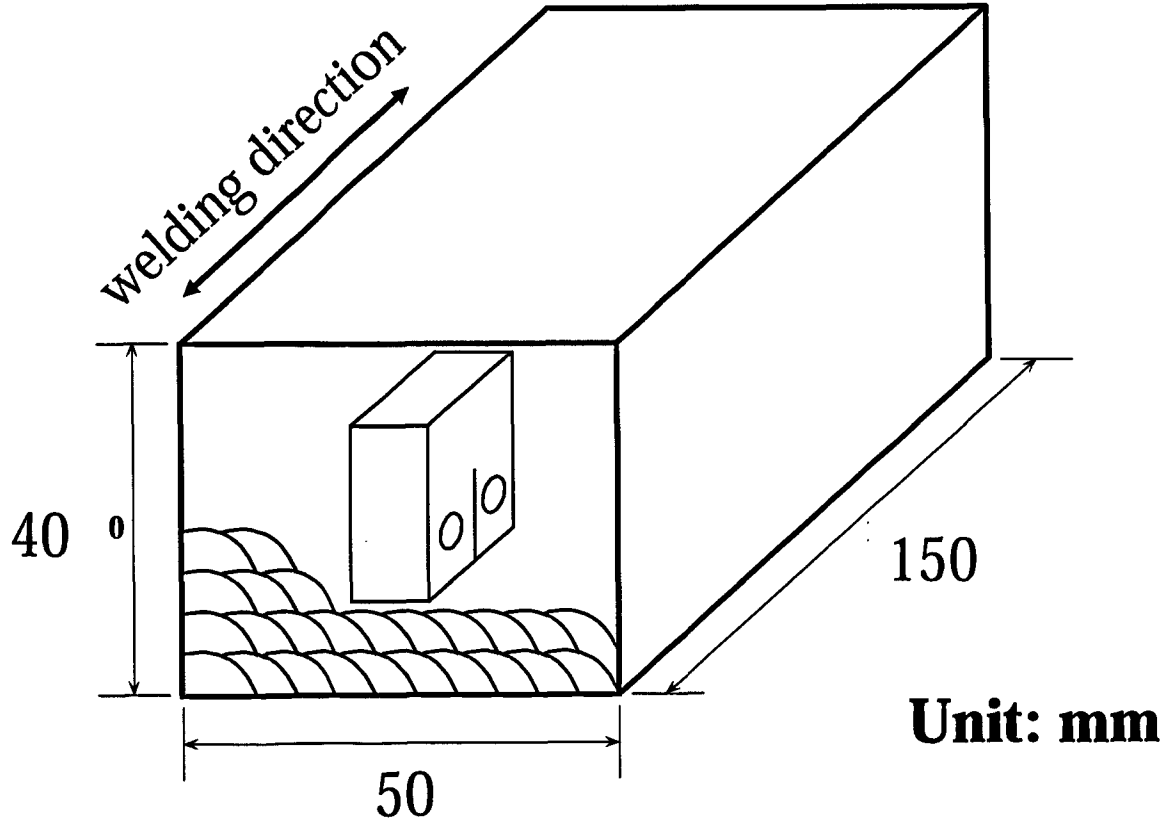

Figure **Machining orientation of CT specimens from deposited metal model of TIG welding by Alloy 82**

EXPERIMENTAL PROCEDURES

MITSUBISHI HEAVY INDUSTRIES, LTD.
TAKASAGO R&D CENTER

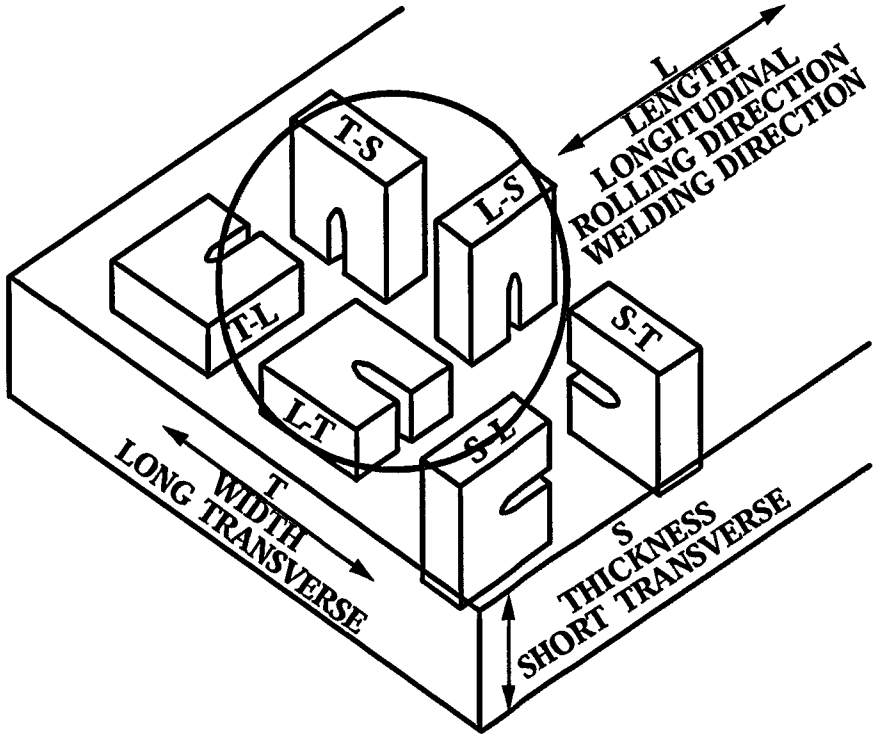

Test Specimens

1/2T CT

Specimen Orientation

TS, LS, LT

The pre-crack length about 1mm

K_I values

20, 35, 60 MPa $\sqrt{m}$

Figure Terminology used for orientation of cracks in the test specimens with respect to the weld

EXPERIMENTAL PROCEDURES

MITSUBISHI HEAVY INDUSTRIES, LTD.
TAKASAGO R&D CENTER

Testing Environment

Temperature	; 325°C
H_3BO_3	; 1800 ppm as Boron
LiOH	; 3.5 ppm as Lithium
DH_2	; 30cc/kg STP H_2O
DO_2	; <5ppb
Autoclave	; refreshed type

EXPERIMENTAL PROCEDURES

MITSUBISHI HEAVY INDUSTRIES, LTD. TAKASAGO R&D CENTER

The periodic unloading conditions for Alloys 132 and 82, to evaluate the effect of the periodic unloading condition on the CGRs of weld metals.

(1) Trapezoidal wave 1 : R = 0.7, holding time : 360 seconds (0.1 hours)
(2) Trapezoidal wave 2 : R = 0.7, holding time : 1,080 seconds (0.3 hours)
(3) Trapezoidal wave 3 : R = 0.7, holding time : 9,000 seconds (2.5 hours)
(4) Constant loading

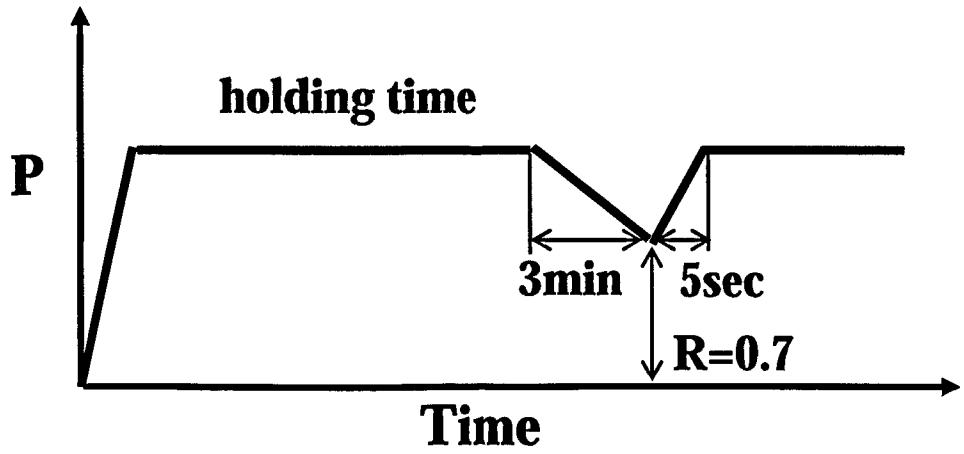

Figure Trapezoidal Wave form

EXPERIMENTAL PROCEDURES

MITSUBISHI HEAVY INDUSTRIES, LTD. TAKASAGO R&D CENTER

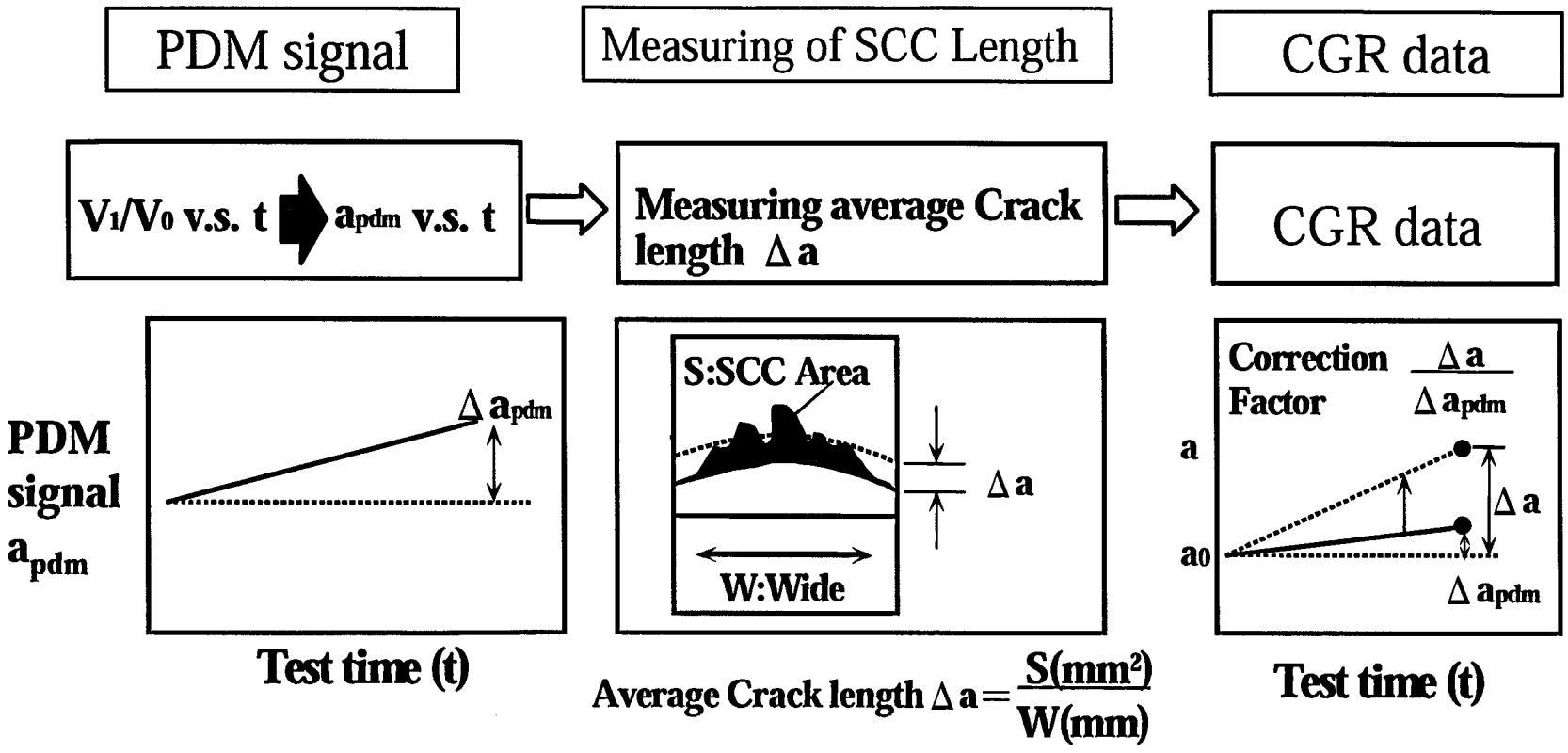

Figure CGR evaluation method

MITSUBISHI HEAVY INDUSTRIES, LTD. TAKASAGO R&D CENTER

CONTENTS

1. INTRODUCTION
2. EXPERIMENTAL PROCEDURES
3. RESULTS
   1) Effect of K value on the PWSCC
   2) Fractography in respect of dendrite orientations
   3) CGR of Alloys 132,82 and 182
4. DISCUSSIONS
5. SUMMARY

RESULTS (Effect of K value)

MITSUBISHI HEAVY INDUSTRIES, LTD. TAKASAGO R&D CENTER

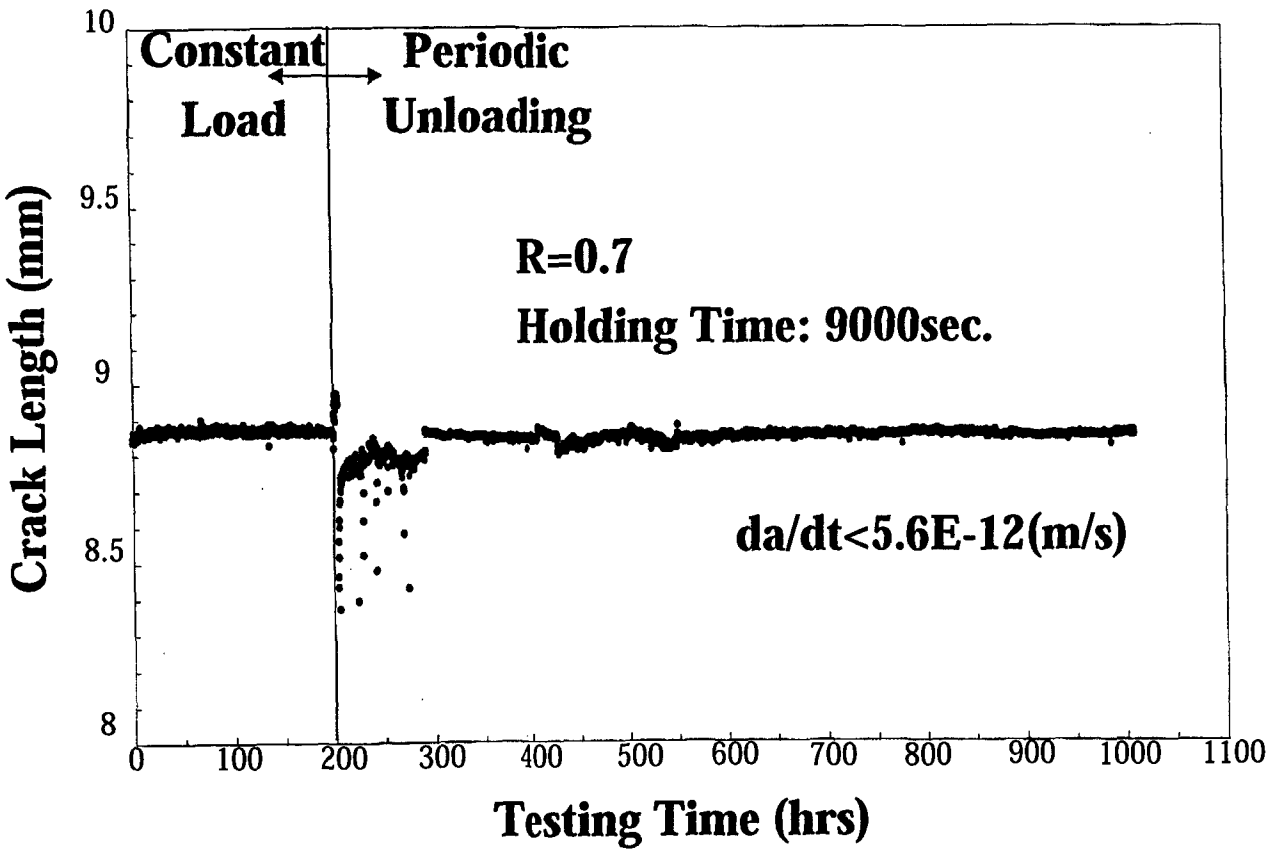

Alloy 132,

K_I values :20 MPa√m,

TS orientation

Figure CGR on-line monitoring results

RESULTS (Effect of K value)

MITSUBISHI HEAVY INDUSTRIES, LTD.
TAKASAGO R&D CENTER

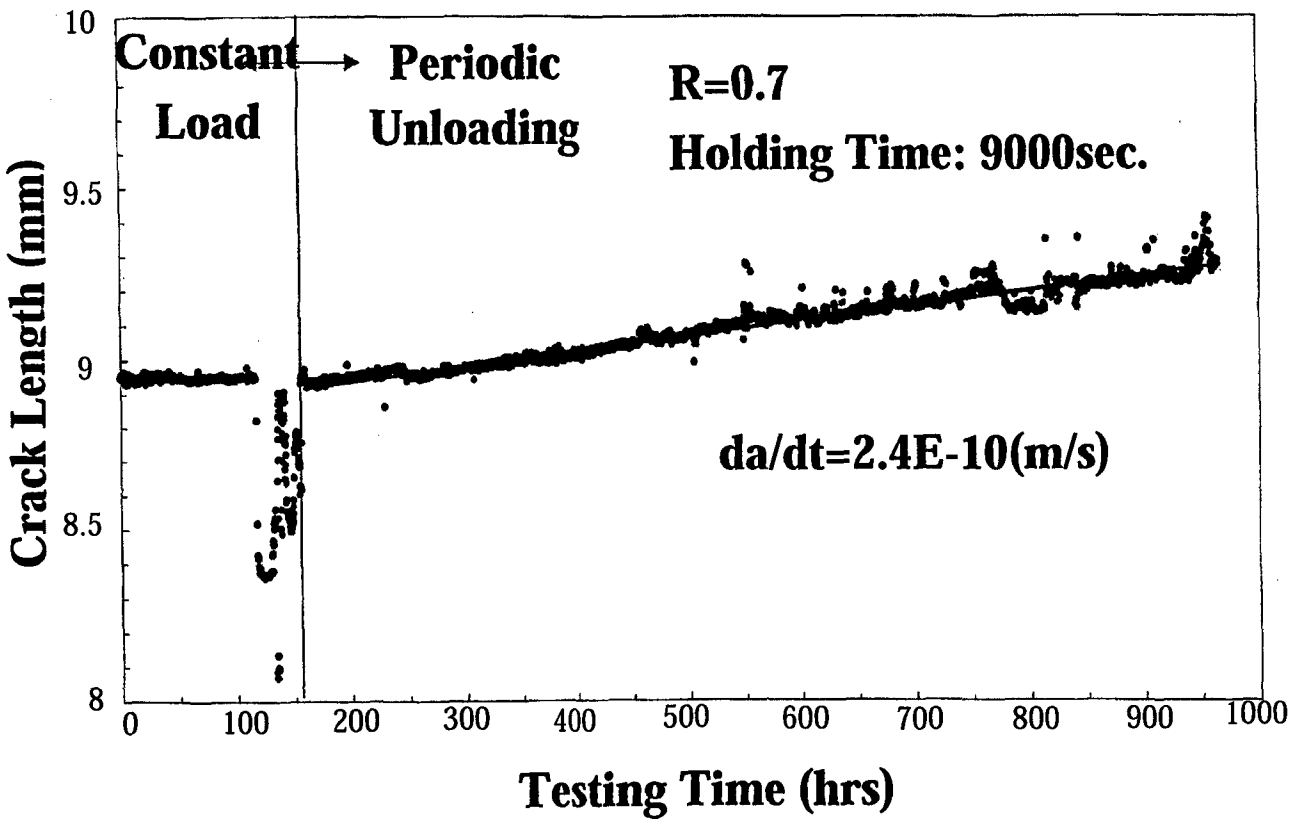

Alloy 132,

K_I values :35MPa√m,

TS orientation

Figure CGR on-line monitoring results

RESULTS (Fractography)

MITSUBISHI HEAVY INDUSTRIES, LTD.
TAKASAGO R&D CENTER

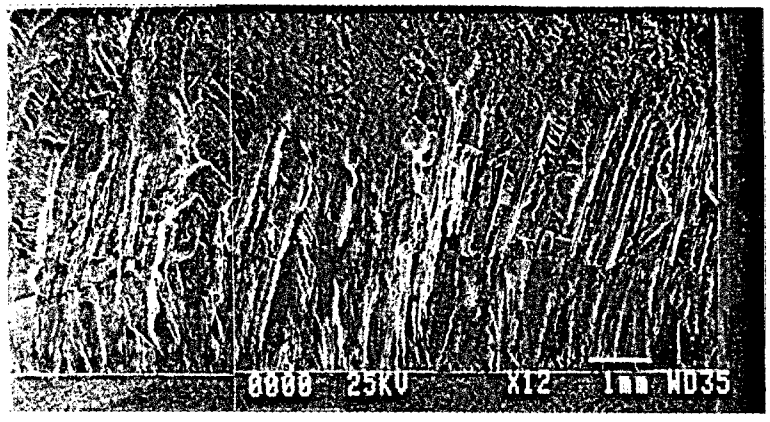

SEM

The crack front of these inter-dendritic PWSCC was not uniform and the area of no ID PWSCC initiation zone was also observed at the fatigue pre-crack tip.

The crack propagation path was inter-dentrite and parallel direction for dendrite.

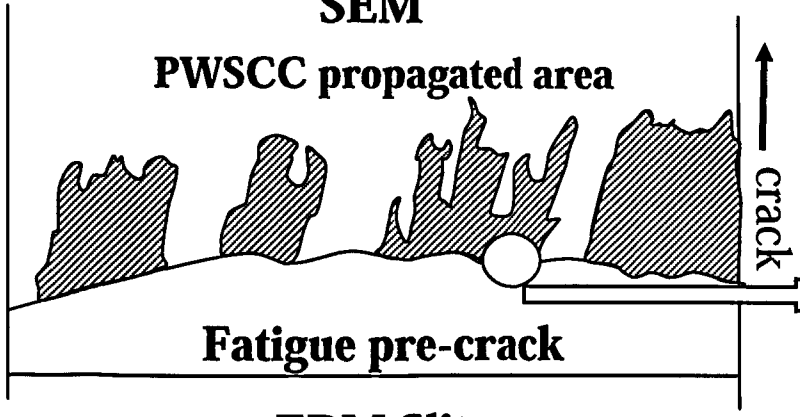

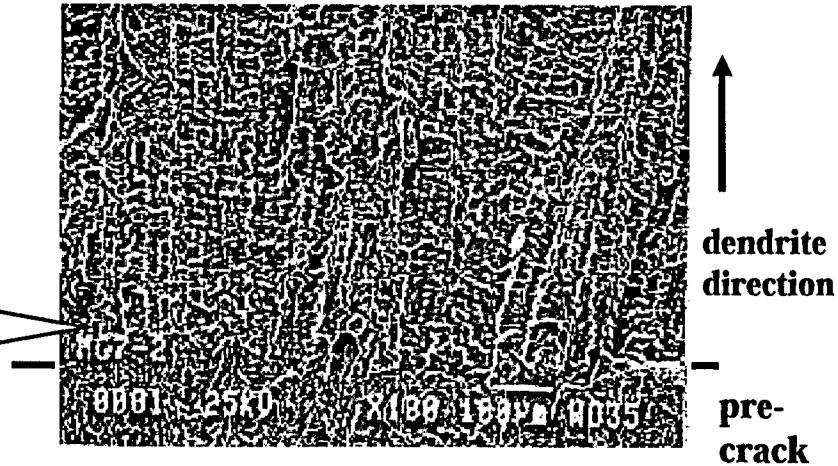

Inter-dentrite

Figure Fractography of TS specimen after SCC test

RESULTS (Fractography)

MITSUBISHI HEAVY INDUSTRIES, LTD.
TAKASAGO R&D CENTER

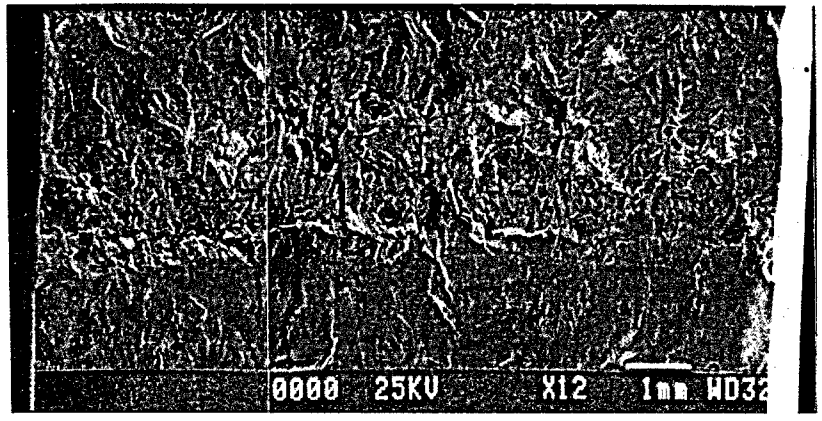

The crack front of these inter-dendritic PWSCC was complicated and not uniform.

The crack propagation path was inter-dentrite and perpendicular direction for dendrite.

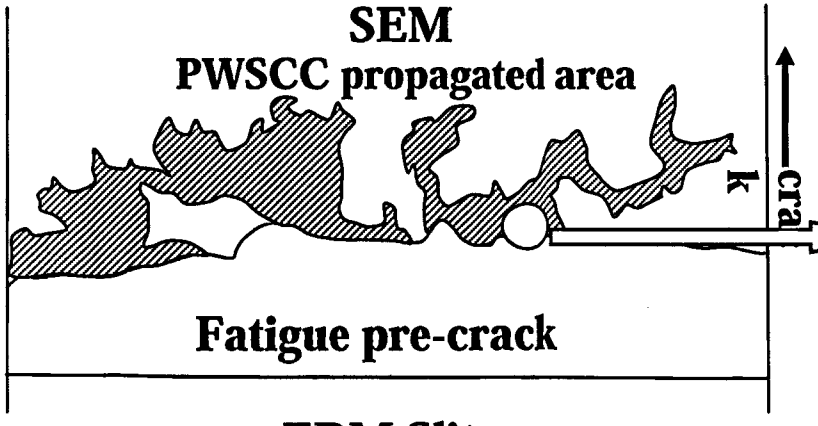

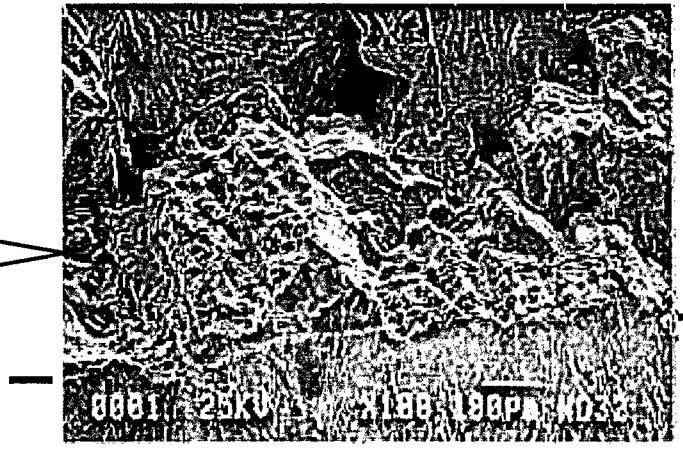

Inter-dentrite

Figure Fractography of LT specimen after SCC test

RESULTS (CGR of Alloys 132, 82 and 182)

MITSUBISHI HEAVY INDUSTRIES, LTD. TAKASAGO R&D CENTER

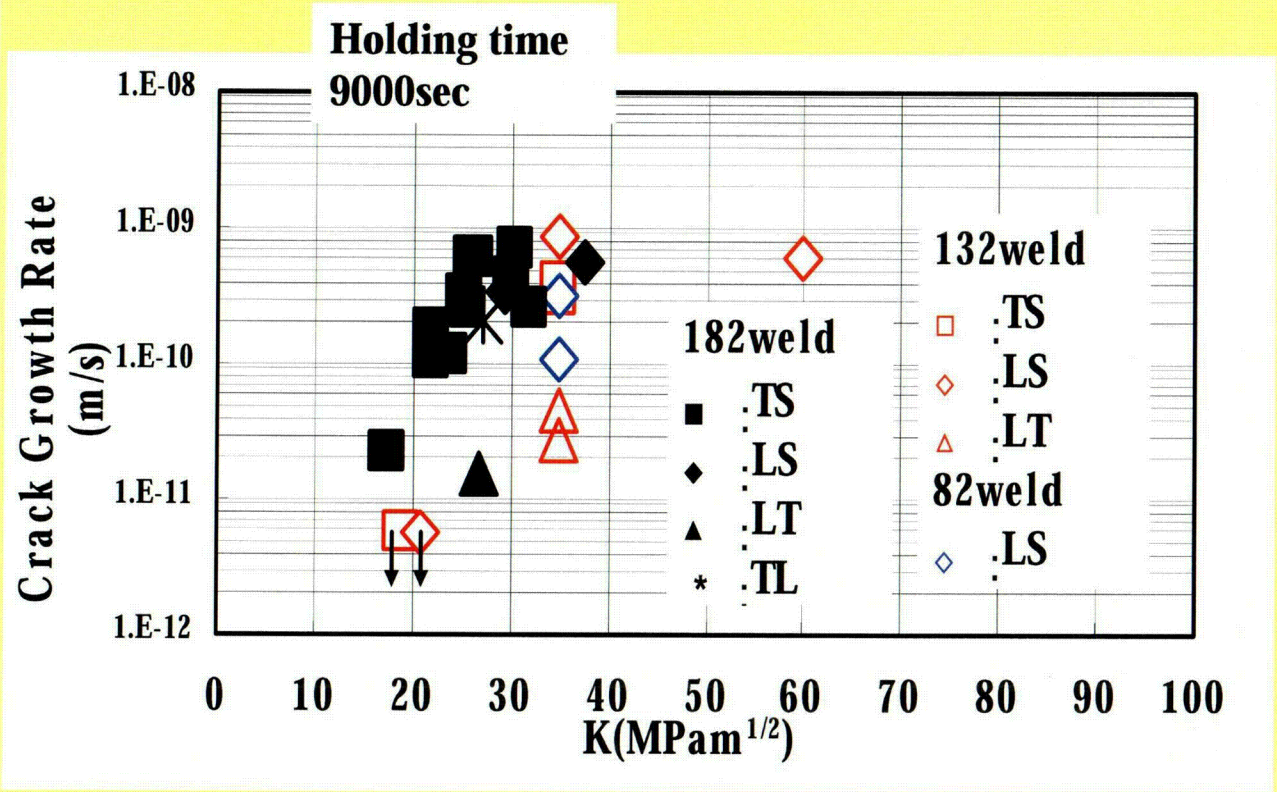

PWSCC CGRs

1) Alloy 132 ≥ Alloy 82
2) LS, TS > LT
3) LS nearly equal to TS

Figure Comparison between CGR of Alloys 132, 82 and 182 weld metal

C44

RESULTS (CGR of Alloys 132,82 and 182)

MITSUBISHI HEAVY INDUSTRIES, LTD. TAKASAGO R&D CENTER

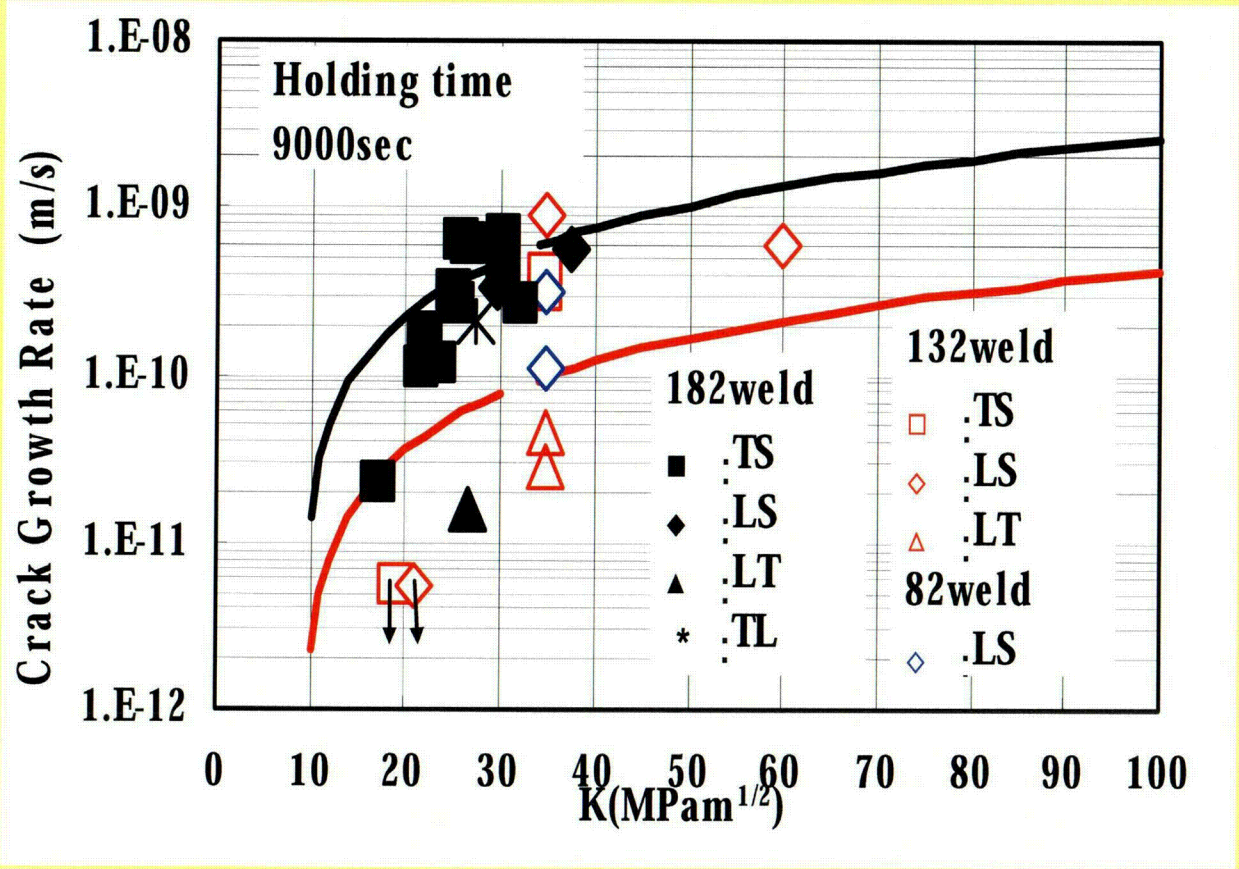

182 weld(325°C)
W.Banford

Alloy 600 (325°C)
P.Scott

PWSCC GRs

Alloy 182

≒ Alloy132

> Alloy600

Figure Comparison between CGR of Alloys 132, 82 and 182 weld metal

C45

MITSUBISHI HEAVY INDUSTRIES, LTD.
TAKASAGO R&D CENTER

CONTENTS

1. INTRODUCTION
2. EXPERIMENTAL PROCEDURES
3. RESULTS
4. DISCUSSIONS
"the effect of periodic unloading on the CGR".
(1) Maintaining of the straight crack front
(2) The effect of the holding time on acceleration of the SCC GR
(3) Reducing SCC incubation time
5. SUMMARY

DISCUSSIONS

MITSUBISHI HEAVY INDUSTRIES, LTD. TAKASAGO R&D CENTER

1. Maintaining of the straight crack front

The straight crack front was not gained for the specimens of the Alloy 132 under constant loading in spite of periodic unloading.

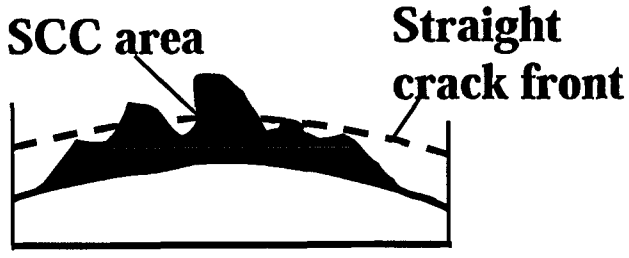

The PWSCC susceptibility is affected by the Metal. Condi. of the G.B. And the Metal. Condi. of G.B. for W.M. is very complicated.

The periodic unloading method has not to be applicable for the ID PWSCC GR measurement of Ni based W. M., to maintain the straight crack front.

DISCUSSIONS

MITSUBISHI HEAVY INDUSTRIES, LTD.
TAKASAGO R&D CENTER

2. The effect of holding time on acceleration of the SCC GR

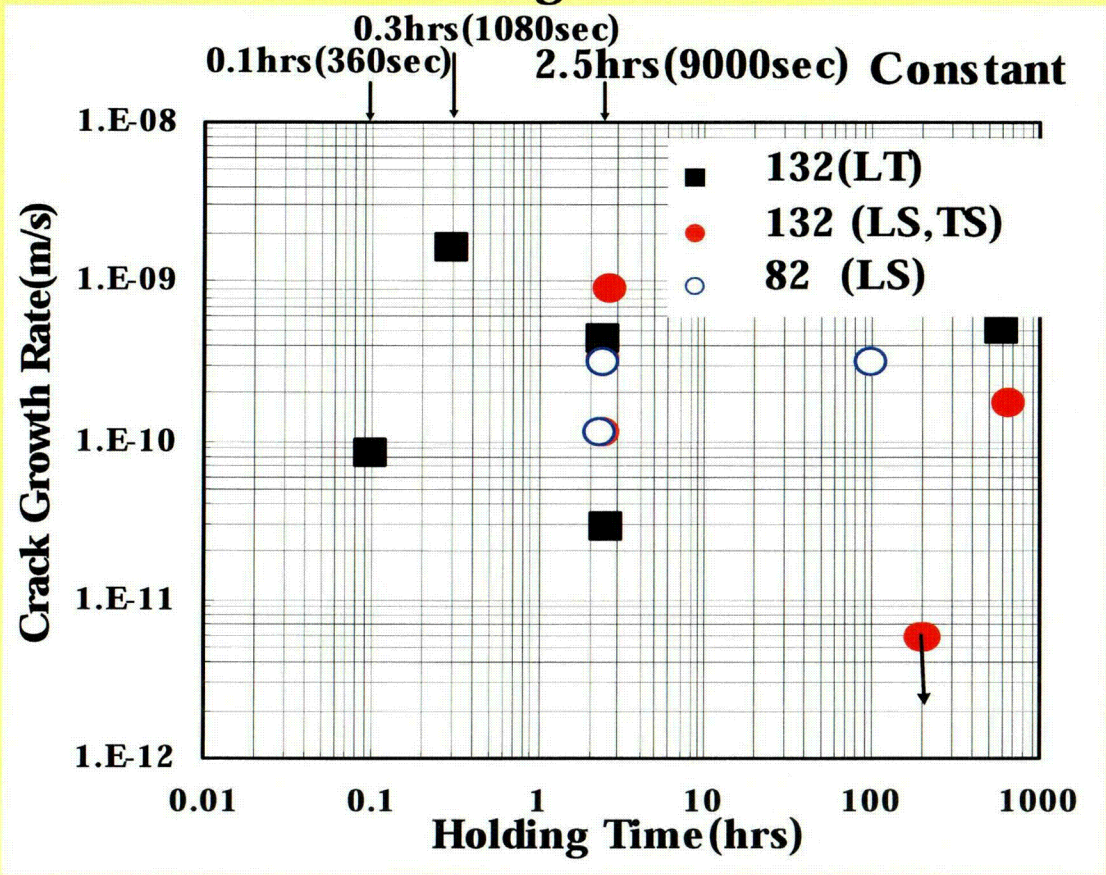

K=35MPa√m
325°C
B/Li:1800/3.5ppm
DO<0.005ppm
DH=30cc/kg H_2O

Figure The effect of holding time for cyclic loading on CGRs

C46

DISCUSSIONS

MITSUBISHI HEAVY INDUSTRIES, LTD. TAKASAGO R&D CENTER

2. The effect of holding time on acceleration of the SCC GR

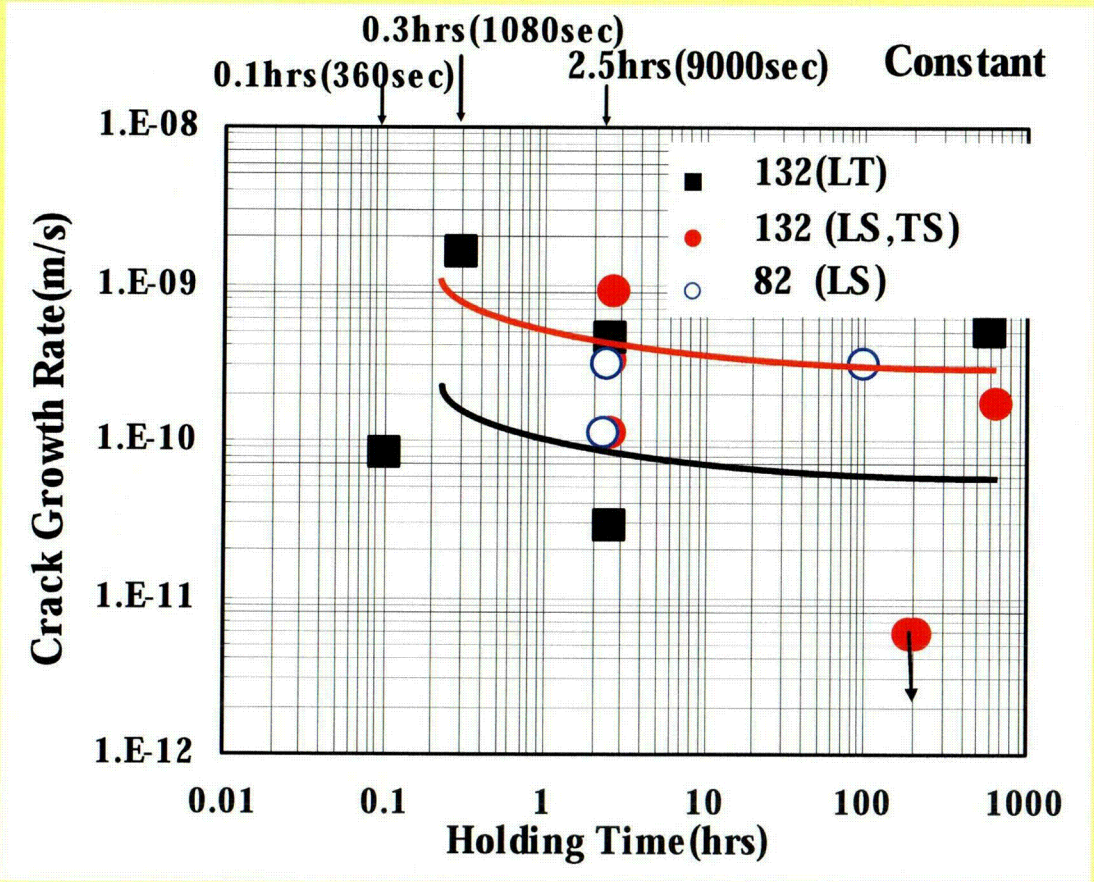

K=35MPa√m
325°C
B/Li:1800/3.5ppm
DO<0.005ppm
DH=30cc/kg H_2O

Figure The effect of holding time for cyclic loading on CGRs

C47

DISCUSSIONS

MITSUBISHI HEAVY INDUSTRIES, LTD. TAKASAGO R&D CENTER

3. Reducing SCC incubation time

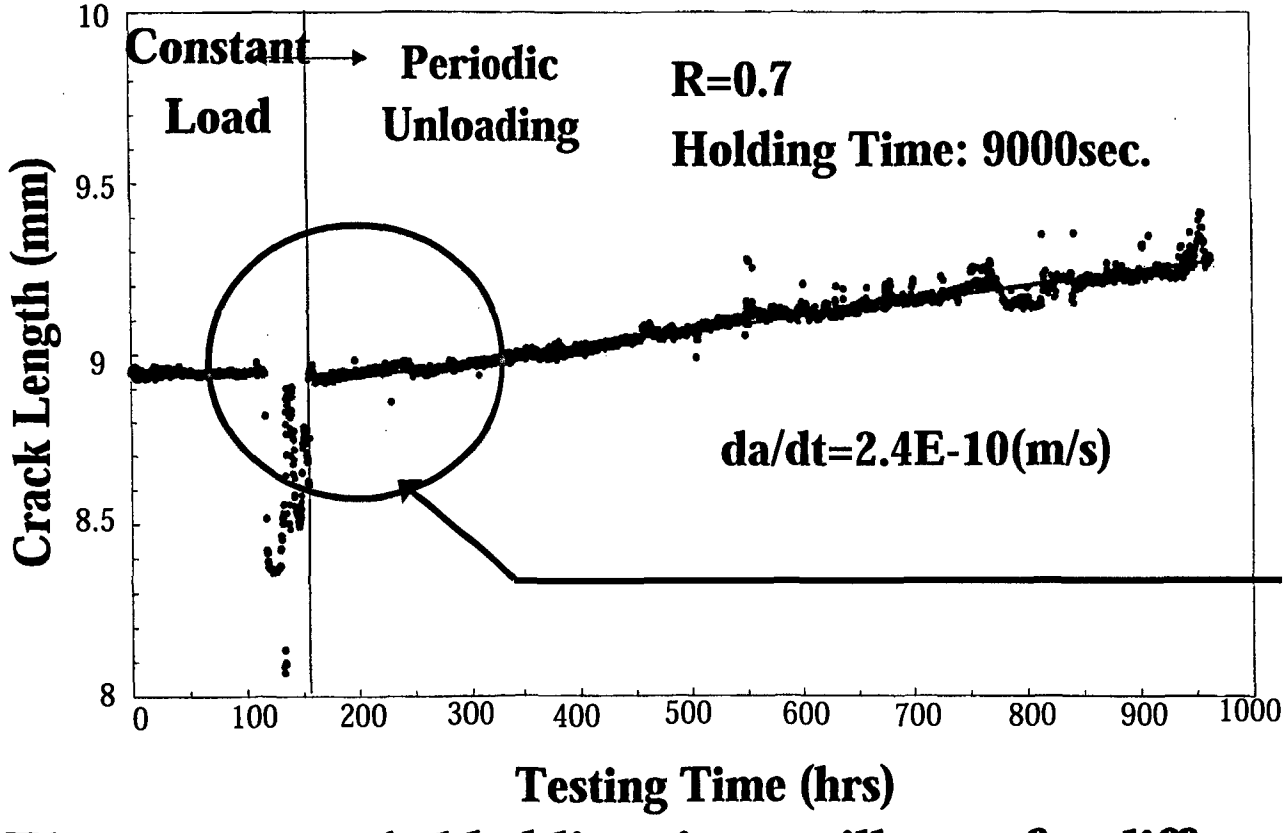

Remarkably changed

The recommended holding times will vary for different materials and specimen orientations.

DISCUSSIONS

MITSUBISHI HEAVY INDUSTRIES, LTD. TAKASAGO R&D CENTER

3. Reducing SCC incubation time

Periodic unloading is recommended for producing the ID pre-crack for the PWSCC GR measurement test. But, the effect of periodic unloading on the real PWSCC GR is not always well known.

The ID PWSCC GR measurement test should be conducted under constant loading or trapezoidal wave with a sufficiently long holding time to eliminate the influence of fatigue.

MITSUBISHI HEAVY INDUSTRIES, LTD.
TAKASAGO R&D CENTER

CONTENTS

1. INTRODUCTION
2. EXPERIMENTAL PROCEDURES
3. RESULTS
4. DISCUSSIONS
5. SUMMARY

SUMMARY

MITSUBISHI HEAVY INDUSTRIES, LTD. TAKASAGO R&D CENTER

(1) The PWSCC GR of Alloy 132 in this study was not larger than that of Alloy 182 reported in the literature.

(1) The PWSCC was propagated along the dendrite, CGRs of the TS and LS specimens were about 3 to 10 times larger than that of the LT specimen.

(1) The crack front of PWSCC on the fracture surface of specimens was not uniform, even under P.U.

(1) P.U. is recommended for producing the ID pre-crack for the PWSCC GR measurement test. The ID PWSCC GR measurement test should be conducted under C.L. or trapezoidal wave with sufficiently long holding time to eliminate the effect of fatigue.

LOCKHEED MARTIN

The Stress Corrosion Crack Growth Rate of Alloy 600 Heat Affected Zones Exposed to High Purity Water

George A. Young, Nathan Lewis,
and David S. Morton

Lockheed Martin Corporation
P.O. Box 1072
Schenectady, NY 12301-1072

LOCKHEED MARTIN

Main Points

- Need to consider SCCGR of HAZ independently of base metal (and weld metal)
- Data presented here likely not worst case
- Other nickel-base alloys (*e.g.* A690) likely show increased susceptibility to PWSCC in the HAZ

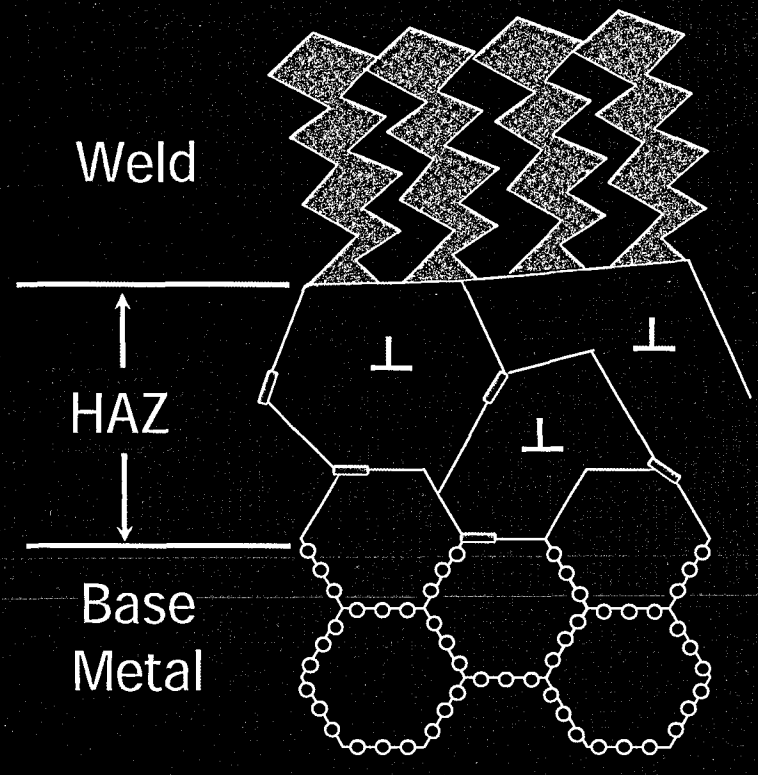

LOCKHEED MARTIN

Background

- **Vessel head penetration SCC in three locations**
  - From A600 penetration ID to OD
  - In E-182 weld metal
  - Near the interface of the A600 penetration and the J-groove weld - ***is this SCC in the HAZ?***

- **Primary water stress corrosion crack growth rate of A600 and its weld metals are well studied - what about the A600 heat affected zone (HAZ)?**

LOCKHEED MARTIN

Machine 1.0 CT Specimens from EN82H/A600 HAZ, no PWHT

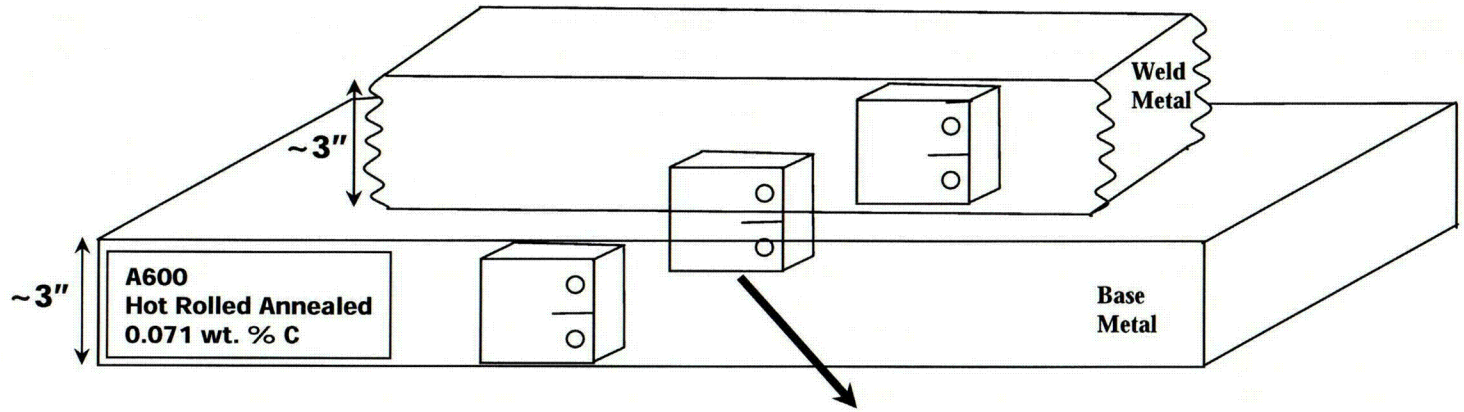

GTAW weld buildup of EN82H

Mill Annealed A600 plate

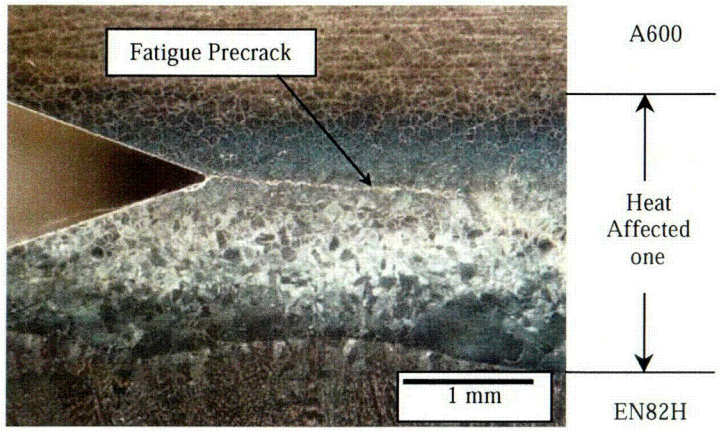

LOCKHEED MARTIN

Notch and precrack entirely in the HAZ

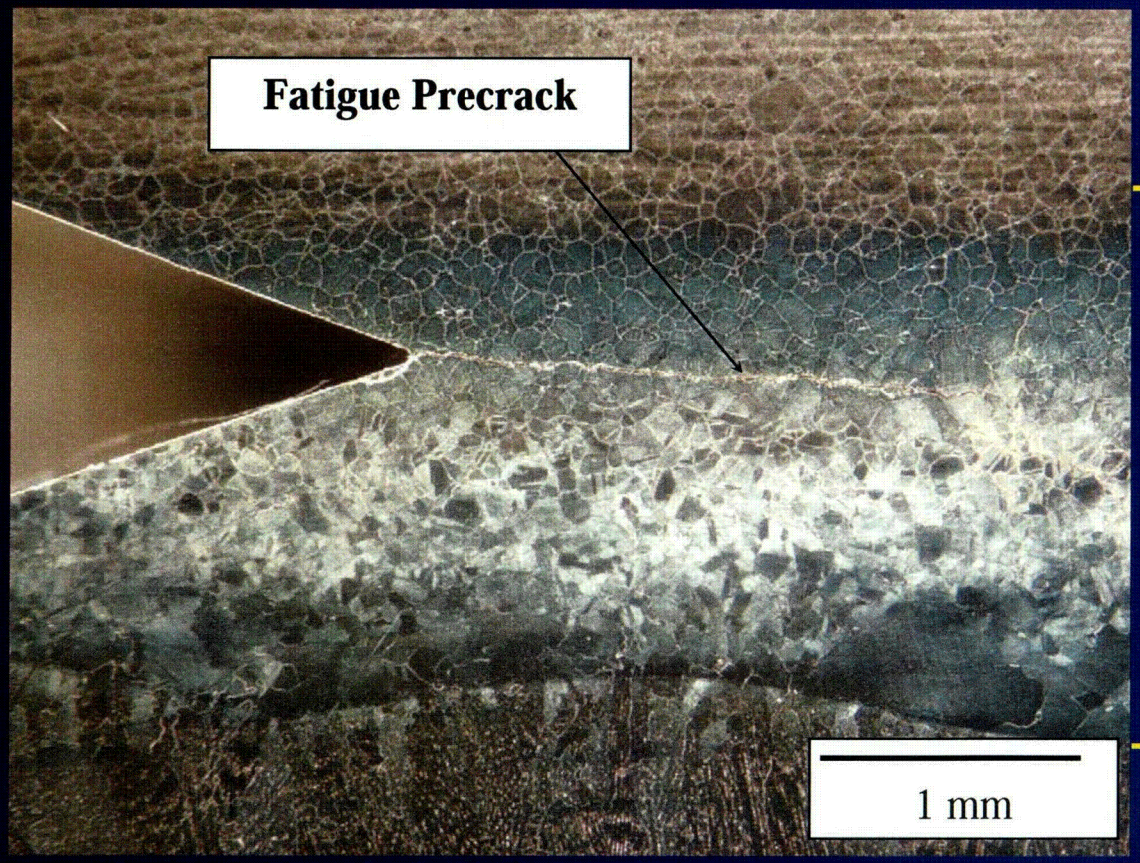

A600

Heat Affected one

EN82H

LOCKHEED MARTIN

Testing Goals and Conditions

- Determine temperature dependence (Q_{SCCGR})
  - Constant electrochemical potential
- Determine effect of coolant H_2 around Ni/NiO
- "Constant" K (constant load)
- Each sample destructively examined post test

Temperature (°F / °C)	Hydrogen (scc/kg)	Approximate ΔECP from Ni/NiO (mV)	Initial Stress Intensity Factor (ksi$\sqrt{in}$)
600 / 316	9	+2	40
640 / 338	1	-41	40
	18	+6	40
	120	+56	40
680 / 360	30	+6	40

LOCKHEED MARTIN

Results

- SCC occurred entirely in the A600 HAZ

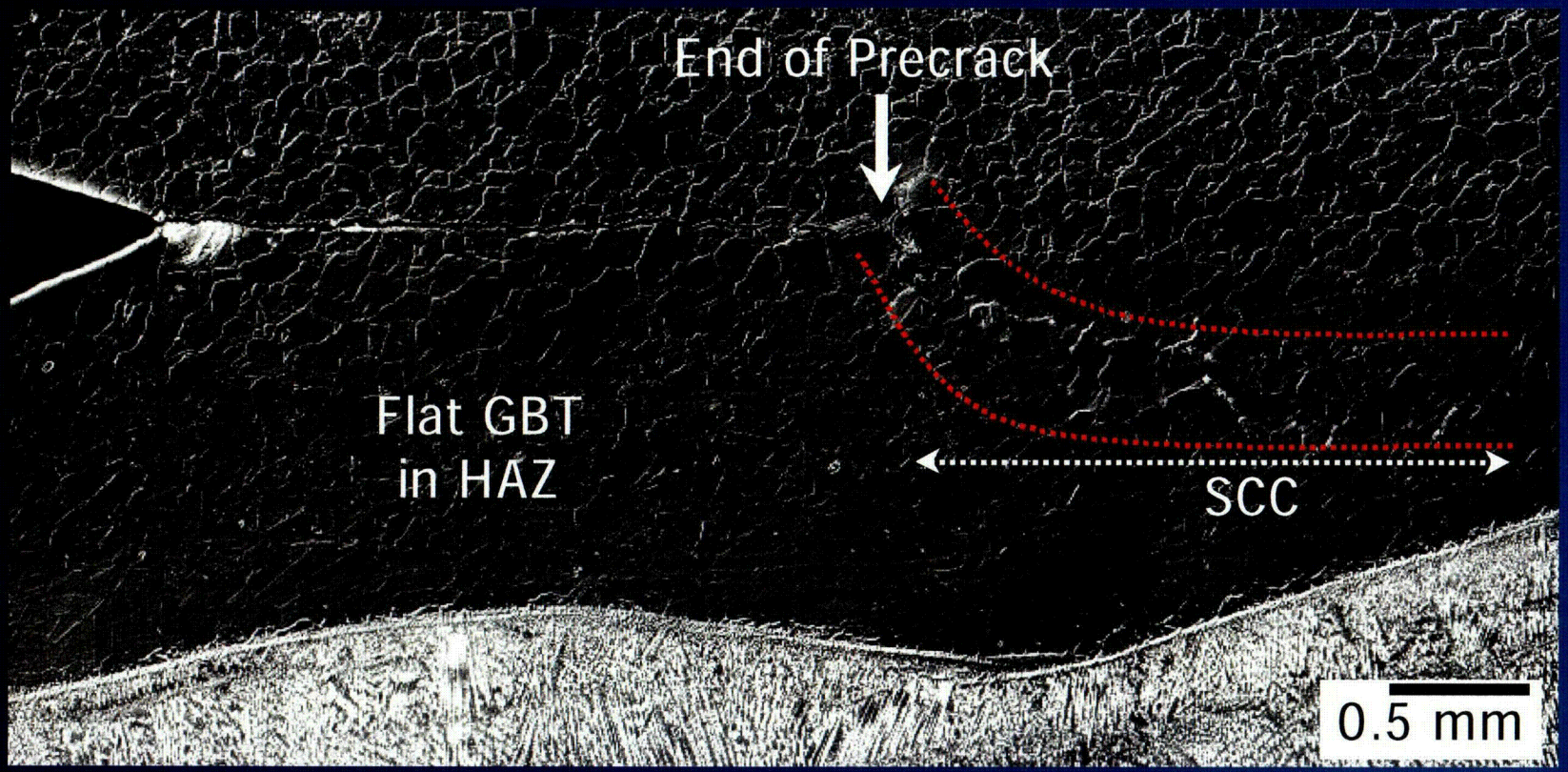

LOCKHEED MARTIN

Branched IGSCC in the A600 HAZ

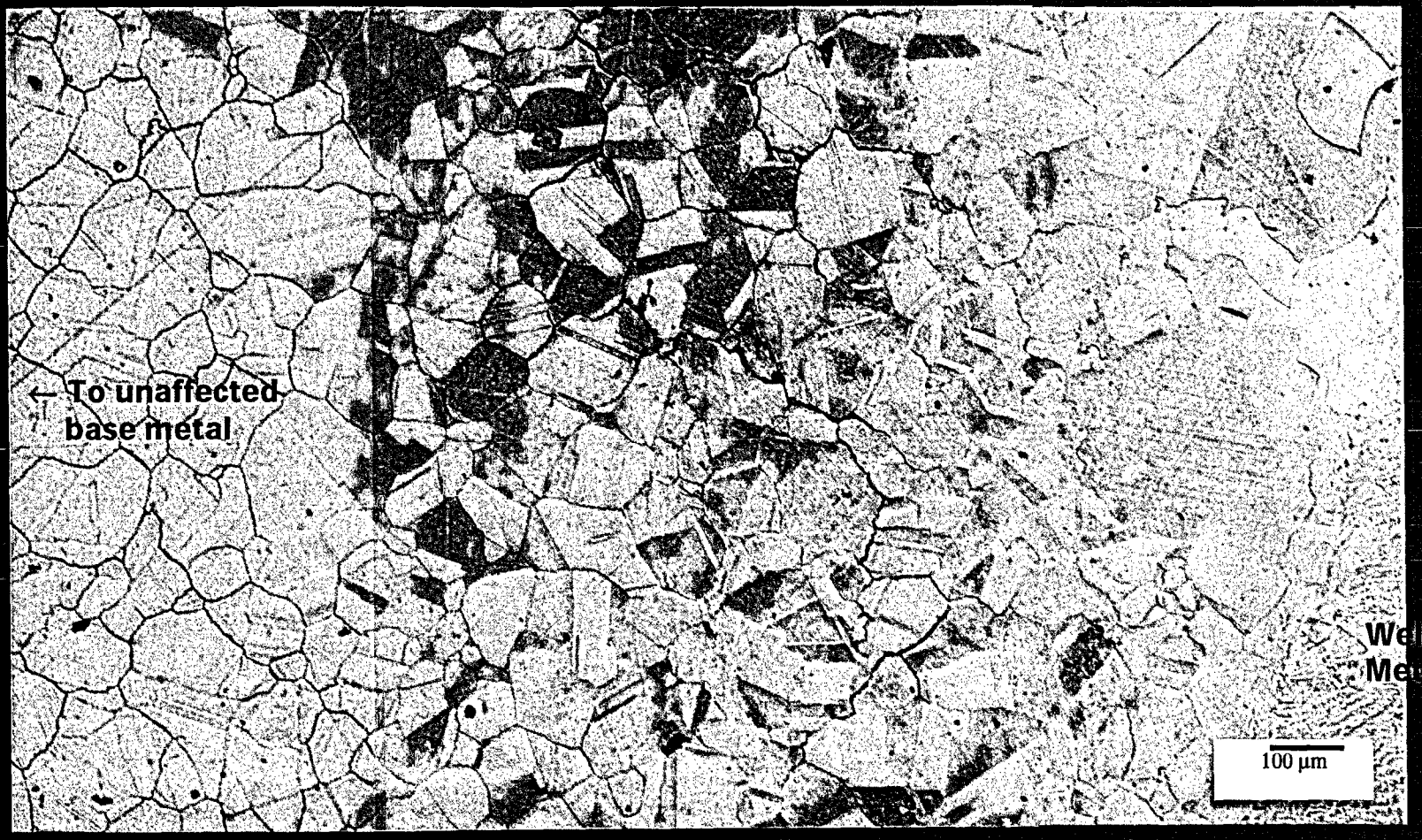

LOCKHEED MARTIN

The A600 HAZ displayed ~30X faster crack growth rates than the base metal

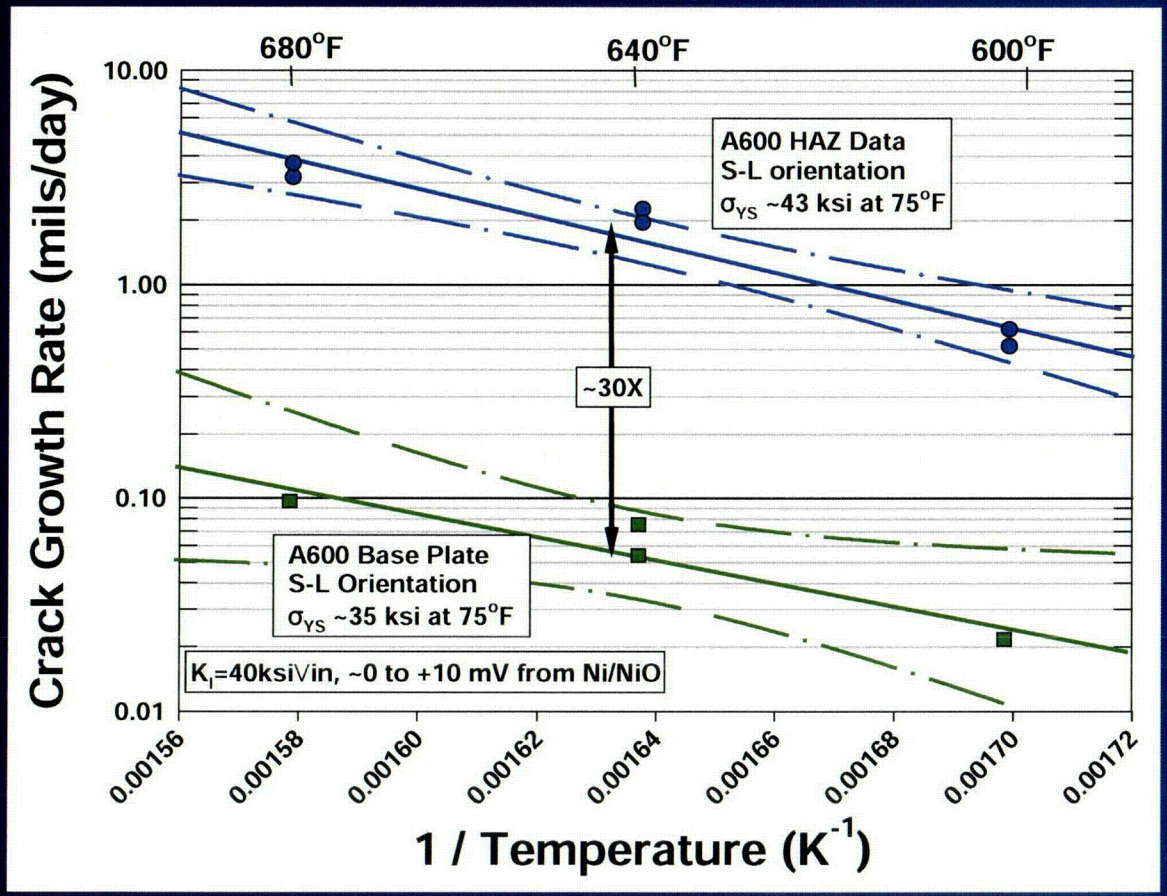

LOCKHEED MARTIN

The Q for the HAZ is ~ 125kJ/mol within experimental error of unaffected base metal

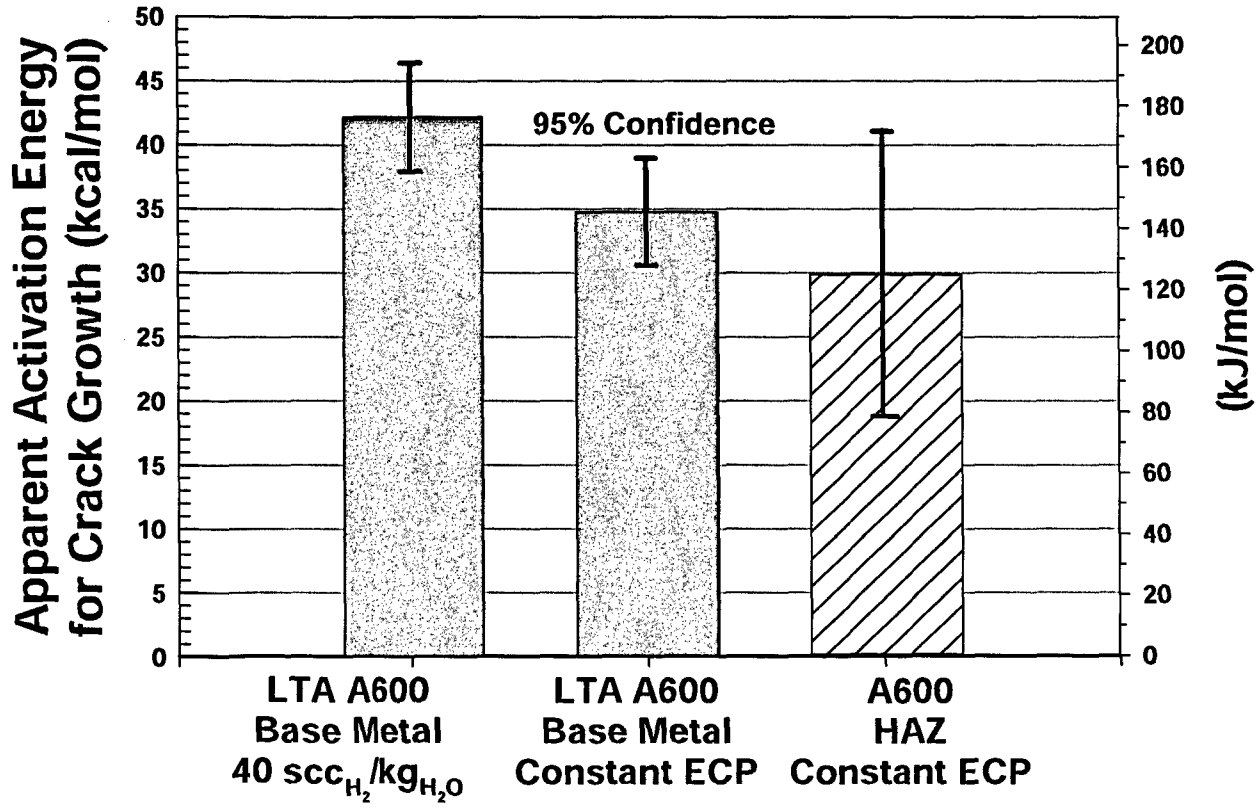

LOCKHEED MARTIN

- Need to consider ΔECP when determining the apparent activation energy, *Q*, for crack growth
- Conduct tests at constant ΔECP or well into Ni metal stability for 'true' *Q*

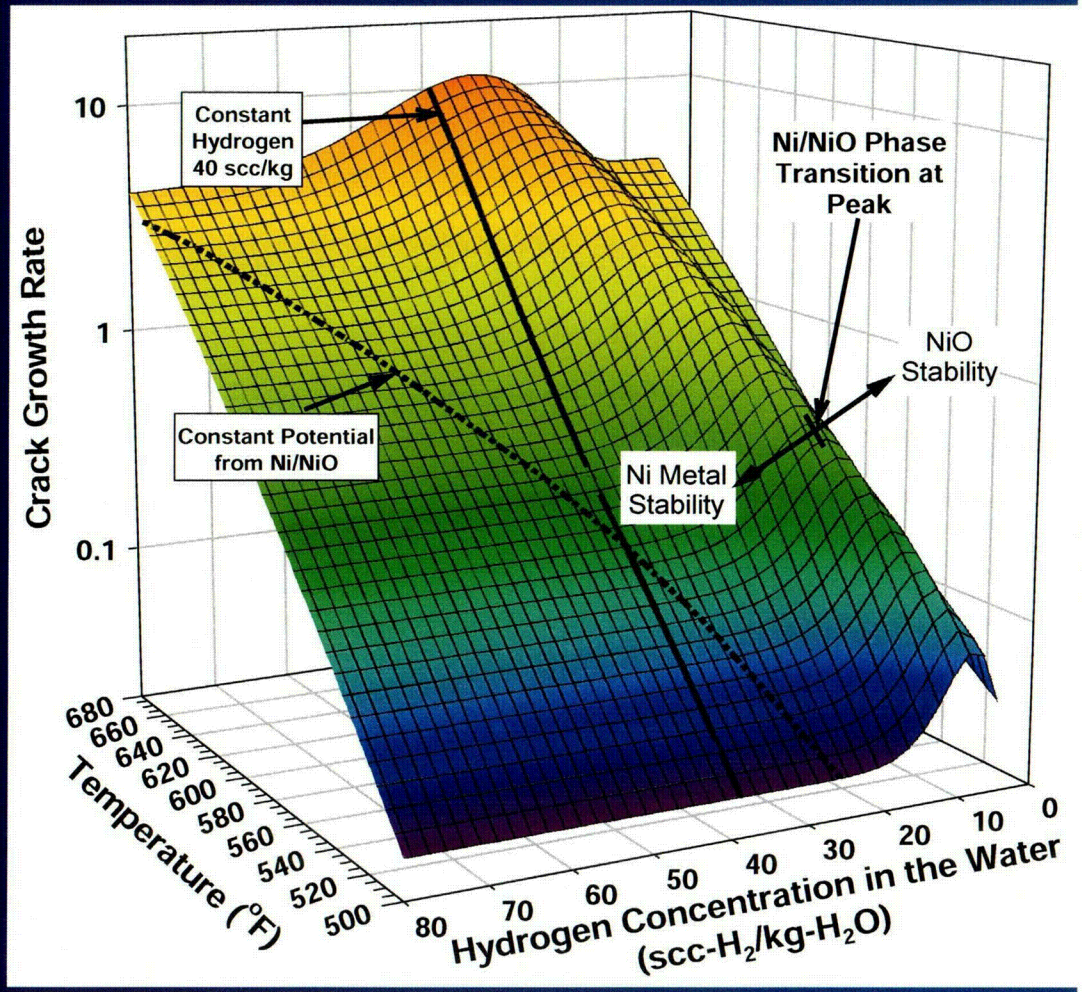

See Morton *et al.*, in 10th Env. Deg. Conf. NACE 2001

C52

LOCKHEED MARTIN

The 'coolant hydrogen effect' for the HAZ is nearly identical the base metal (~2.8X)

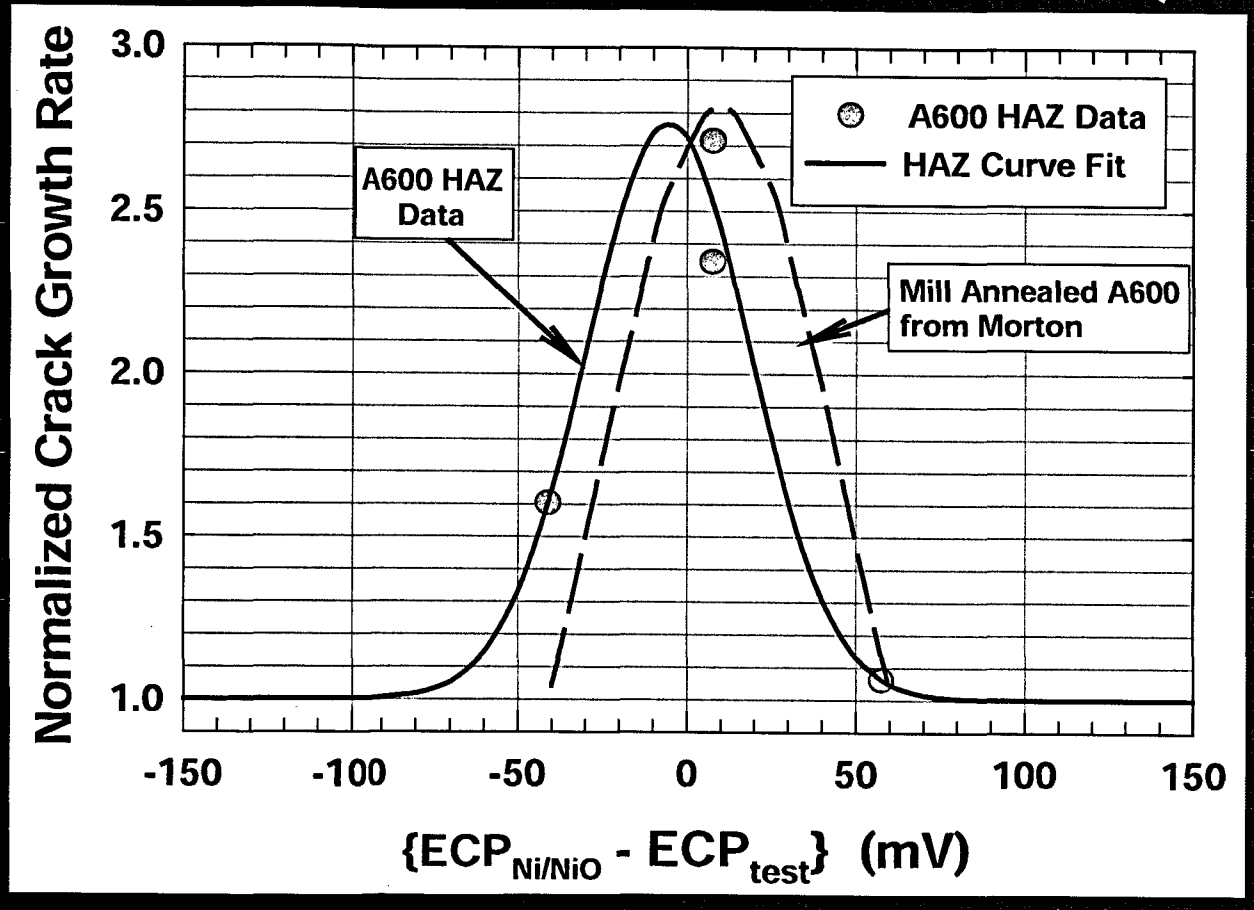

LOCKHEED MARTIN

Why does the A600 HAZ SCC at fast rates?

→ Fewer grain boundary Cr-rich carbides

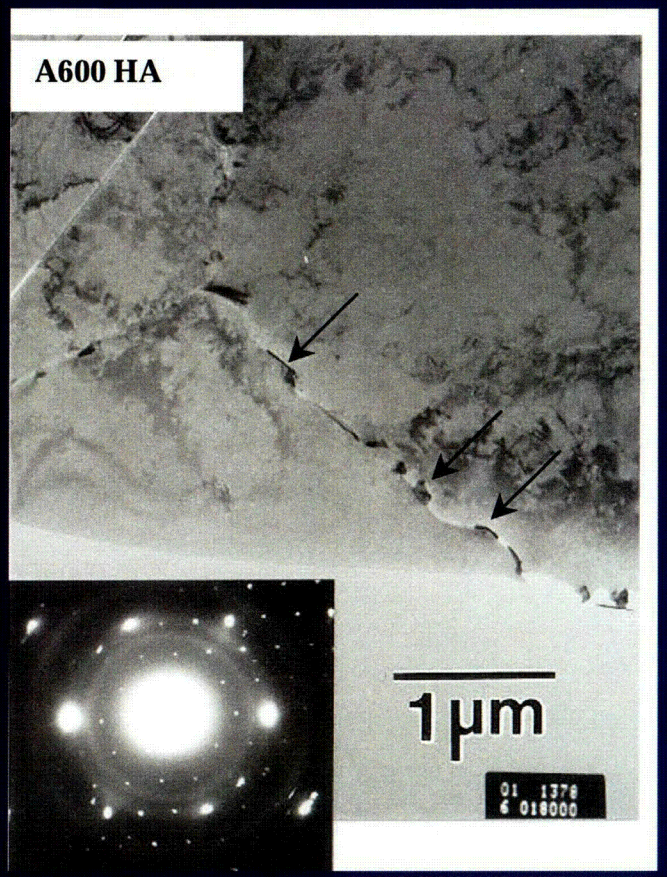

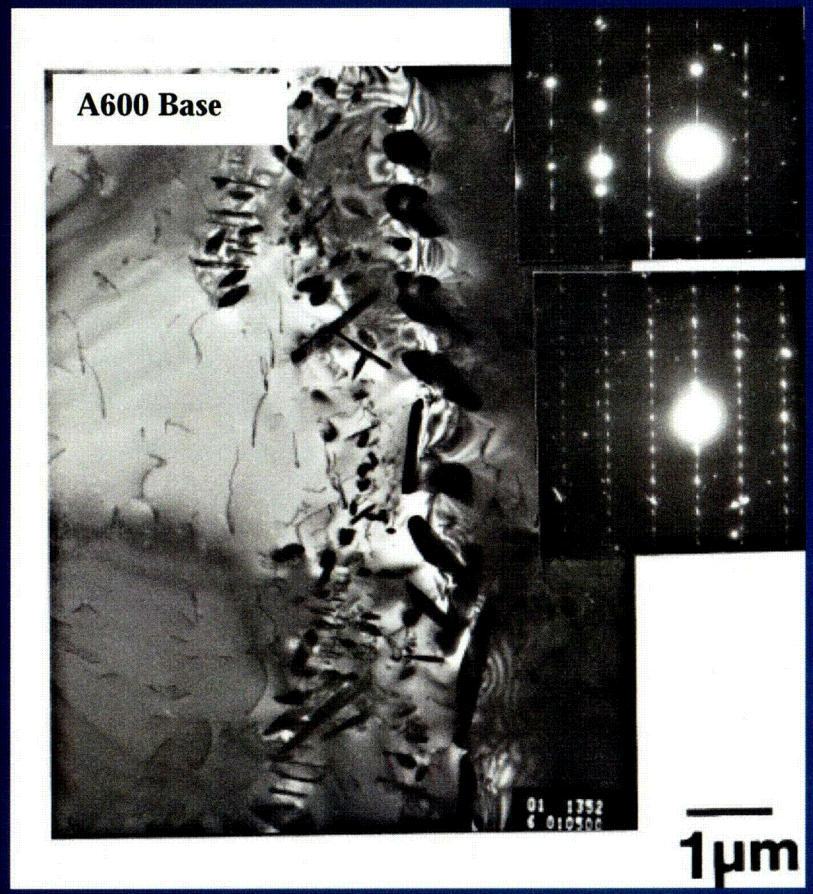

LOCKHEED MARTIN

(1) Microhardness
(2) Strain Quantification via EBSD
(3) Strain Mapping via EBSD

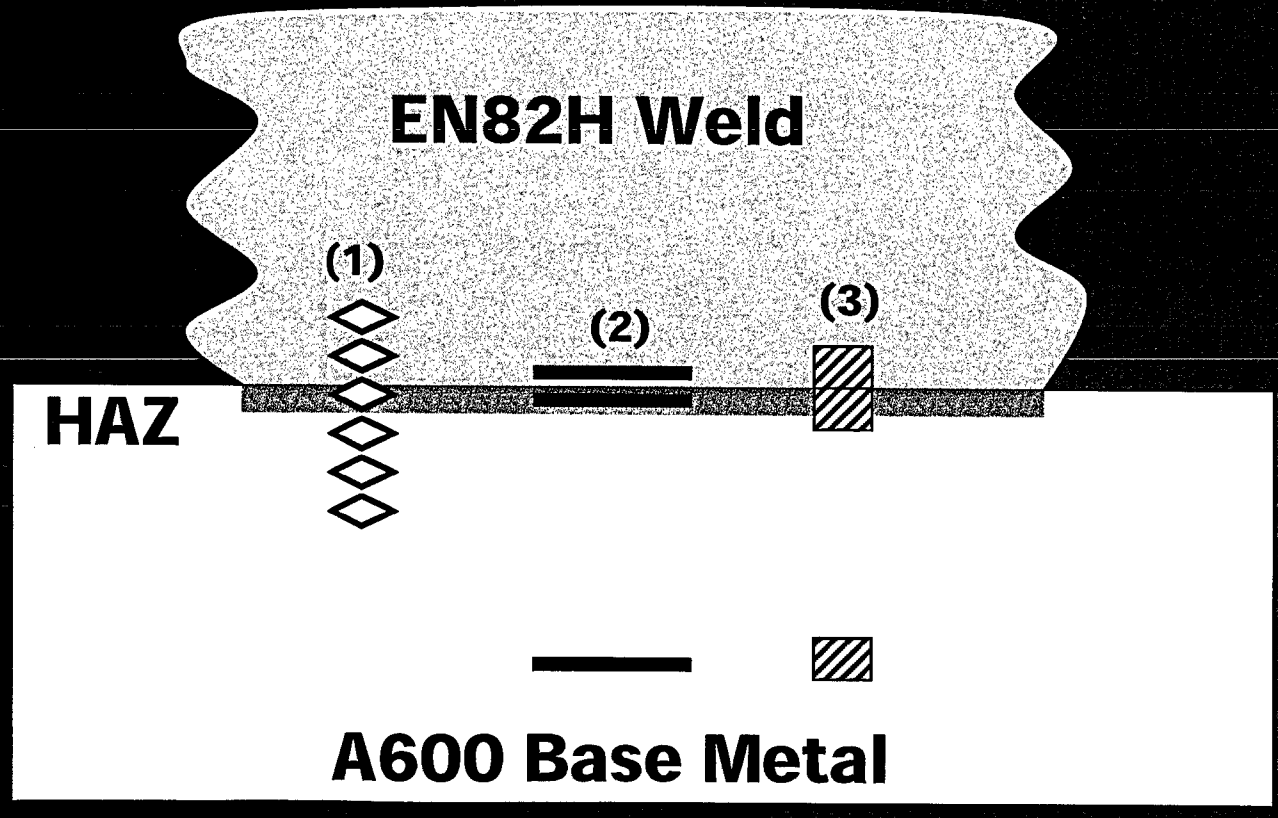

LOCKHEED MARTIN

The HAZ shows increased hardness relative to the unaffected base metal

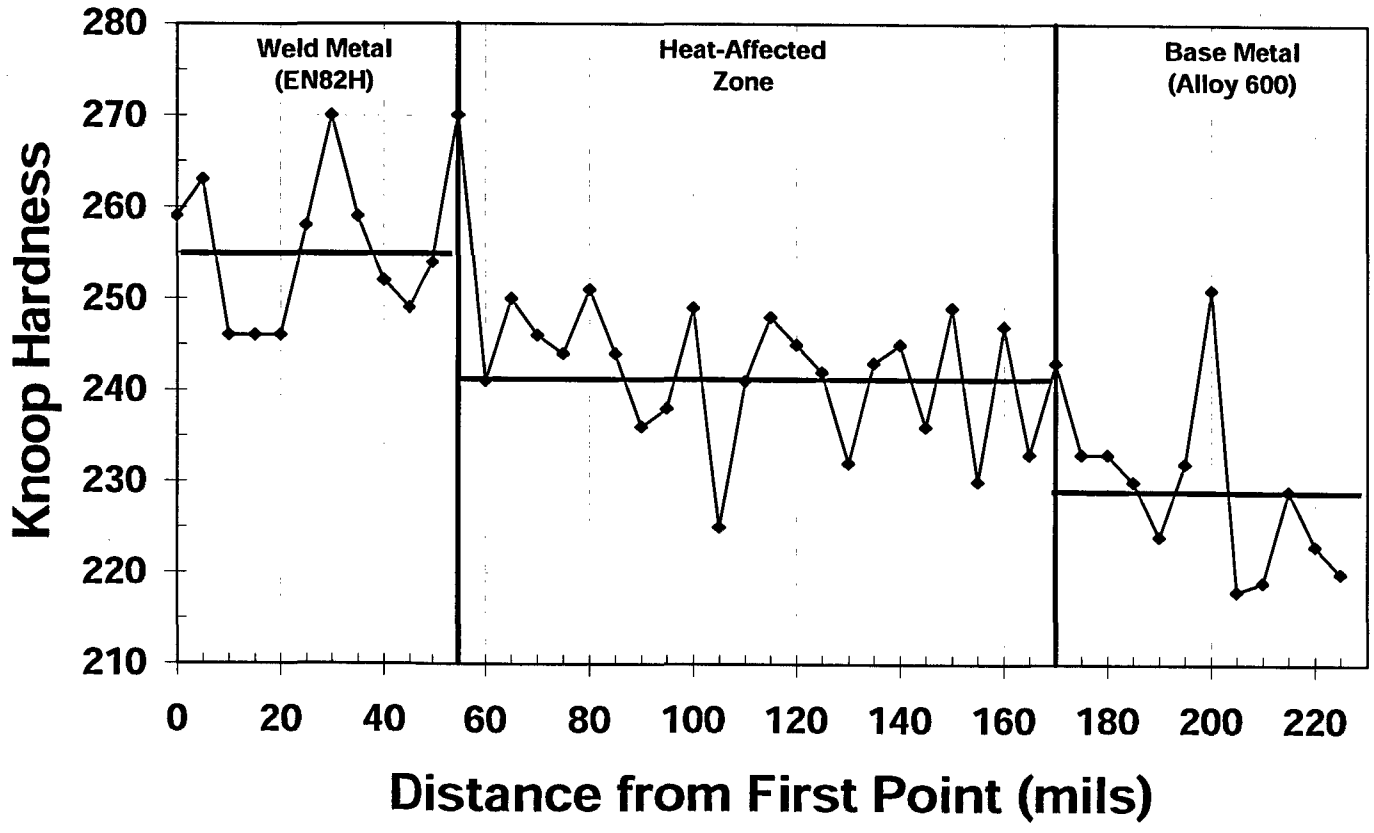

LOCKHEED MARTIN

Why does the A600 HAZ SCC at fast rates?

→ increased plastic strain (~6%) in the HAZ

Far from Weld ← A600 HAZ → EN82H GTA Weld

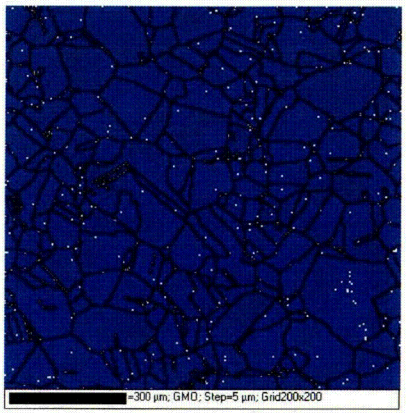

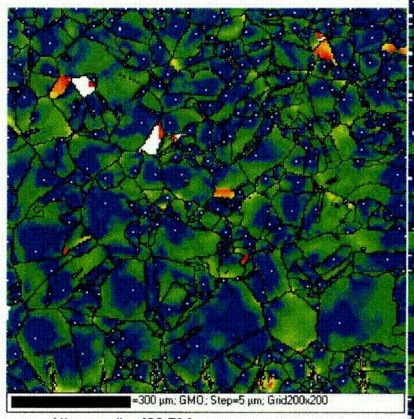

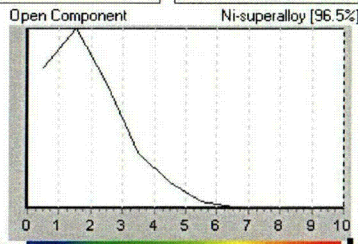

Low strain — High strain

Misorientation (°)

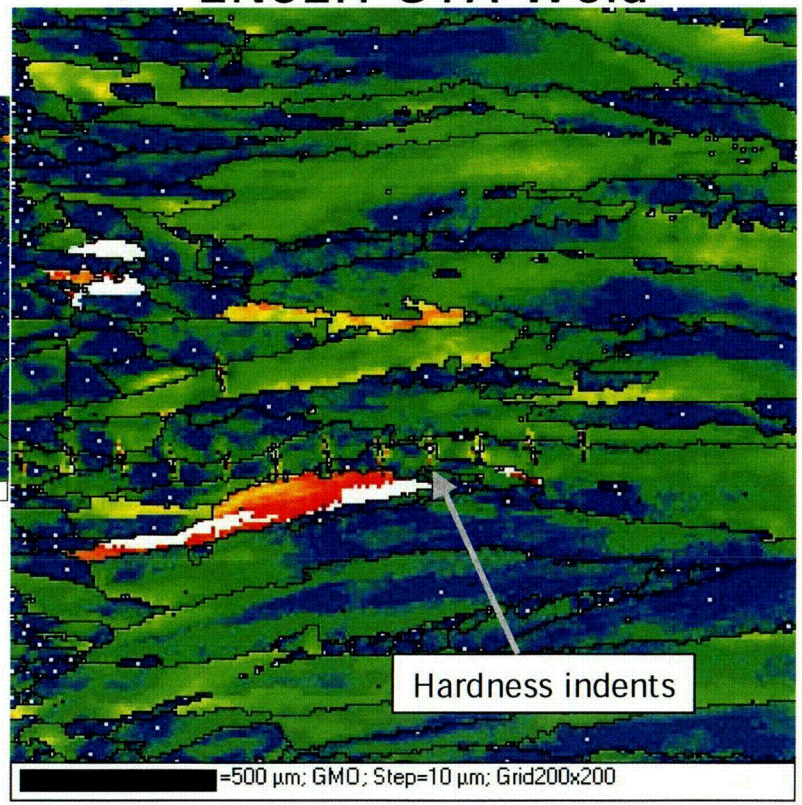

LOCKHEED MARTIN

Discussion

- The HAZ tested was from a very PWSCC resistant base plate (well annealed, good microstructure). Other heats may show significantly different crack growth rates.

- The HAZ tested was low constraint (~6% ε). Higher constraint welds may contain higher plastic strains (~15% ε ?) and exhibit faster crack growth rates.

  See Young *et al.* in 6th International Conference on Trends in Welding Research, ASM, 15 April 2002, pp. 912-917.

LOCKHEED MARTIN

Discussion

- Other nickel-base alloys which rely on grain boundary Cr-rich precipitates for PWSCC resistance (*e.g.* A690) may show increased susceptibility to PWSCC in the HAZ.

- Post weld heat treatment / bead tempering may help recover PWSCC resistance but ...
  - plastic strain may promote intra vs. intergranular carbide precipitation
  - may need significantly longer PWHT times (or higher T) than are typical

LOCKHEED MARTIN

Conclusions

- **Need to consider PWSCC of the HAZ separately from the base metal and weld metal.**
- **The susceptibility of the HAZ is due to:**
  - Loss of grain boundary Cr_7C_3 carbides
  - (Less grain boundary Cr depletion)
  - Residual plastic strain from welding
- **The temperature dependence of the A600 HAZ SCC is very similar to unaffected base metal**

A600 HAZ	125 kJ/mol ± 47 kJ/mol	95%
'Typical' A600 base metal	145 kJ/mol ± 18 kJ/mol	95%

LOCKHEED MARTIN

Conclusions

- The 'coolant hydrogen effect' in the A600 HAZ is ~2.8X, similar to the unaffected base metal
- The A600 HAZ studied is likely not the worst case HAZ
- Other nickel-base alloys which rely on grain boundary Cr-rich precipitates for PWSCC resistance (*e.g.* A690) may show increased susceptibility to PWSCC in the HAZ.

In-situ Raman Spectroscopic Study on Alloy 600 CRDM Nozzle Material and Its Implications

Ji Hyun Kim, Il Soon Hwang
Department of Nuclear Engineering, Seoul National University
and
Tae Ryong Kim
Korea Electric Power Research Institute
Republic of Korea

Conference on Vessel Penetration Inspection, Cracking and Repairs
2003. 9. 29 ~ 10. 2
Gaithersburg. MD, U.S.A.

Outlines

- 1. Introduction
- 2. Rationale and Approach
- 3. In-situ Raman Spectroscopy
- 4. Results
- 5. Ni/NiO Equilibrium & Implication to PWSCC
- 6. Conclusions

1. Introduction: PWSCC

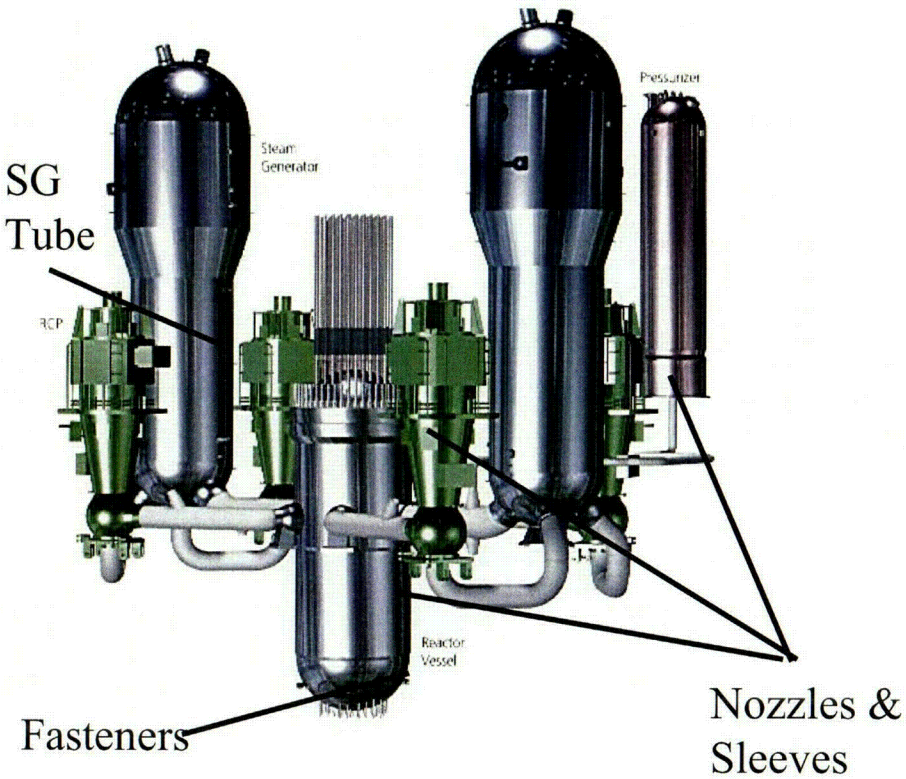

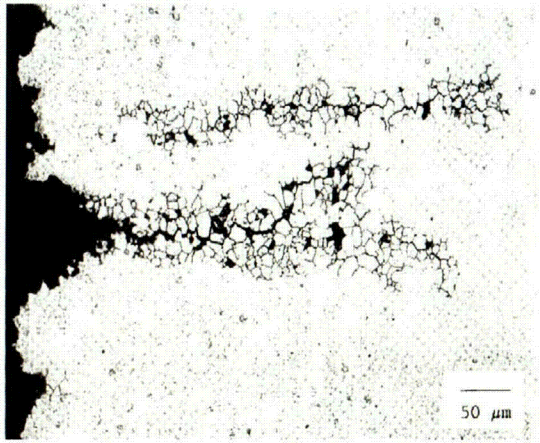

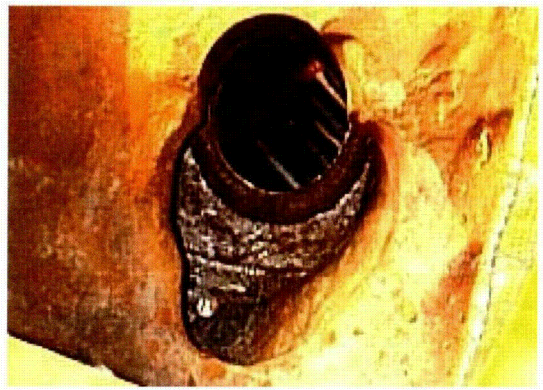

1. Introduction: PWSCC

- No general agreement on the mechanism of PWSCC

- It is conceivable that the damage to the alloy substrate is related with the integrity of surface oxide film

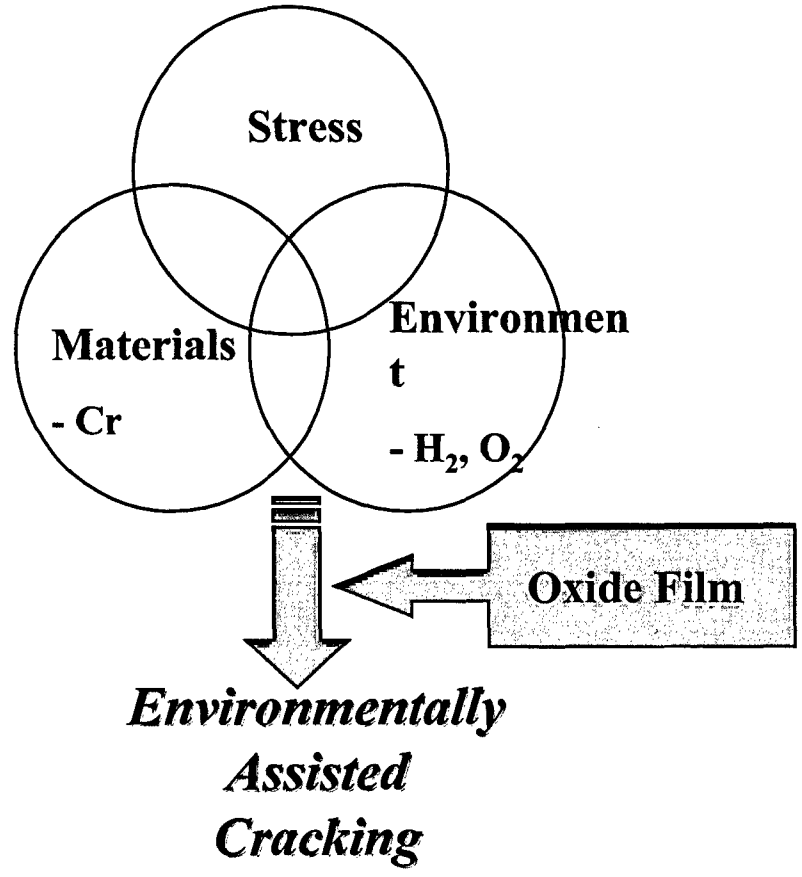

1. Introduction: PWSCC

Influence of [H_2] on PWSCC initiation

(G. Airey. '80)

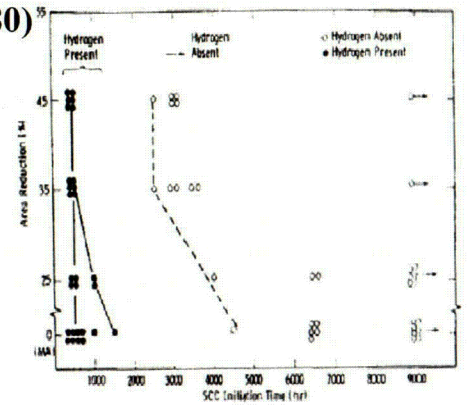

(T. Cassagne et al. '93)

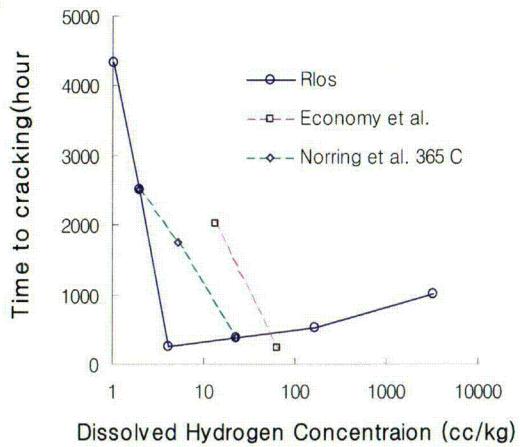

Influence of [H_2] on PWSCC

(T. Cassagne et al. '93)

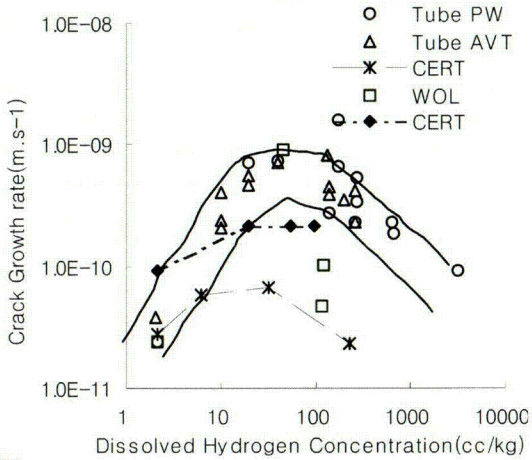

(D. Caron '06)

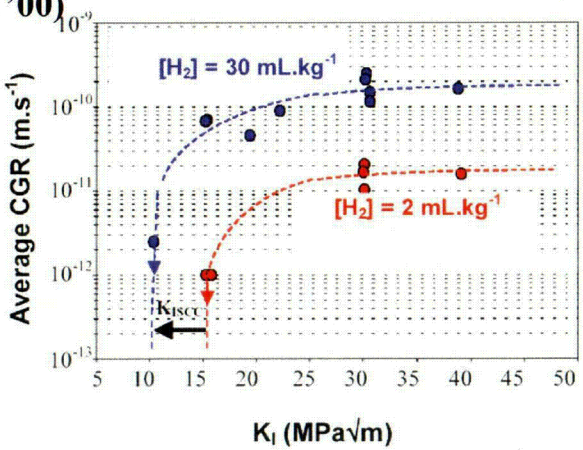

1. Introduction: PWSCC

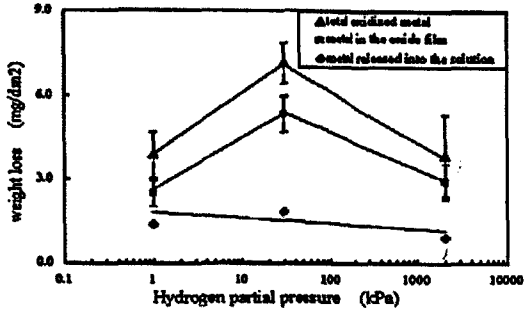

Figure 7: Weight measurements of oxidized metal on alloy 600

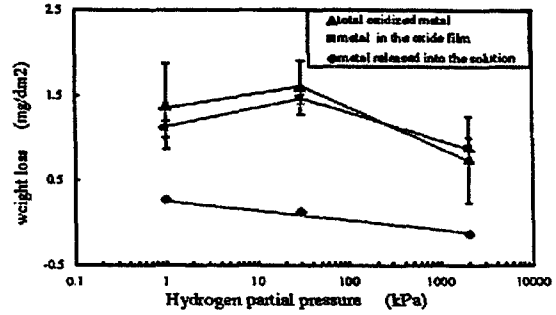

Figure 8: Weight measurements of oxidized metal on alloy 690

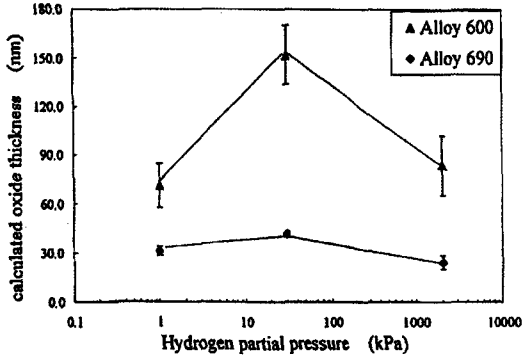

Figure 9: thickness of the oxide layers calculated from the weight measurements (assuming an oxide density of 5)

H_2 overpressure (kPa)	<1	30	2000
Alloy 600 -Weight measurement -X-ray diffraction	60nm 80nm	150nm 175nm	90nm 60nm
Alloy 690 - Weight measurement	30nm	40nm	25nm

(C. Soustelle et al. '99)

- Total amount of oxidized metal(oxide+dissolved cations) as well as oxide thickness are maximum at the intermediate hydrogen overpressure.

2. Rationale and approach

- **The characterization of the oxide film of alloy 600 under PWR primary water conditions**
  - **one of key elements for understanding how the oxide film behaves in the cracking process.**
- **In-situ study can give potentially a clearer picture of the corrosion mechanism**
  - **Removal of the material from the corrosion environment can result in modification of the oxide film structure and chemistry.**
- **In-situ oxide study in high temperature water**
  - **for pure metals and alloys in <u>air-saturated</u> or <u>BWR</u> water**
  - **by T. Devine et al. and J. Maslar et al.**

⇨ ***Need in-situ information on oxide film of alloy 600 in <u>PWR</u> environment***

2. Rationale and approach

- Characterization of oxide structure and chemistry under various PWR environments by in-situ experimental method
  - Ex-situ reference oxide powder experiment
  - In-situ experiment at various PWR conditions

  - Ni/NiO domain on ECP-T coordinate
  - Comparison with thermochemical calculations on Ni/NiO

  - Oxide structure examination
  - Comparison of oxide chemistry with earlier ex-situ results

3. In-situ Raman Spectroscopy

- **Raman spectroscopy**
  - the measurement of the wavelength and intensity of inelastically scattered light from molecules by irradiating a sample with the monochromatic radiation from a laser.
  - Performed by collecting the light that is inelastically scattered by the sample.

Raman Scattering

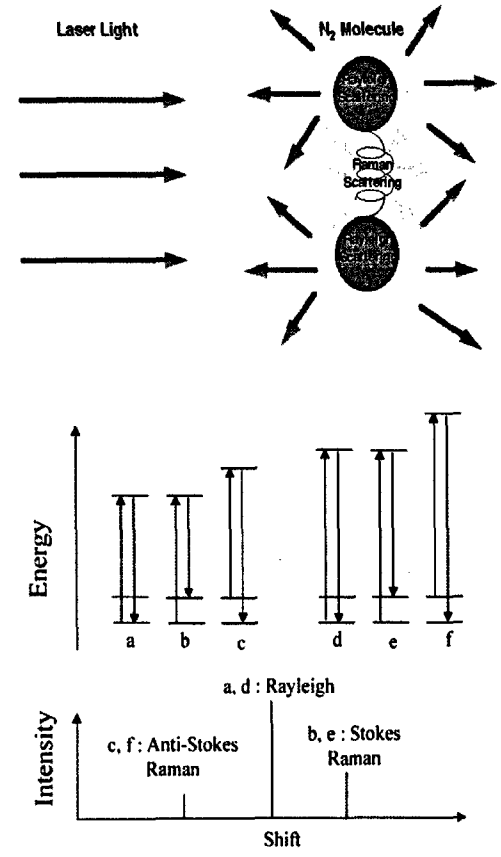

3. In-situ Raman Spectroscopy

➢ Material

- Alloy 600 : hot forged, SA at 1050°C for 2hrs and water cooled

Elem.	C	Mn	Fe	S	Si	Cu	Ni	Cr	Al	Ti	Nb	P	B	N
Comp.	0.06	0.26	8.31	0.001	0.3	0.12	75.12	15.25	0.16	0.36	0.04	0.009	0.002	0.001

➢ Water environment

- PWR primary water chemistry
  - ✓ Deionized and deaerated water : DO_2 < 10 ppb (inlet)
  - ✓ Boron: 1,000 ppm, Lithium : 2 ppm
- Hydrogen gas injection
  - ✓ Pure hydrogen gas of 0.7 atm overpressure : ~ 30 cm^3(STP)/kg
  - ✓ 5% hydrogen & 95 % He of 0.6 atm overpressure : ~ 1 cm^3(STP)/kg
- Temperature : 250 ~ 350 ℃
- Pressure : 180 atm

3. In-situ Raman Spectroscopy

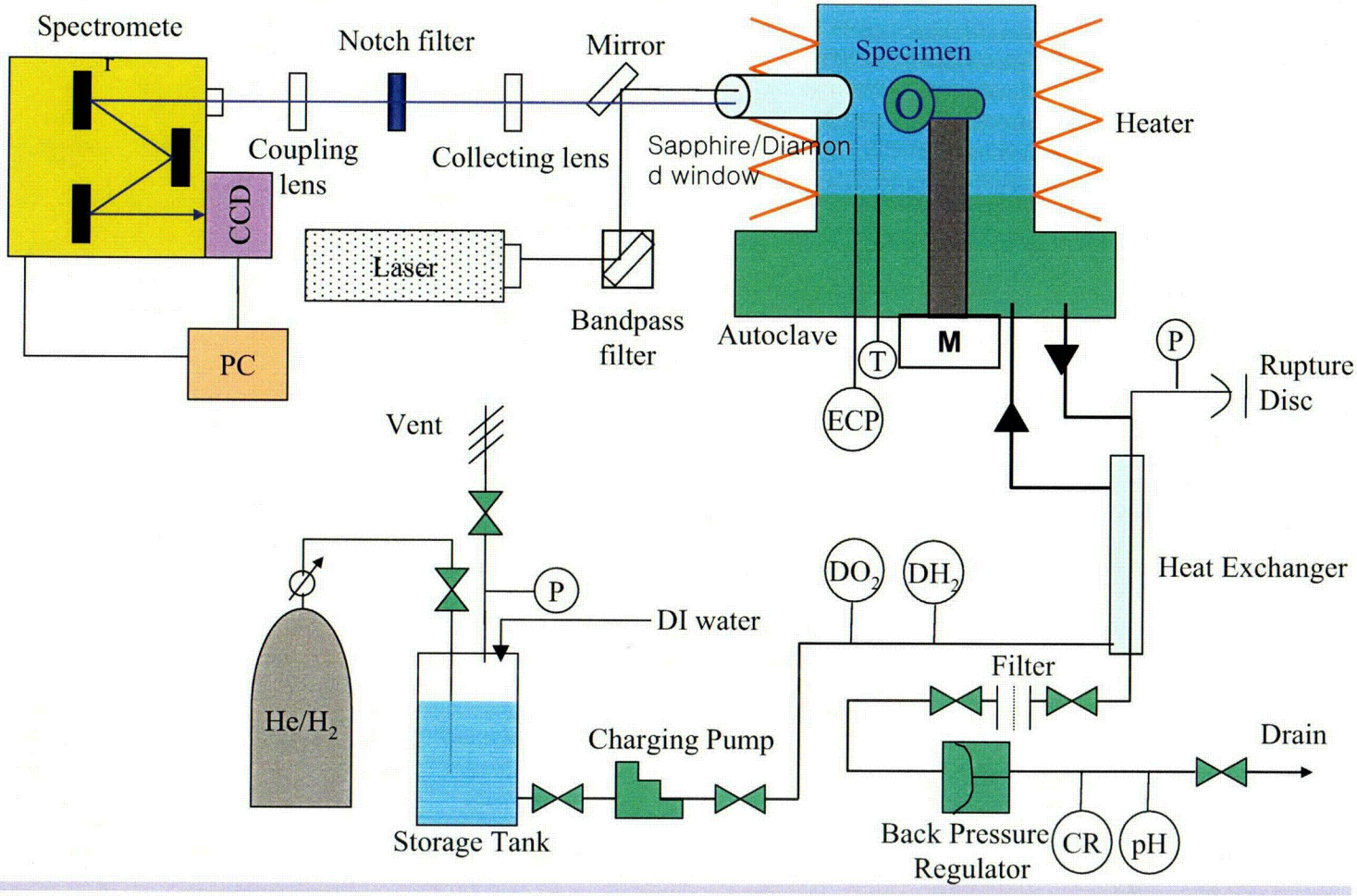

C57

3. In-situ Raman Spectroscopy

➢ Bird's-eye view of Raman system

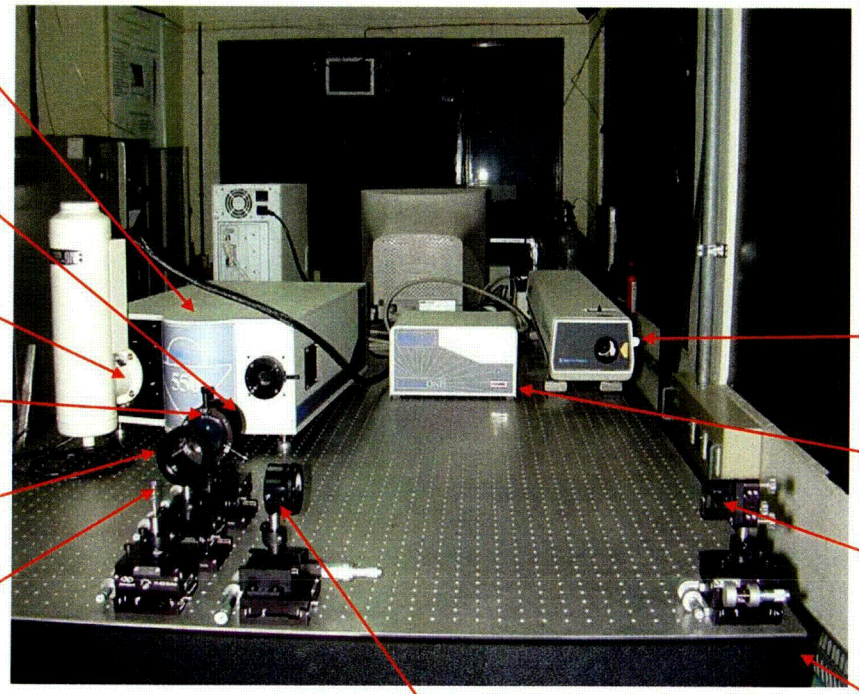

C58

3. In-situ Raman Spectroscopy

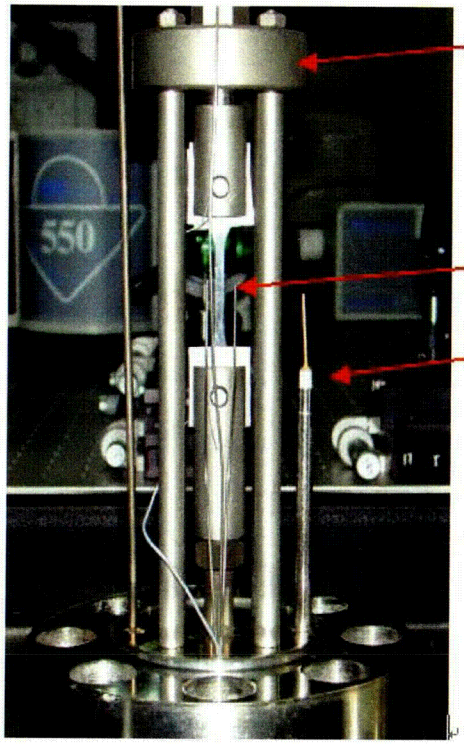

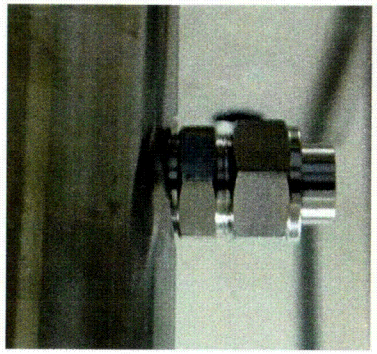

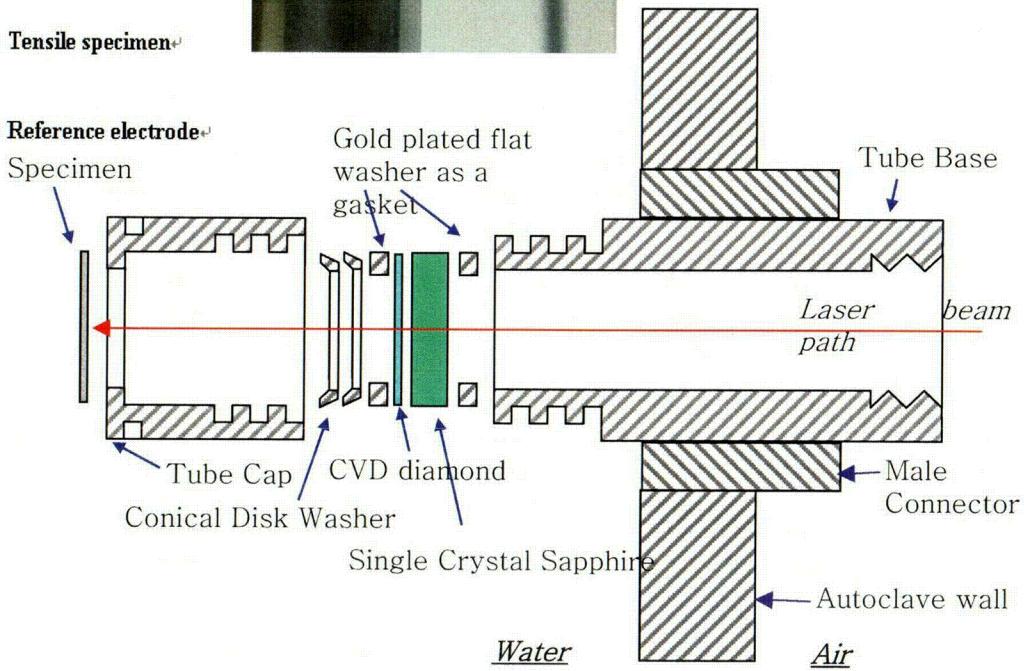

C59

3. In-situ Raman Spectroscopy

- **Reference Raman spectra measurement in air**
  - **NiO**
  - **$NiFe_2O_4$**
  - **Cr_2O_3**
  - **$NiCr_2O_4$**

- **In-situ Raman spectra measurement**
  - **Dissolved hydrogen concentration variation**
  - **Temperature variation**

4. Results : Reference Powder in Air at RT

- **NiO**

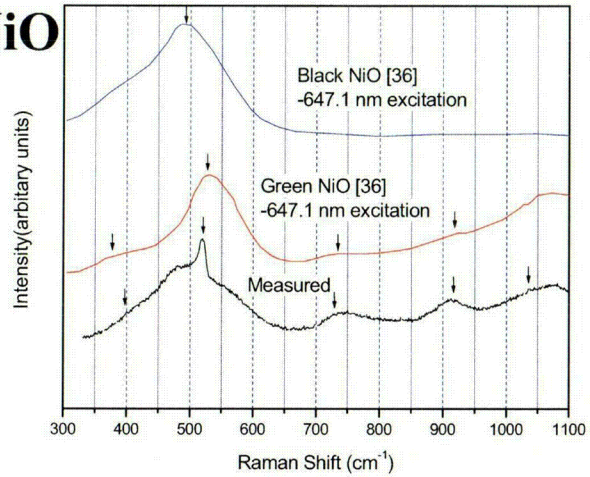

- **$NiFe_2O_4$**

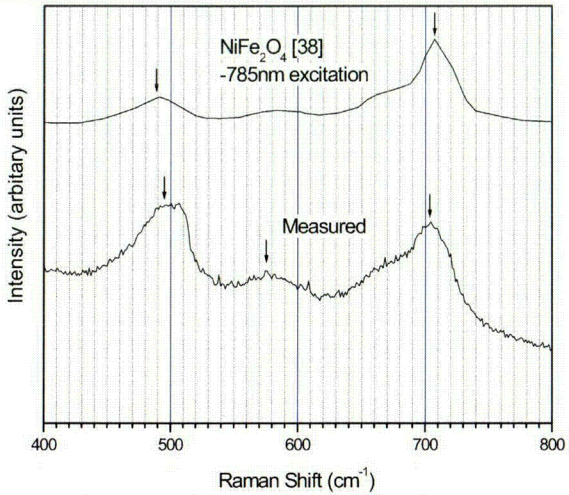

- **Cr_2O_3**

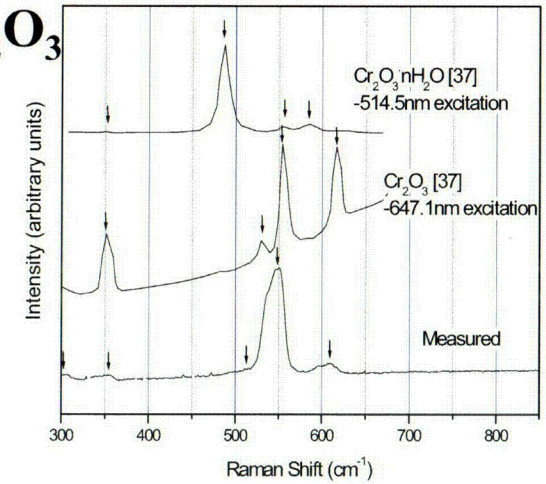

- **$NiCr_2O_4$**

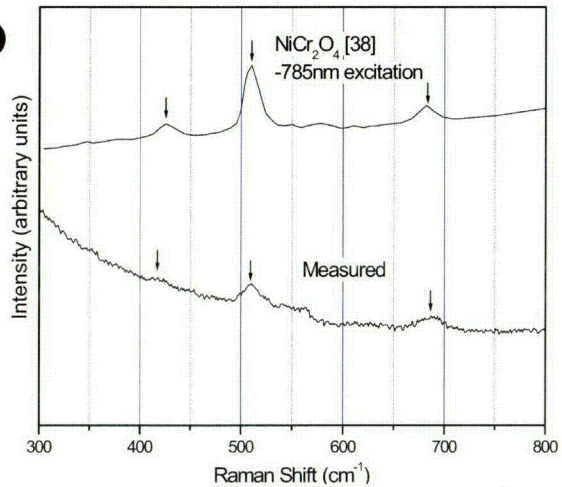

C60

4. Results in PWR conditions

➢ **Temperature and alloy 600 exposure time prior to in-situ Raman spectra measurements**

Temperature (℃)	Total exposure time prior to first measurement at temperature (h)	Hold time at each temperature prior to first measurement (h)
250	28	2
290	33.5	3
320	42	7
350-I	47.5	3.5
350-II	69.5	20.5

4. Results in PWR conditions

➢ In-situ Raman Spectra with DH_2=30cc/kg

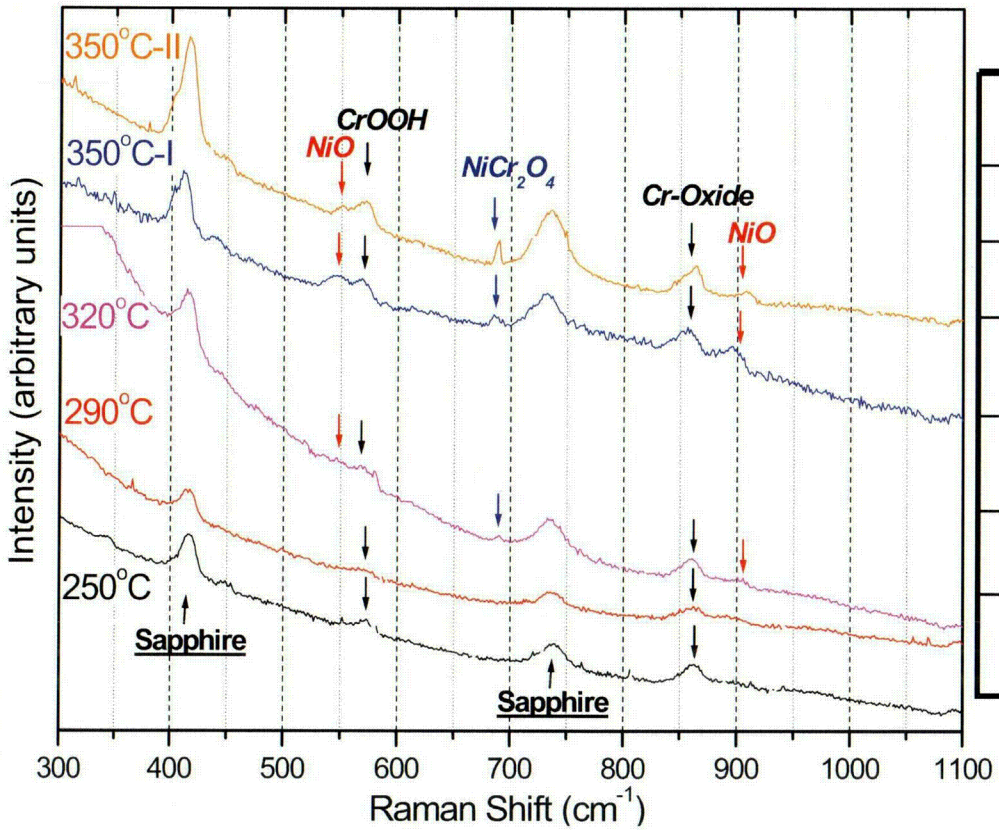

Species	Peaks
$NiCr_2O_4$	430 510 682
CrOOH	ca. 546-587
Cr^{III}/Cr^{VI} oxide	340-350 840-880
$NiFe_2O_4$	570 704
NiO	550 910
Sapphire	417 751

4. Results in PWR conditions

➢ In-situ Raman Spectra with DH_2=1cc/kg

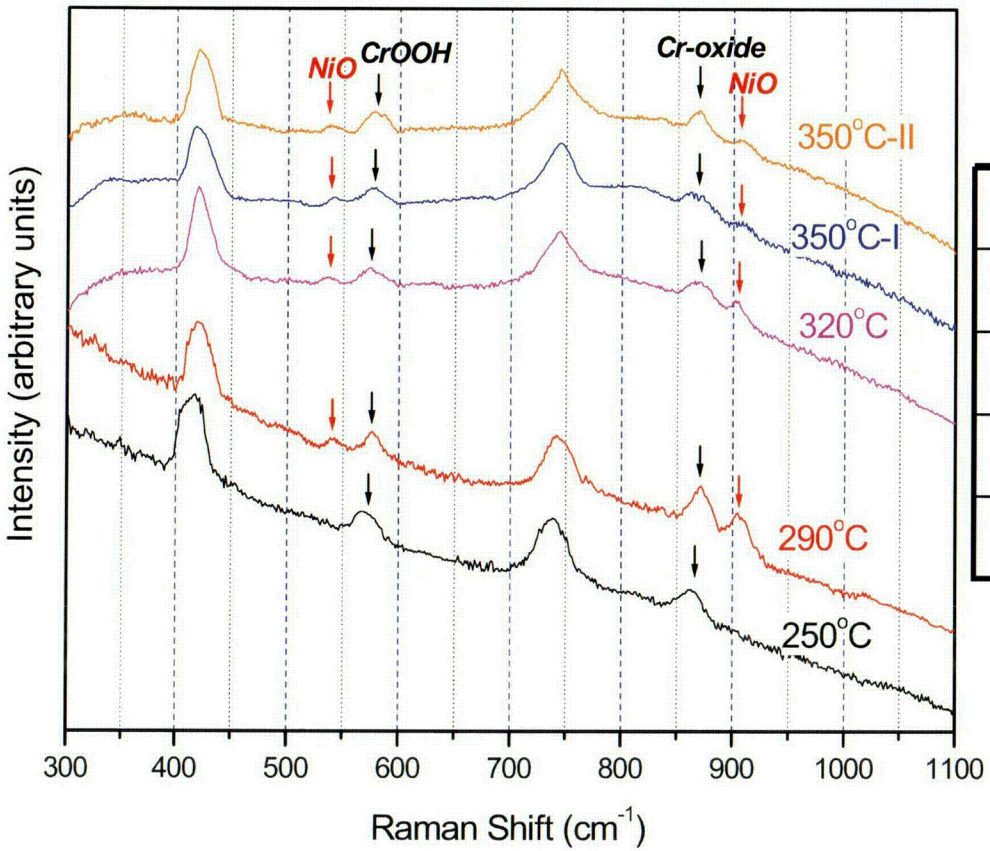

Species	Peaks
CrOOH	ca. 546-587
Cr^{III}/Cr^{VI} oxide	340-350 840-880
NiO	550 910
$NiCr_2O_4$	430 510 682

C62

4. Results in PWR conditions

Change of dissolved hydrogen concentration

- 1cc/kg -> 30cc/kg

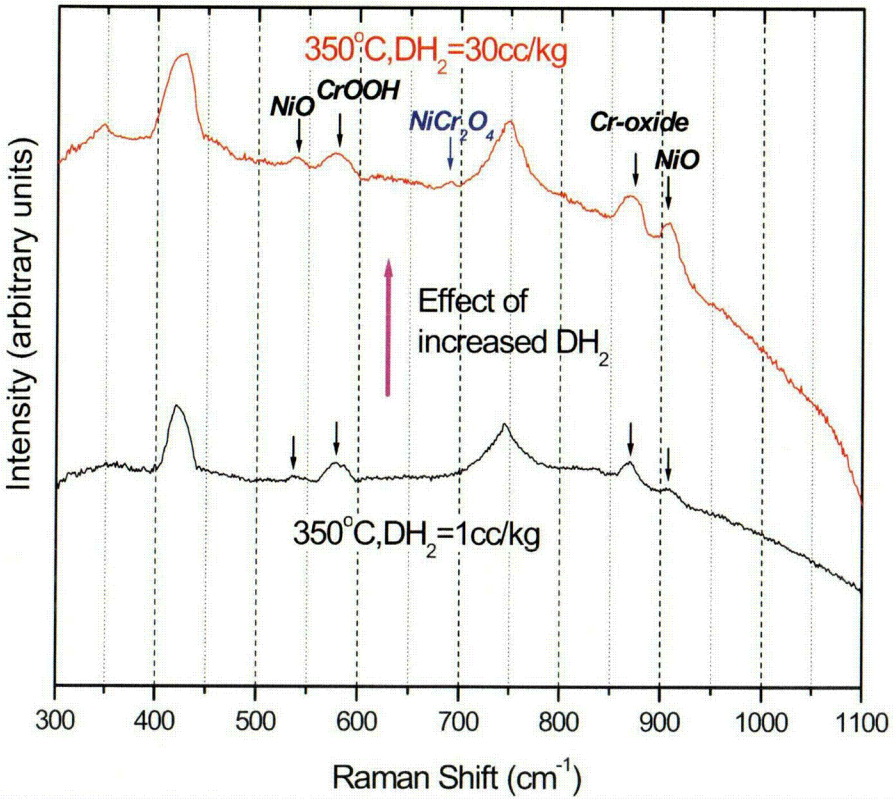

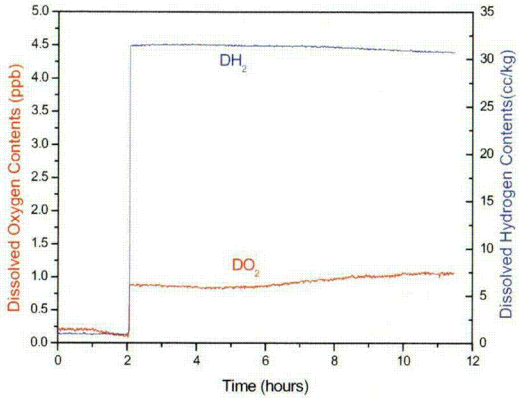

Species	Peaks
CrOOH	ca. 546-587
Cr^{III}/Cr^{VI} oxide	340-350 840-880
NiO	550 910
$NiCr_2O_4$	510 682

C63

4. Results: in-situ vs. ex-situ

- After cool-down to room temp. and exposure to air
  - No remarkable change in Raman spectrum
  - lower of Cr-oxide peak(~870cm^{-1}) : absence of borate

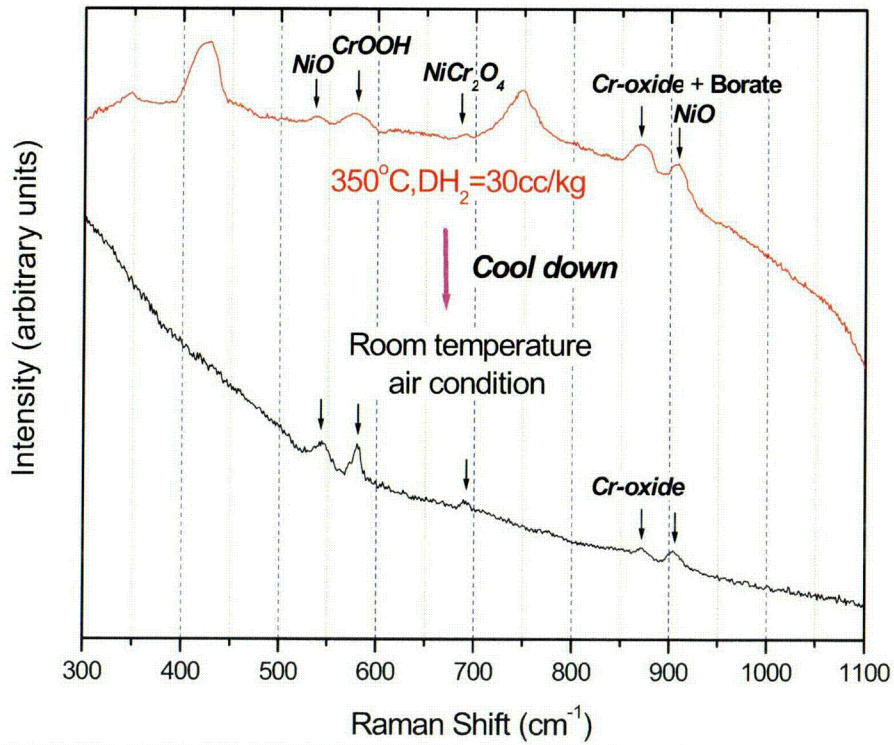

C64

4. Results: in-situ vs. ex-situ

➢ Comparison with past work

	In-situ (This work)	Soustelle et al.	Caron	Nakagawa et al.
Method	In-situ Raman	GDOS+EDS	XPS	Synchrotron XRD + TEM
T (°C)	350	360	330	320
Exposure time (hrs)	71	300	1869	1000
Oxide(s) at high DH_2	CrOOH, Cr-Oxide, NiO +$NiCr_2O_4$	Compact layer ($NiCr_2O_4$) + Precipitates ($NiFe_2O_4$)	$NiCr_2O_4$	(Ni+Cr-rich) oxide + Ppt. ($NiFe_2O_4$)
Oxide(s) at low DH_2	CrOOH, Cr-Oxide, NiO	Compact layer ($NiCr_2O_4$)	NiO	NiO

4. Results: in-situ vs. ex-situ

- $NiFe_2O_4$ detected at high DH_2 condition in ex-situ studies could not be observed in-situ at above 290℃. Suppression of precipitate layers in this work is attributed as the cause for the difference. But FE-SEM post-examination of oxide showed scarcity of precipitates on film.
- CrOOH that was not detected in the past was observed by Raman.
- NiO, Cr_2O_3, $NiCr_2O_4$ were observed in agreement with results of earlier ex-situ studies.

FE-SEM micrograph

TEM micrograph

5. Ni/NiO equilibrium: measured & predicted

- **Regular solution theory**
  - **Enthalpy of mixing**
    - ✓ Hertzman & Sundman (1985)
    - ✓ Use binary interaction coefficients to describe the enthalpy of mixing and extrapolation of high temperature (> 1100 K) thermodynamic data
  - **Standard Gibbs energy of formation of austenitic Ni-Cr-Fe solid solution**

$$\Delta_f G_T^o(alloy) = \sum_i^3 x_i \Delta_f G_T^o(i, fcc) + RT \sum_i^3 x_i \ln x_i + {}^E G_T^o + {}^{mag} G_T^o$$

where $\Delta_f G_T^o(alloy)$ = standard Gibbs energy of formation of the alloy

$\Delta_f G_T^o(i, fcc)$ = standard Gibbs energy of formation of component i in the fcc structure of alloy

${}^E G_T^o$ = excess Gibbs energy

${}^{mag} G_T^o$ = standard Gibbs energy due to magnetic ordering

- **Chemical thermodynamic data**
  - Room temperature data: standard literature source and HSC database
  - HT data by Criss-Cobble, HKF relation and extrapolation procedure
  - Data for chromium hydrolysis species : Ziemniak (1998)
  - Data for nickel and iron hydrolysis species : Tremaine et al. (1980)

5. Ni/NiO equilibrium: measured & predicted

➢ **DH2 vs. T and Comaprision with Earlier Work**

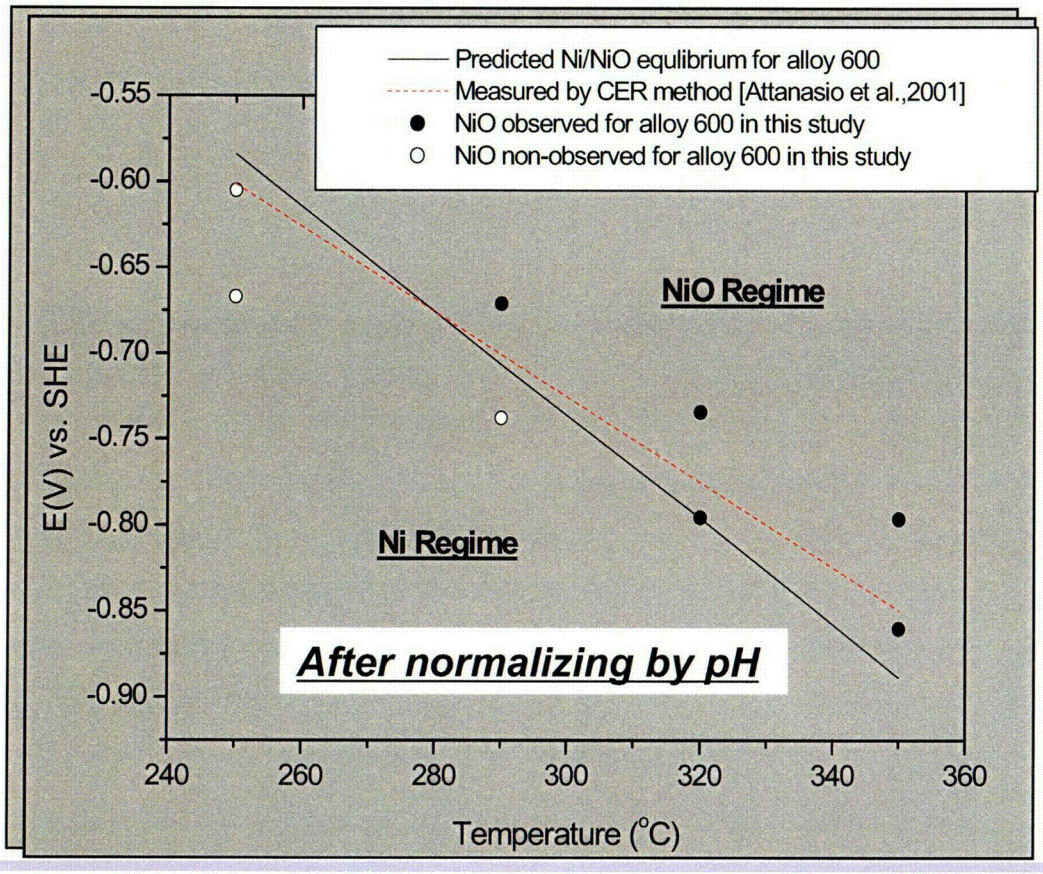

C65

5. Ni/NiO equilibrium: Implication to PWSCC

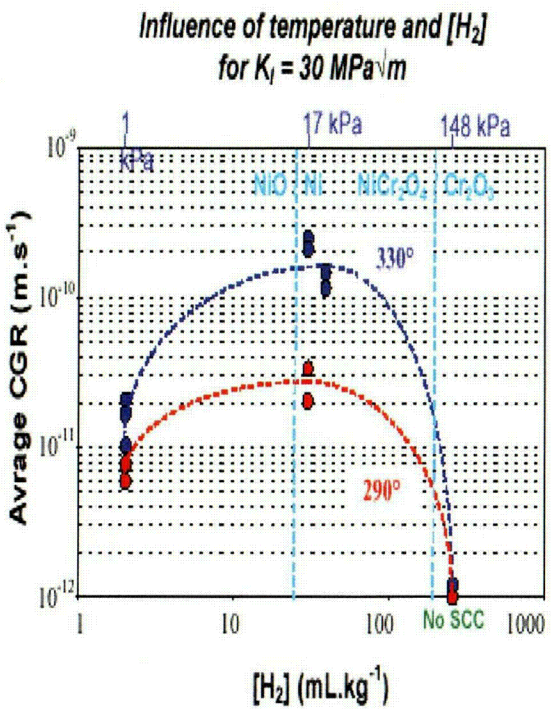

(T. Cassagne et al. '97 @ 330C)

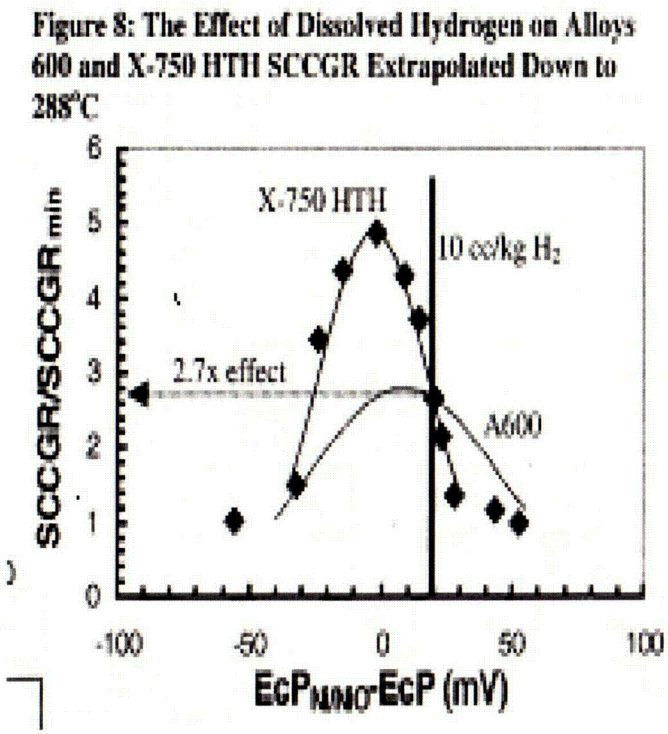

(S. Attanasio et al., '01 @ 288C)

5. Ni/NiO equilibrium: Implication to PWSCC

Accelerated corrosion due to Tetragonal/Monoclinic phase transition of ZrO2

New Hypothesis on PWSCC
Redox alteration of Ni/NiO may enhance film-percolation and PWSCC

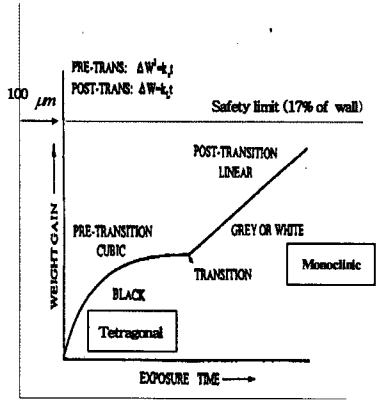

Oxidation behavior of zirconium alloys in nuclear power plants [Edward Hillner, 1977]

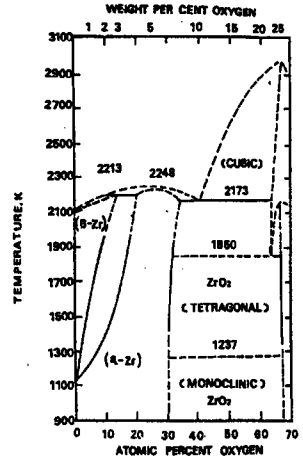

Phase diagram of Zirconium oxide [F. Garzarolli,1991]

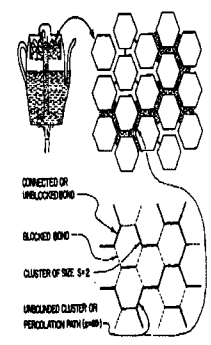

Percolation model of a flow through a porous medium that is modeled as a network of interconnected channels..

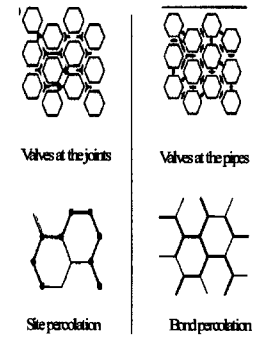

Plumbing analogy for the distinction Between site percolation and bond percolation

Nuclear Materials Laboratory 16

Nuclear Materials Laboratory 5

5. Ni/NiO equilibrium: Implication to PWSCC

Implication to Mitigation Effort

- Tighter DH2 Control at PWR
  - DH2 controlled by cover gas pressure in CVCS
  - H2 pressure may vary with time(0~50 cc/kg?)

- Systematic investigation on DH2 effect
  - Initiation and crack growth rate study as function of DH2, temperature and stress
  - Explore alternate DH2 levels;
    - either lower or higher than now (30 cc/kg H2O)

845

6. Conclusions

- In-situ Raman spectroscopy system was developed to obtain needed information on oxide films on Alloy 600 in in PWR water conditions .
- Some unique observations were made, compared with earlier ex-situ results;
  - CrOOH phase, undetected by ex-situ methods, was observed under most conditions.
  - $NiFe_2O_4$ usually found in precipitate layer was not observed, conceivably due to the suppression of precipitate layers in this work.
- NiO, Cr_2O_3 and $NiCr_2O_4$ phases were observed, in reasonable agreement with ex-situ results.

6. Conclusions

- Ni/NiO equilibrium was determined as function of dissolved hydrogen concentration and temperature.
  - Comparison of observed results with thermodynamic predictions showed a good agreement on Ni/NiO equilibrium at the temperature range from 250 to 350 degree C.
  - A good agreement was found between in-situ Raman results and those from contact electrical resistance (CER) measurements on Ni/NiO equilibrium.

- Fluctuation in DH2 in PWR may cause Ni/NiO alternation and accelerate PWSCC
  - Stable DH2 control at PWR is suggested
  - Systematic study is needed for lower/higher DH2 control for mitigation.